

Hydrodynamic and biochemical impacts on the development of hypoxia in the Louisiana–Texas shelf Part 1: numerical modeling and hypoxia mechanisms

Yanda Ou¹ and Z. George Xue^{1,2,3}

¹Department of Oceanography and Coastal Sciences, Louisiana State University, Baton Rouge, LA, 70803, USA.

²Center for Computation and Technology, Louisiana State University, Baton Rouge, LA, 70803, USA.

³Coastal Studies Institute, Louisiana State University, Baton Rouge, LA, 70803, USA

Correspondence to: Z. George Xue (zxue@lsu.edu)

Abstract. A three-dimensional coupled hydrodynamic–biogeochemical model with nitrogen, phosphorus, silica cycles, and multiple phytoplankton and zooplankton functional groups was developed and applied to the Gulf of Mexico to study bottom dissolved oxygen dynamics. A 15-year hindcast was achieved covering the period of 2006–2020. Extensive model validation against in situ data demonstrates that the model was capable of reproducing vertical distributions of dissolved oxygen (DO), spatial distributions of bottom DO concentration as well as its interannual variations. Horizontal advection, vertical advection, vertical diffusion, and sedimentary oxygen consumption (SOC) were found as the major factors modulating summer bottom DO dynamics. SOC contributes 33%–51% of summer bottom DO variability over the nearshore regions. Hydrodynamic impacts on the summer bottom DO are also remarkable as the joint contribution of the advection and vertical diffusion reaches 28%–55% and 51%–59% in nearshore and offshore regions, respectively. Sensitivity experiments were carried out to assess the changes in the size of the hypoxic zone due to riverine nutrient reductions. Results of sensitivity experiments highlighted the nonlinear relationship between the reduction of river nutrients and changes in the size of the hypoxic zone, which can be explained by the complexity of the lower-trophic community (e.g., competition on nutrients, grazing, and predation behaviors). Nutrient reductions would not necessarily lead to a decrease in the size of the hypoxic zone. Instead, due to the interactions among different plankton groups, the hypoxic area could even increase under some nutrient-reduction conditions. A triple riverine nutrient reduction (nitrogen, phosphorus, and silica) of 80% is needed to reach the goal of a 5000 km² hypoxic zone.

1 Introduction

The Louisiana–Texas (LaTex) shelf in the northern Gulf of Mexico (nGoM) has one of the most notorious recurring hypoxia in the world (bottom dissolved oxygen (DO) < 2 mg L⁻¹, Rabalais et al., 2002; Rabalais et al., 2007a; Justić and Wang, 2014). Regular mid-summer cruises since 1985 have shown that hypoxia usually first emerges in mid-May and persists through mid-September. The hypoxic zone can cover as big as 23,000 km² and has a volume of up to 140 km³ (Rabalais and Turner, 2019; Rabalais and Baustian, 2020). Sensitivity experiments of hypoxia area reduction to different nutrient reduction strategies by

Formatted	[1]
Deleted: Biochemical Impacts	
Deleted: Development	
Formatted	[2]
Formatted	[3]
Deleted: Hypoxia	
Deleted: Shelf	
Deleted: I: Numerical Modeling	
Formatted	[4]
Formatted	[5]
Formatted	[6]
Deleted: Hypoxia Mechanisms	
Formatted	[7]
Formatted	[8]
Formatted	[9]
Deleted: N, P, Si	
Formatted	[10]
Deleted: -	
Formatted	[11]
Deleted: is	
Formatted	[12]
Deleted: frequency distributions of hypoxia thickness,	
Deleted: and	
Deleted: of hypoxic area. The impacts of river plume and	[15]
Formatted	[13]
Formatted	[14]
Deleted: and water stratification (measured by potential e	[17]
Deleted: the variability of bottom DO concentration. Gen	[19]
Formatted	[16]
Formatted	[18]
Deleted: . The analysis indicates that SOC is the main regulator in	
Deleted: , and water stratification outcompetes the sedime	[22]
Formatted	[20]
Formatted	[21]
Deleted: (20–50 m)	
Deleted: . A strong quadratic	
Formatted	[23]
Formatted	[24]
Deleted: was found between	
Deleted: volume and hypoxic area	
Deleted: suggests that the volume mostly results from the	[28]
Formatted	[25]
Formatted	[26]
Formatted	[27]
Formatted	[29]
Deleted: potentially estimated based on	
Formatted	[30]
Deleted: Shelf	
Deleted: is	
Deleted: affected areas	
Formatted	[31]
Formatted	[32]
Formatted	[33]
Deleted: water	
Formatted	[34]

117 Fennel and Laurent (2018) suggested that to meet the hypoxic area reduction goal (< 5,000 km² in a 5-year running average)

118 set by the Hypoxia Task Force (2008), a dual nutrient strategy with a reduction of 48 % of total nitrogen and inorganic

119 phosphorus would be the most effective way. Although nitrogen is the ultimate limiting nutrient, phosphorus load reduction

120 would also lead to a significant reduction of the hypoxia area (Fennel and Laurent, 2018). Transient phosphorus limitation on

121 the shelf (Laurent et al., 2012; Sylvan et al., 2007) was deemed to be associated with the delayed onset and reduction of the

122 hypoxia area.

123

124 Coastal eutrophication in the LaTex shelf leads to a high rate of microbial respiration and depletion of DO (Rabalais et al.,

125 2007b). Incubation studies in the LaTex shelf suggested that SOC accounted for 20±4 % (Murrell and Lehrter, 2011) or

126 25±5.3 % (McCarthy et al., 2013) of below-pycnocline respiration, nearly 7-fold greater than the corresponding percentage at

127 the water overlying sediments (3.7±0.8 %, McCarthy et al., 2013). The fraction of SOC over the total respiration rate at

128 sediments and overlying water was ~87 % according to the measurements by McCarthy et al. (2013). As mentioned by Fennel

129 et al. (2013), the corresponding SOC fraction reached 60 % when applying the water respiration rates of Murrell and Lehrter

130 (2011) and sediment respiration rates of Rowe et al. (2002). Another numerical study (Yu et al., 2015) also pointed out that in

131 the LaTex shelf, oxygen consumption at the bottom water layer was more associated with SOC rather than water column

132 respiration. As it was commonly accepted that SOC was driven by the abundance of organic matter in the sediment, numerical

133 studies developed SOC schemes following this nature (e.g., Justić and Wang, 2014; Fennel et al., 2006; 2011). For example,

134 the instantaneous remineralization parameterization used by Fennel et al. (2006, 2011) estimated SOC as a function of sediment

135 detritus and phytoplankton. Using this scheme, Große et al. (2019) found that the simulated SOC was supported by Mississippi

136 nitrogen supply (51±9 %), Atchafalaya nitrogen supply (33±9 %), and open-boundary nitrogen supply (16±2 %). However,

137 the instantaneous parameterization tends to underestimate SOC at the peak of blooms yet overestimate SOC once the blooms

138 start. In a realistic environment, there should be a lag between the blooms and the peak SOC (Fennel et al., 2013). Recently,

139 developments of coupled sediment–water models emphasized the importance of sedimentary biochemical processes on the

140 SOC dynamics and evolution of bottom hypoxia in the shelf (Moriarty et al., 2018; Laurent et al., 2016). However, coupled

141 sediment–water models are computationally more expensive than simple parameterization of SOC. Therefore, it is crucial to

142 balance the model efficiency and complexity, especially for long-term hindcasts.

143

144 The phytoplankton bloom on the shelf results from both cyanobacteria and diatoms (Wawrik and Paul, 2004; Schaeffer et al.,

145 2012; Chakraborty et al., 2017). Cruises data in the nGoM indicated that diatoms accounted for ~50 to ~65 % (inner-shelf) and

146 ~33 to ~64 % (mid-shelf) of chlorophyll a in winter and spring, and ~30 % to ~46 % (inner-shelf) during summer and fall,

147 respectively (Chakraborty and Lohrenz, 2015). A field survey documented that the biovolume contribution of diatoms to the

148 total phytoplankton could be as high as 80 % and 70 % during the upwelling seasons in 2013 and 2014, respectively (Anglès

149 et al., 2019). In the Mississippi River plume, diatoms were found as the most diverse algal class accounting for over 42 % of

150 all unique genotypes observed (Wawrik and Paul, 2004). The phytoplankton community was highly simplified in previous

- Deleted: (reduce to <
- Formatted ... [36]
- Formatted ... [37]
- Deleted: shrinkage
- Deleted: Phosphorus limitation was deemed to be associat ... [39]
- Formatted ... [38]
- Deleted: Laurent and Fennel, 2014).
- Formatted ... [40]
- Formatted ... [41]
- Deleted: Shelf was deemed to be important
- Deleted: Conley et al., 2009; Rabalais et al., 2007b).
- Formatted ... [42]
- Deleted: Shelf
- Formatted ... [43]
- Formatted ... [44]
- Formatted ... [45]
- Formatted ... [46]
- Formatted ... [47]
- Deleted: Shelf
- Formatted ... [48]
- Deleted: While it is commonly accepted that bottom water ... [49]
- Moved down [1]: Hetland and DiMarco, 2008;
- Deleted: Murrell and Lehrter, 2011; Justić and Wang, 201 ... [51]
- Deleted: estimates
- Formatted ... [50]
- Formatted ... [52]
- Formatted ... [53]
- Deleted: only
- Formatted ... [54]
- Deleted: started
- Formatted ... [55]
- Deleted: emphasize
- Formatted ... [56]
- Deleted: couple
- Formatted ... [57]
- Deleted: It
- Deleted: , therefore,
- Formatted ... [58]
- Formatted ... [59]
- Deleted: model
- Deleted: hindcast
- Formatted ... [60]
- Formatted ... [61]
- Moved down [2]: the biovolume contribution of diatoms to the
- Moved down [3]: the most diverse algal class accounting for
- Deleted: Cruises data in the nGoM indicated that diatoms ... [62]
- Deleted: In the Mississippi River plume, diatoms are
- Deleted: The phytoplankton bloom in
- Formatted ... [63]
- Formatted ... [64]
- Formatted ... [65]
- Moved (insertion) [2]
- Formatted ... [66]
- Moved (insertion) [3]
- Formatted ... [67]

241 numerical studies, usually with only one phytoplankton functional group considered (e.g., Fennel et al., 2006, 2011, 2013;
242 Laurent et al., 2012; Justić and Wang, 2014).

243

244 In addition to SOC and excess nutrient supply from the rivers, water column stratification also plays an important role in
245 regulating the variability of bottom DO concentration in the LaTex shelf. Strong stratification prohibits ventilation of DO and
246 thus results in reduced DO supply to the bottom water layer (Hetland and DiMarco, 2008; Bianchi et al., 2010; Fennel et al.,
247 2011, 2013, 2016; Justić and Wang, 2014; Wang and Justić, 2009; Feng et al., 2014; Yu et al., 2015; Laurent et al., 2018). On
248 the shelf, the river freshwater plume supported by the Mississippi and the Atchafalaya Rivers introduces buoyancy, leading to
249 a stable water column and weak DO ventilation processes (Mattern et al., 2013; Fennel and Testa, 2019). Due to the different
250 distances from major river mouths, the influence of freshwater-induced buoyancy would vary along the shelf. Moreover, the
251 transports and deposition processes of organic matter are affected by the coastal along-shore current systems resulting in
252 different SOC gradients across the shelf. For instance, Hetland and DiMarco (2008) pointed out that in the west of Terrebonne
253 Bay where stratification is usually weak, bottom hypoxia is controlled by bottom respiration.

254

255 Despite the above efforts, there are still knowledge gaps in our understanding of the mechanism of hypoxia development as
256 well as a feasible way to reduce the size of the hypoxic zone. First of all, the LaTex shelf is a vast water body and the
257 contribution of sedimentary biochemical and hydrodynamics to hypoxia development is location-dependent. Fennel et al.
258 (2016)(Fennel et al., 2016) divided the shelf into six subregions for model validation purposes instead of for quantifying
259 biochemical and hydrodynamic impacts on bottom DO variability in different shelf regions. A recent study by Ruiz Xomchuk
260 et al. (2021) tried to fill such a gap by decomposing the oxygen equation and found that advection and sediment oxygen
261 demand were the two main contributors to the oxygen budget. But they focused more on the impacts of the temporal and spatial
262 scales of physical processes on bottom DO variability over the west shelf (between 95°W and 92.5°W). Secondly, existing
263 biogeochemical models (e.g., Hetland and DiMarco, 2008; Fennel et al., 2006, 2011, 2013; Laurent et al., 2012; Laurent and
264 Fennel, 2014; Fennel and Laurent, 2018; Justić et al., 2003; Justić et al., 2007; Justić and Wang, 2014; Große et al., 2019;
265 Moriarty et al., 2018) utilized an over-simplified lower-trophic ecosystem (one phytoplankton + one zooplankton function
266 groups or only one phytoplankton group) with one or two embedded nutrient flows (nitrogen or nitrogen+phosphorus). These
267 models could not differentiate the contribution of different plankton groups or the interaction among them in hypoxia
268 development. The nutrients reduction strategies proposed by existing models (mostly based on nitrogen loads; Scavia et al.,
269 2013; Obenour et al., 2015; Turner et al., 2012; Laurent and Fennel, 2019) may be problematic as bottom DO's responses to
270 decreased nutrient loads may not be linear or quasilinear due to the complexity of the lower trophic community.

271

272 In this study, we adapted and modified a coupled physical-biogeochemical model covering the entire Gulf of Mexico (GoM)
273 by introducing the oxygen and phosphorus cycles to the North Pacific Ecosystem Model for Understanding Regional
274 Oceanography (NEMURO, Kishi et al. 2007). The model has two phytoplankton and three zooplankton functional groups for

Formatted [69]

Deleted: Shelf. Stronger

Formatted: English (US)

Deleted: less

Formatted [70]

Deleted: In

Formatted [71]

Deleted: would introduce

Formatted [72]

Deleted: However, due

Formatted [73]

Deleted: matters would be

Formatted: English (US)

Deleted: Although...or instance, Hetland and DiMarco (2008) pointed out that in the west of Terrebonne Bay where stratification is usually weak, bottom hypoxia is controlled by bottom respiration, there is still a lack of discussions of dominated factors of bottom DO dynamics in different parts of the shelf. [74]

Formatted: English (US)

Moved (insertion) [1]

Deleted: In this study, we adapted and modified a coupled physical-biogeochemical model to the Gulf of Mexico. We introduced an oxygen and a phosphorus cycle to the North Pacific Ecosystem Model for Understanding Regional Oceanography (NEMURO, Kishi et al. 2007). The model has two phytoplankton and three zooplankton, functional groups, for a more comprehensive representation of the plankton community. An additional silicate limitation term is applied for the growth of the diatom functional group. We developed a simplified yet efficient SOC parameterization with two sedimentary organic pools to account for the time lags between bottom hypoxia peaks and bloom peaks. Based on a 15-year (2006–2020) hindcast, we aim to 1) understand the contributions of different factors in hypoxia evolution in different parts of the LaTex shelf; and 2) to provide daily hindcasts of physical and biochemical conditions to develop a hypoxia prediction model using machine learning techniques (see an accompanying paper in Part II). In the following sections, model description and modification, model set-ups, and data availability are given in Methods (Section 2), followed by extensive model validations from time series to spatial patterns and vertical structure (Section 3). The main findings of this study and discussion of the relative importance of different factors in modulating bottom DO variability are given in Section 4. Conclusions are addressed in the last section. [1]

Formatted [75]

343 a more comprehensive representation of the plankton community. We also modified the instantaneous remineralization
344 parameterization by adding a conceptual sedimentary organic pool (represented by a sedimentary particulate organic nitrogen
345 pool, PONsed; Fig. 1) to allow the accumulation of organic matter in the sediment. Although the SOC scheme applied is
346 similar to that in Justić and Wang (2014), the sedimentary organic matter pool in our study is supported by a more complex
347 plankton community, including three phytoplankton functional groups and two zooplankton functional groups. The influence
348 of the community complexity can be reflected in the SOC and eventually in the bottom DO variability. Based on a 15-year
349 (2006–2020) numerical hindcast, we aimed to 1) understand the contributions of different factors in hypoxia development in
350 different parts of the LaTex shelf; and 2) assess the outcomes of different riverine nutrient reduction scenarios regarding the
351 reduction of the hypoxic zone. In addition, the daily outputs of physical and biochemical conditions will be used to develop a
352 hypoxia prediction model using machine learning techniques (see an accompanying paper in Part 2). In the following sections,
353 model description and modification, model set-ups, and data availability were given in Section 2 (Methods), followed by
354 extensive model validations (Section 3). The main findings of this study and relevant discussion are presented in Section 4.

355 2 Methods

356 2.1 Coupled hydrodynamic–biogeochemical model

357 We adapted the three-dimensional, free-surface, topography-following community model, the Regional Ocean Model System
358 (ROMS, version 3.7) on the platform of Coupled Ocean–Atmosphere–Wave–Sediment Transport (COAWST) modeling
359 system (Warner et al., 2010) to the GoM (Gulf–COAWST). ROMS solves finite difference approximations of Reynolds
360 Averaged Navier–Stokes equations by applying hydrostatic and Boussinesq approximations with a split explicit time-stepping
361 algorithm (Haidvogel et al., 2000; Shchepetkin and McWilliams, 2005, 2009). The biogeochemical model applied is primarily
362 based on the NEMURO developed by Kishi et al. (2007). NEMURO is a concentration-based, lower-trophic-level ecosystem
363 model developed and parameterized for the North Pacific. The original NEMURO model has 11 concentration-based state
364 variables, including nitrate (NO₃), ammonium (NH₄), small and large phytoplankton biomass (PS and PL), small, large, and
365 predatory zooplankton biomass (ZS, ZL, and ZP), particulate and dissolved organic nitrogen (PON and DON), particulate
366 silica (Opal), and silicic acid (Si(OH)₄). NEMURO is known for its capability to distinguish ZS, ZL, and ZP, and provides a
367 detailed analysis of the dynamics of different functional groups. It was widely used in studies of plankton biomass on regional
368 scales (Fiechter and Moore 2009; Gomez et al., 2018; Shropshire et al., 2020). The embedded silicon cycle permits the
369 inclusion of a diatom group (i.e., PL), the dominant phytoplankton group in the nGoM.

370 2.2 Model modification

371 In a recent effort, Shropshire et al. (2020) adapted and modified NEMURO to the GoM with five structural changes, (1) The
372 grazing pathway of ZL on PS was removed since, in the GoM, the PS group is predominated by cyanobacteria and
373 picoeukaryotes, which are too small for direct feeding by most mesozooplankton (i.e., PL). (2) Linear function of mortality

Formatted	... [76]
Deleted: adapt	
Deleted:	
Deleted: numerical	
Formatted	... [77]
Formatted	... [78]
Formatted	... [79]
Deleted:)	
Formatted	... [80]
Deleted: (COAWST,	
Formatted	... [81]
Deleted: largely	
Formatted	... [82]
Deleted: SP	
Deleted: LP	
Formatted	... [83]
Formatted	... [84]
Deleted: SZ, LZ	
Deleted: PZ	
Formatted	... [85]
Formatted	... [86]
Deleted: in distinguishing SZ, LZ	
Deleted: PZ	
Formatted	... [87]
Formatted	... [88]
Deleted: in	
Formatted	... [89]
Deleted: Gomez et al., 2018;	
Formatted	... [90]
Deleted: which is deemed to be	
Formatted	... [91]
Deleted: as follows	
Formatted	... [92]
Formatted	... [93]
Deleted: LZ	
Deleted: SP	
Deleted: SP	
Formatted	... [94]
Formatted	... [95]
Formatted	... [96]
Deleted: LP	
Formatted	... [97]

414 was applied for PS, PL, ZS, and ZL, while quadratic mortality was used for ZP, accounting for predation pressure of unmodeled
 415 predators, like planktivorous fish. (3) The ammonium inhibition term in nitrate limitation function was no longer considered
 416 exponentially but followed the parameterization by Parker (1993). (4) Light limitation on photosynthesis was replaced with
 417 Platt et al.'s (1980) functional form, which was also implemented in the newer version of NEMURO. (5) Constant C: Chl ratio
 418 was replaced with a variable C: Chl model according to the formulation by Li et al. (2010).

- Deleted: SP, LP, SZ
- Deleted: LZ
- Deleted: PZ
- Formatted: English (US)
- Formatted: English (US)
- Formatted: ... [98]

420 However, neither the modified (Shropshire et al., 2020) nor the original (Kishi et al., 2007) NEMURO model considered
 421 phosphorus and oxygen cycles. In this study, we introduced a phosphorus cycle into NEMURO, including three concentration-
 422 based state variables as phosphate (PO₄), particulate organic phosphorus (POP), and dissolved organic phosphorus (DOP). The
 423 phosphate limitation on phytoplankton growth was introduced using the Michaelis–Menten formula. In the NEMURO model,
 424 nitrogen serves as the common “currency”, while phosphorus and silicon are converted to nitrogen using the Redfield ratio of
 425 P: N: Si=1: 16: 16. In the river-dominated LaTex shelf, inorganic and organic nutrients are supplied mainly by rivers. In our
 426 model, riverine PO₄(Fig. C1), DOP, and POP were prescribed based on water quality measurements at river gages. When no
 427 measurement was available, the PO₄, DOP, and POP were approximated using total nitrate+nitrite (NO₃+NO₂), dissolved
 428 organic nitrogen (DON), and particulate organic nitrogen (PON) measurements, respectively, via the Redfield ratio of P: N=1:
 429 16. We neglected the POP settling process but preserved these pools by introducing the stoichiometric ratio between
 430 phosphorus and nitrogen instead. In other words, the sinking process of POP was implicitly included by building linkages
 431 between PON and POP concentrations, as the sinking of PON was considered in the model. Governing equations for
 432 phosphorus state variables were given according to Equations 1–3. Please also refer to the appendices for more details on
 433 expressions of modified terms (Appendix A), state variables (Appendix Table B1), source and sink terms (Appendix Table
 434 B2), and values of parameters (Appendix Table B4).

- Formatted: ... [99]
- Deleted: which includes
- Formatted: English (US)
- Deleted: (Michaelis and Menten, 1913).
- Formatted: English (US)
- Deleted: Shelf
- Deleted: mostly
- Formatted: English (US)
- Formatted: ... [100]
- Deleted: is
- Formatted: ... [101]
- Deleted:)
- Formatted: ... [102]
- Deleted: of
- Formatted: English (US)

$$436 \frac{d(PO_4)}{dt} = (ResPSn + ResPLn) \cdot RPO4N$$

$$437 + (DecP2N + DecD2N) \cdot RPO4N$$

$$438 + (ExcZSn + ExcZLn + ExcZPn) \cdot RPO4N$$

$$435 - (GppPSn + GppPLn) \cdot RPO4N, \quad (1)$$

- Formatted: ... [103]
- Formatted: ... [104]
- Formatted: ... [105]
- Formatted: ... [106]
- Formatted: ... [107]

$$440 \frac{d(DOP)}{dt} = (DecP2D - DecD2N) \cdot RPO4N$$

$$439 + (ExcPSn + ExcPLn) \cdot RPO4N, \quad (2)$$

- Formatted: ... [109]
- Formatted: ... [108]

$$441 \frac{d(POP)}{dt} = (MorPSn + MorPLn + MorZSn + MorZLn + MorZPn) \cdot RPO4N$$

$$442 + (EgeZSn + EgeZLn + EgeZPn) \cdot RPO4N$$

$$443 - (DecP2N + DecP2D) \cdot RPO4N, \quad (3)$$

- Formatted: ... [110]
- Formatted: ... [111]

465 We further adapted the oxygen cycle developed by Fennel et al. (2006, 2013) to NEMURO for hypoxia simulations. However,
 466 ~~our model's~~ biochemical dynamics of oxygen are slightly different due to the different plankton functional groups considered.
 467 Biochemical sources for oxygen are contributed by photosynthesis of two phytoplankton functional groups, while the sinks
 468 are attributed to respirations of two phytoplankton functional groups, metabolism of three zooplankton functional groups, light-
 469 dependent nitrification (Olson, 1981; Fennel et al., 2006), aerobic decomposition of particulate and dissolved organic matter
 470 (measured as PON, and DON, respectively), and SOC. Wanninkhof's (1992) parameterization was implemented for estimates
 471 of oxygen air-sea flux. The biochemical dynamics of oxygen ~~were~~ adopted as follows (see detailed descriptions of variables
 472 and parameters in Appendix A-B):

$$\begin{aligned}
 474 \frac{d(Oxyg)}{dt} = & (rOxNO_3 \cdot GppNPS + rOxNH_4 \cdot GppAPS) \\
 475 & + (rOxNO_3 \cdot GppNPL + rOxNH_4 \cdot GppAPL) \\
 476 & - ResPSn \cdot [RnewS \cdot rOxNO_3 + (1 - RnewS) \cdot rOxNH_4] \\
 477 & - ResPLn \cdot [RnewL \cdot rOxNO_3 + (1 - RnewL) \cdot rOxNH_4] \\
 478 & - rOxNH_4 \cdot (ExcZSn + ExcZLn + ExcZPn) \\
 479 & - 2 \cdot Nit \cdot LgtlimN \cdot r_s \\
 480 & - rOxNH_4 \cdot DecD2N \cdot r_s \\
 481 & - SOC \cdot THK_{pote}
 \end{aligned}
 \tag{4}$$

482 A sedimentary particulate organic nitrogen (PON_{sed}) pool due to vertical sinking processes of PON was introduced for
 483 parameterization of SOC. The SOC scheme (Fennel et al., 2006) ~~is~~ known as the instantaneous consumption of DO. ~~As~~ soon
 484 as the PON falls into the sediment bed, ~~PON will be decomposed instantaneously. This scheme~~ tends to underestimate SOC at
 485 the peak of blooms and to overestimate SOC after blooms since the lag in SOC demand is neglected (Fennel et al., 2013). We
 486 considered such temporal delays ~~in~~ SOC by introducing a PON_{sed} pool. A portion of sinking PON ends up with PON_{sed}, while
 487 the rest is buried (PON_{burial}) and is removed ~~from~~ the system. The parameterization is shown in the following. 1) Organic
 488 matter settling down at the conceptual sediment layer is remineralized at a temperature-dependent aerobic remineralization
 489 rate, K_{P2N} . 2) Sediment oxygen is consumed only in the oxidation of sedimentary organic matter (represented by PON_{sed}) and
 490 the nitrification of ammonium to nitrate (Fennel et al., 2006). 3) Oxygen consumption at the conceptual sediment layer directly
 491 contributes to oxygen concentration ~~decreases~~ only at the overlying water or bottom water column. ~~Here, we did not distinguish~~
 492 ~~the overlying water and bottom water column since no dynamic sediment module was considered.~~ 4) Sediment denitrification
 493 is linearly related to SOC according to observational-based estimates by Seitzinger and Giblin (1996), but the relationship was
 494 modified by Fennel et al. (2006) with a slightly smaller slope of denitrification on SOC rate, i.e.,

$$495 \text{denitrification } (\mu\text{molN m}^{-2} \text{day}^{-1}) = 0.105 \times \text{SOC } (\mu\text{molO}_2 \text{m}^{-2} \text{day}^{-1}).
 \tag{5}$$

496 5) Aerobic decomposition of PON_{sed}, sediment nitrification, and denitrification follow chemical equations according to
 497 (Fennel et al., 2006):

- Formatted [112]
- Deleted: the
- Deleted: in our model
- Formatted: English (US)
- Formatted [113]
- Deleted: are
- Formatted: English (US)
- Formatted [114]
- Formatted [115]
- Formatted [116]
- Formatted [117]
- Deleted: (ExcZS + ExcZL + ExcZP)
- Formatted [118]
- Formatted: English (US)
- Formatted [119]
- Formatted [120]
- Formatted [121]
- Deleted: is
- Deleted: as
- Formatted [122]
- Formatted: English (US)
- Deleted: which
- Formatted [123]
- Deleted: of
- Formatted: English (US)
- Deleted: out of
- Formatted [124]
- Deleted: decreases of
- Formatted [125]
- Formatted [126]
- Formatted [127]

518 $C_{106}H_{263}O_{410}N_{46}P + 106O_2 \leftrightarrow 106CO_2 + 16NH_4 + H_2PO_4 + 122H_2O$, (R1) Formatted ... [128]

519 $NH_4 + 2O_2 \rightarrow NO_3 + 2H + H_2O$, (R2) Formatted ... [129]

520 $C_{106}H_{263}O_{410}N_{46}P + 84.8HNO_2 \rightarrow 106CO_2 + 42.4N_2 + 16NH_4 + H_2PO_4 + 148.4H_2O$, (R3) Formatted ... [130]

521

522 6) Only a portion of NH_4 provided by the aerobic respiration (Eq. (R1)) is used as the source element in the nitrification (Eq.

523 (R2)), while all NO_3 produced by nitrification is used as the source element in denitrification (Eq. (R3)). The linear assumption

524 in 4) implicitly builds relationships among the reactions listed in assumption 5). Let's assume that the production rate of NH_4

525 by aerobic decomposition (Eq. (R1)) of organic matter is M $mmol\ m^{-3}\ day^{-1}$, and that the fraction of denitrification-produced

526 CO_2 (Eq. (R3)) to the total CO_2 production (Eq. (R1) and (R3)) is x . According to the linear assumption abovementioned, the

527 consumption rate of NO_3 during denitrification (Eq. (R3)) is proportional to the total consumption rate of O_2 in the sediment

528 (Eq. (R1) and (R2)), yielding $\frac{84.8Mx}{16(1-x)} = 0.105 \times \left[\frac{106M}{16} + \frac{84.8Mx}{16(1-x)} \right]$ and further $x \approx 0.1425$. The oxygen consumption rate (Eq. (6))

529 and organic matter consumption rate (Eq. (7)) due to the coupled aerobic decomposition, nitrification, and denitrification

530 processes can be obtained by substituting the x value into the stoichiometric ratios according to Eq. (R1)–(R3).

531 $Oxygen_{consumption} = \frac{106M}{16} + \frac{84.8Mx}{16(1-x)} = 8.3865M$, (6) Formatted ... [132]

532 $OM_{consumption} = \frac{M}{16} + \frac{Mx}{16(1-x)} = 0.0729M$, (7) Formatted ... [133]

533 Accordingly, the SOC and consumption rate of PON_{sed} are given, respectively as follows:

534 $SOC = Oxygen_{consumption} \cdot THK_{bot} = 8.3865M \cdot THK_{bot}$, (8) Formatted ... [134]

535 $PON_{sed,consumption} = 16 \cdot OM_{consumption} \cdot THK_{bot} = 1.1662M \cdot THK_{bot}$, (9) Formatted ... [135]

536 where,

537 $M = \frac{PON_{sed} \cdot VP2N_0 \cdot \exp(Kp2N \cdot TMP)}{THK_{bot}}$, (10) Formatted ... [137]

538 THK_{bot} = thickness of bottom water column, (11) Formatted ... [138]

539 Formatted ... [139]

540 For further comparison with the DO concentration, we transferred the SOC rate into a volume-based unit ($mg\ L^{-1}\ day^{-1}$) dividing

541 the rate by THK_{bot} . For simplification, the terminology of SOC was still applied to represent the transferred SOC rate in the

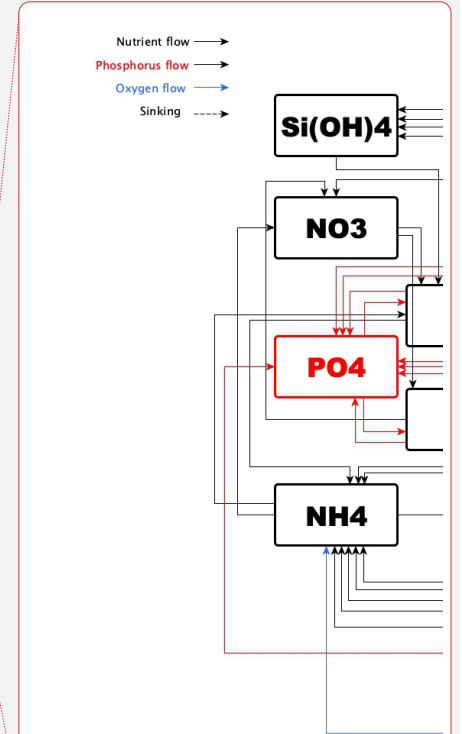
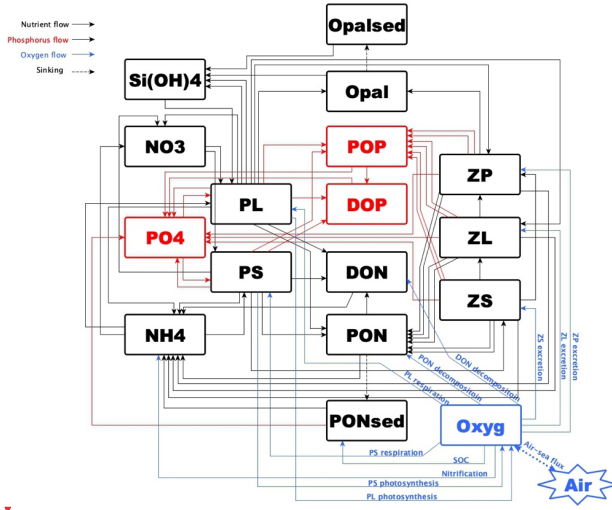
542 following discussion. We further added light inhibition on the nitrification (Olson, 1981) and oxygen dependency on

543 nitrification and aerobic decomposition. These parametrizations were applied following descriptions by Fennel et al. (2006,

544 2013). For the oxygen-dependent term, an oxygen threshold was specified below which no aerobic respiration or nitrification

545 occurred. Detailed equations were listed in Appendix A. The structure of the newly modified NEMURO model was shown in

546 a schematic diagram in Figure 1.



559
 560 **Figure 1.** Schematic diagram of the modified NEMURO model. Note that the phosphorus flow and the oxygen flow are two newly
 561 added flows to the original NEMURO model.

562 **2.3 Model set-ups**

563 The coupled model was applied to the GoM using Arakawa C-grid with a horizontal resolution of ~5 km (Figure 2a). There
 564 are 334 and 357 interior rho points in the east-west and north-south directions, respectively. The model includes 36 sigma
 565 layers vertically. The wetting and drying scheme (Warner et al., 2013) was implemented for a more accurate representation of
 566 shallow water. The computational time step (i.e., baroclinic time step) was set to 240 seconds while the number of barotropic
 567 time steps between each baroclinic time step was set to 30. Model hindcast was carried out from 1 August 2006 to 26 August
 568 2020 with the first 5 months as a spin-up period. Model results were output on a daily interval at UTC 00: 00.

569 The physical model set-ups largely followed an earlier Gulf-COAWST application (Zang et al., 2018, 2019, 2020). Open
 570 boundaries were set at the south and east forced by daily water level, horizontal components of 3-D current velocity, horizontal
 571 components of depth-integrated current velocity, 3-D water salinity, and 3-D water temperature derived from the Hybrid
 572 Coordinate Ocean Model (HYCOM) global analysis products (Bleck and Boudra, 1981; Bleck, 2002) with data assimilated
 573 via the Navy Coupled Ocean Data Assimilation system (Cummings, 2005; Cummings and Smedstad, 2013; Fox et al., 2002;
 574 Helber et al., 2013). For lateral boundary conditions, we utilized Chapman implicit for free surface and water level (Chapman,
 575 1985), Flather for depth-integrated momentum (Flather, 1976), gradient for mixing total kinetic energy, and mixed radiation-
 576 nudging conditions for 3-D momentum, temperature, and salinity (Marchesiello et al., 2001). The nudging time steps for the

Deleted:
Formatted: English (US)
Formatted: ... [141]
Deleted: be
Formatted: English (US)
Deleted: be
Formatted: English (US)
Formatted: ... [142]
Deleted: (i.e., GLBu0.08 expt_19.1, GLBu0.08 expt_90.9, GLBu0.08 expt_91.0, GLBu0.08 expt_91.1, GLBu0.08 expt_91.2, GLBv0.08 expt_93.0, and GLBy0.08 expt_93.0, for detailed information, seeing <https://www.hycom.org/hycom>)
Formatted: ... [143]

591 mixed radiation-nudging condition were set to 1 day for inflows and 30 days for outflows. The boundary nudging technique
592 was performed at the computational grids along the open boundary. The boundary condition types for passive biochemical
593 tracers (i.e., PS, PL, ZS, ZL, ZP, NO₃, NH₄, PON, DON, Si(OH)₄, opal, PO₄, POP, DOP, and Oxyg) were all prescribed as
594 radiation.

Formatted: English (US)

Deleted: passive

Formatted: English (US)

595

596 Initial conditions for water level, horizontal components of 3-D current velocity, horizontal components of depth-integrated
597 current velocity, 3-D water salinity, and 3-D water temperature were provided by the same HYCOM products as well. Initial
598 conditions for concentrations of NO₃, PO₄, and Si(OH)₄ were interpolated from measurements provided by the World Ocean
599 Database (WOD, Boyer et al., 2018). Initial conditions for DO concentration were given by World Ocean Atlas (WOA, Garcia
600 et al., 2018). Other biochemical tracers were initialized as 0.1 mmol m⁻³ due to the lack of observations.

Formatted: English (US)

Formatted: English (US)

Formatted: English (US)

Deleted: Garcia et al., 2018)

Formatted: English (US)

Formatted: English (US)

601
602 Atmospheric forcings, including surface wind velocity at 10 m height above sea level, net longwave radiation flux, net
603 shortwave radiation flux, precipitation rate, air temperature 2 m above sea level, sea surface air pressure, and relative humidity
604 2 m above sea level, were derived from the National Centers for Environmental Prediction (NCEP) Climate Forecast System
605 Reanalysis (CFSR) 6-hourly products (for years prior to 2011, Saha et al., 2010) and NCEP CFS Version 2 (CFSv2) 6-hourly
606 products (for years starting from 2011, Saha et al., 2011) with a horizontal resolution of ~35 km and ~22 km, respectively. In
607 our model, 63 rivers were considered as horizontal point source forcings along the coastal GoM. They were split into 280
608 points (red dots in Fig. 2a) sources transporting time-varying salinity (nearly zero), temperature, 3-D horizontal momentum
609 (based on the magnitude of river discharges), nutrients (NO₃, NH₄, PO₄, Si(OH)₄, PON, DON, POP, and DOP; Fig. C1), and
610 DO to the computational domain. Locations of river point sources of the Mississippi and the Atchafalaya Rivers were shown
611 as red dots in Figure 2b. For reconstructions of time series of river forcing terms, we composed measurements from various
612 sources, including U.S. Geological Survey (USGS) National Water Information System (NWIS), National Oceanic and
613 Atmospheric Administration (NOAA) Tides and Currents System (TCS), NOAA National Estuarine Research Reserve System
614 (NERRS), and Mexico National Water Commission (CONAGUA, for rivers in Mexico's territory). Daily averaged river
615 discharges were given based on measurements by USGS NWIS and CONAGUA. The magnitude of river discharges was
616 multiplied by 1.4 to account for adjacent watershed areas and lateral inflow of tributaries (Warner et al., 2005). River
617 temperature and salinity time series were reconstructed from measurements by USGS NWIS, NOAA TCS, and NOAA
618 NERRS. River nutrient concentrations were provided monthly by USGS NWIS and NOAA NERRS and were extended to
619 daily time series with values in the corresponding months. Riverine DO concentration was set to be a constant (258 mmol m⁻³)
620 assuming that riverine DO was saturated at 25 °C under 1 atm. Besides, tidal forcings were introduced in the hydrodynamic
621 model taking into account of influences of tidal elevations and tidal currents. There were 13 tidal constituents considered in
622 the model including M2, S2, N2, K2, K1, O1, P1, Q1, MF, MM, M4, MS4, and MN4.

Formatted: English (US)

Formatted: English (US)

Formatted: English (US)

Formatted: English (US)

Deleted: point

Formatted: English (US)

Formatted: English (US)

Deleted: are

Formatted: English (US)

Formatted: English (US)

Formatted: English (US)

Formatted: English (US)

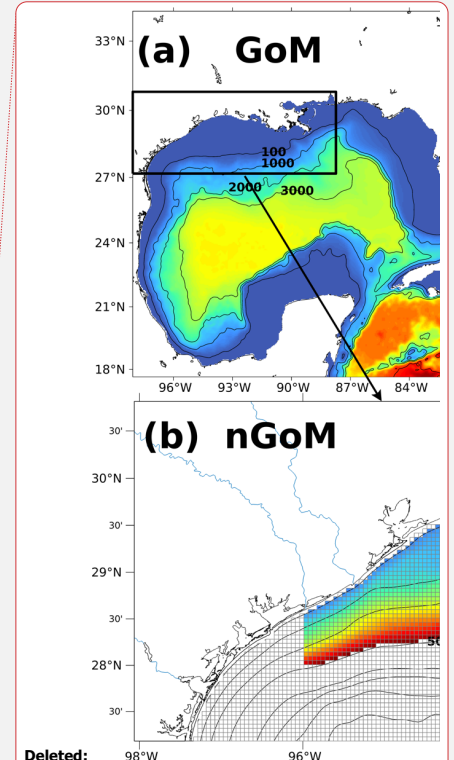
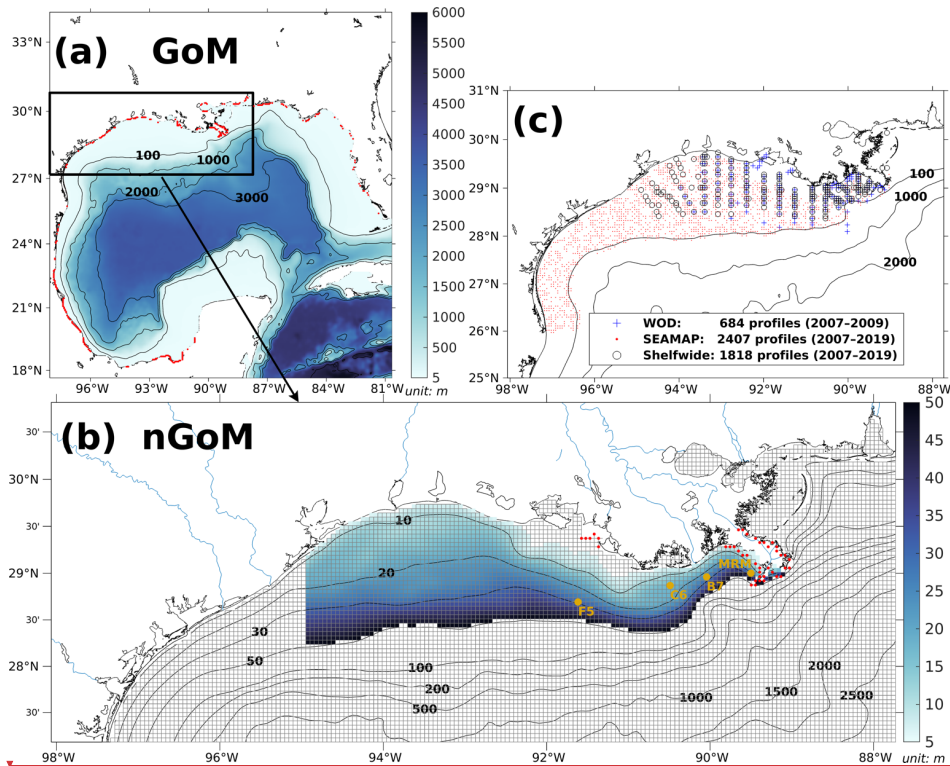
Deleted: 511

Formatted: English (US)

Deleted: highly oversaturated

Formatted: English (US)

623



Deleted: Figure 2. (a) Bathymetry of the entire domain of the Gulf-COAWST, (b) zoom-in bathymetry plot of the northern Gulf of Mexico (nGoM), and (c) locations of observed inorganic (... [144])

Formatted: English (US)

Moved (insertion) [4]

Deleted: profile comparisons between

Deleted: results and observations from various sources

Deleted: concentrations of

Formatted: English (US)

Formatted: English (US)

Formatted: English (US)

Deleted: , and DO.

Formatted: English (US)

630
631 **Figure 2. (a) Bathymetry of the entire domain of the Gulf-COAWST, (b) zoom-in bathymetry plot of the northern Gulf of Mexico**
632 **(nGoM), and (c) locations of observed inorganic nutrient and DO profiles derived from WOD, SEAMAP, and NOAA's shelf-wide**
633 **cruises. In (a), locations of river point sources are denoted by red dots. In (b), only bathymetry between 6 and 50 m was mapped**
634 **with colors; computational meshes were split by solid grey lines; main river channels are denoted by solid blue curves; locations of**
635 **river point sources of the Mississippi and the Atchafalava rivers are indicated by red dots; sampling locations for SOC and**
636 **overlying water respiration measurements by McCarthy et al. (2013) are denoted by dark yellow dots.**

637 3 Biogeochemical model validations

638 3.1 Available measurements

639 In this section, **biogeochemical model validations** were conducted for **inorganic nutrient concentration profiles (i.e., NO₃, PO₄,**
640 **and Si(OH)₄), ratios of diatom and total phytoplankton, SOC, ratios of SOC and overlying water respiration, DO concentration**

662 profiles, spatial distributions of bottom DO concentration, and temporal variability of the hypoxic area against multiple data
663 sets derived from cruise measurements and literature. Model simulated profiles were linearly interpolated to depths of the
664 observed profiles for a quantitative comparison. Validation of the hydrodynamic model can be found in Zang et al. (2019).

665
666 Inorganic nutrient concentration profiles from WOD were used for model validation. WOD measurements cover the period
667 from 11 January 2007 to 5 July 2009 including 478 NO₃ profiles, 409 PO₄ profiles, and 217 Si(OH)₄ profiles. The diatom
668 percentage of total phytoplankton was derived from measurements by Chakraborty and Lohrenz (2015) and Schaeffer et al.
669 (2012). The SOC and overlaying water respiration measurements were from an incubation study (McCarthy et al., 2013).
670 Available DO concentration profiles were obtained from the WOD, NOAA-supported mid-summer shelf-wide cruises, and
671 Summer Groundfish Survey in GoM supported by Southeast Area Monitoring and Assessment Program (SEAMAP) conducted
672 annually by the Gulf States Marine Fisheries Commission. There were 445 DO profiles (11 January 2007 to 5 July 2009) from
673 WOD. The shelf-wide cruises provided 1818 measured profiles with 85140 available records from 2007 to 2019. There were
674 at least 83 DO profiles for each summer (June–August, except 2016) from the shelf-wide cruise observations. The selected
675 SEAMAP DO dataset covers a time range from 2007 to 2019 with measurements including 2407 profiles with 77415 sampled
676 records. Locations of the selected profiles from different archives were shown in Figure 2c. Summer measurements by the
677 shelf-wide cruises were used for the validation of spatial patterns of bottom DO concentration and time series of summer
678 hypoxic areas. Estimated hypoxic areas by the cruises are available from 2007 to 2020 with a range from 5,480 km² to 22,720
679 km².

680 3.2 Nutrients concentration profiles

681 Modeled results showed good agreements with WOD nutrient profiles (Fig. 3a, 3d, and 3g, averaged every 2 m from the
682 surface to 50 m depth) in terms of vertical patterns and magnitudes. The surface waters were rich in NO₃ (Fig. 3a) but
683 oligotrophic in PO₄ (Fig. 3d) and Si(OH)₄ (Fig. 3g), indicating a possibly high diatom productivity (Baronas et al., 2016) and
684 possible phosphorous or silicon limitation in the photic zone. NO₃ concentrations decreased drastically at a depth between 10
685 and 15 m and were maintained at a low level from 15 to 50 m. A bi-peak structure was found in both PO₄ and Si(OH)₄
686 concentration profiles. The first peak (also the higher ones) of PO₄ concentration occurred at around 10–20 m depth while the
687 second peak was at around 35 m depth as illustrated by the averaged values and corresponding 10–90 percentiles. In contrast,
688 the high peak of Si(OH)₄ concentration occurred at around 35 m depth while the low peak at the depth of around 15 m, which
689 is consistent with biogenic silica remineralization at lower water columns (Baronas et al., 2016). The simulated profiles were
690 linearly interpolated to the observed depth for point-to-point comparisons. The probability histograms of concentration
691 differences illustrated that our model generally overestimated NO₃ (Fig. 3b) and PO₄ (Fig. 3e) but underestimated Si(OH)₄
692 (Fig. 3h). About 60% of total NO₃ differences fell within a range from -10 to 10 mmol m⁻³ with 43 % in the positive interval
693 (i.e., from 0 to 10 mmol m⁻³). The corresponding statistics of PO₄ comparisons within a range of ±0.4 mmol m⁻³ were 53 % (-
694 0.4–0.4 mmol m⁻³), 31 % (0–0.4 mmol m⁻³), and 22 % (-0.4–0 mmol m⁻³), respectively. Approximately 13 % of observed

Deleted: the specific depth

Formatted: English (US)

Formatted: English (US)

Deleted: We also provided detailed comparisons of frequency distributions of hypoxic thickness, spatial distributions of bottom DO, and temporal variability of the hypoxic area between the model results and the Shelfwide measurements.

Formatted: English (US)

Formatted: English (US)

Formatted: English (US)

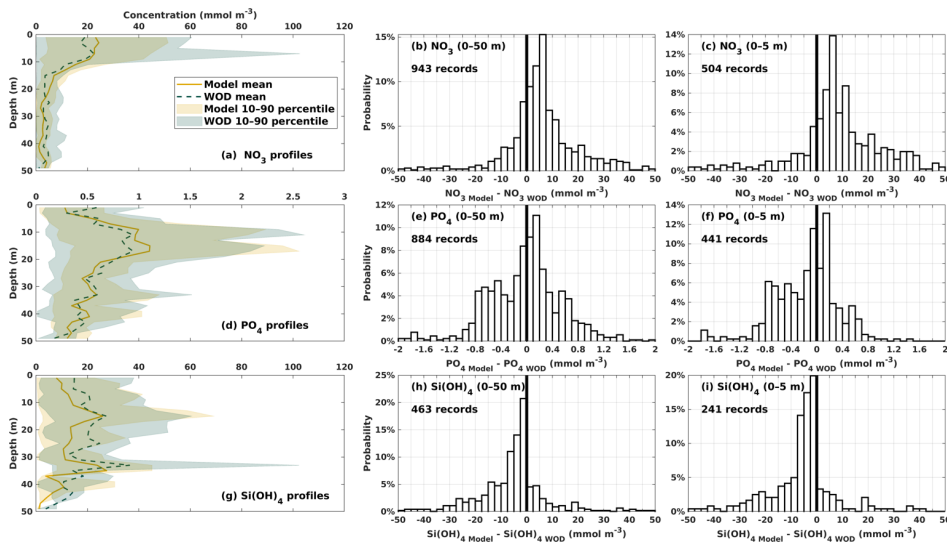
Moved up [4]: 3.1 Available measurements

Deleted: Inorganic nutrient concentration profiles from WOD were used for model validation. Measurements cover a period from 11 January 2007 to 5 July 2009 including 436 NO₃ profiles, 377 PO₄ profiles, and 215 Si(OH)₄ profiles. Available DO concentration profiles were obtained from the WOD, NOAA-supported midsummer Shelfwide cruises, and Summer Groundfish Survey in GoM supported by Southeast Area Monitoring and Assessment Program (SEAMAP) and conducted annually by the Gulf States Marine Fisheries Commission. There were 410 DO profiles (11 January 2007 to 5 July 2009) available provided by WOD. There were at least 77 DO profiles for each summer (July–August for years 2012, 2013, 2014, 2015, 2017, and 2018) derived from the Shelfwide cruises observations. More than 3,000 measurements were conducted each summer except 2017 summer (909 in total) by Shelfwide cruises. Selected SEAMAP summer DO measurements covered a time range from 2007 to 2019 with higher data coverage (152–331 DO profiles including 4,141–12,550 measurements for each summer) than the WOD and Shelfwide observations. Locations of the selected profiles from different archives are shown in Figure 2c. We estimated the hypoxia thickness (Figure 5) and spatial extents of bottom hypoxic water (Figure 6) based on the Shelfwide DO profiles measurements. The observed spatial patterns were obtained by interpolating the measured bottom DO concentration to the computational grids. Time series of summer hypoxic areas estimated by the Shelfwide cruises were available from 2008 to 2020 with a range from 5,480 km² to 22,720 km² (<https://gulfhypoxia.net/research/shelfwide-cruises/>, Figure 7).
3.2 Inorganic nutrients

Formatted: English (US)

Deleted: WOD-derived and modeled nutrient profiles show a good agreement in terms of vertical distributions and magnitudes (Figure 3). Both simulations and measurements are relatively higher in shallow water areas (within 10 m). Higher PO₄ and Si(OH)₄ concentrations were found at the lower water layers for both simulated and measured profiles in waters deeper than 10 m. Nonetheless, NO₃ and PO₄ concentration were both slightly overestimated by the model, while Si(OH)₄ concentration was marginally underestimated. The probability histogram of NO₃ concentration differences between simulations and measurements illustrates that ~60 % of total simulation–measurement pairs drop within a range from -10 to 10 mmol m⁻³ with ~40 % in the positive interval (i.e., from 0 to 10 mmol m⁻³). The same statistics were also found for PO₄ comparisons within a range of ±0.4 mmol m⁻³. However, there were ~15 % of observed Si(OH)₄ being overestimated by within 10 mmol m⁻³ and ~50 % being underestimated by within 10 mmol m⁻³. Mean NO₃ concent... [145]

772 Si(OH)_4 were overestimated within 10 mmol m^{-3} and $\sim 51 \%$ were underestimated within 10 mmol m^{-3} . At surface layers (0–5
 773 m), similar probability patterns in nutrient biases were found but with slightly different statistics (Fig. 3c, 3f, and 3i). For
 774 example, about 34 % of NO_3 concentrations were overestimated within 10 mmol m^{-3} compared to 10 % of surface
 775 measurements underestimated within 10 mmol m^{-3} . Mean NO_3 concentrations from the Mississippi and the Atchafalaya Rivers
 776 were $99 \pm 34 \text{ mmol m}^{-3}$ (mean $\pm 1\text{sd}$) and $66 \pm 29 \text{ mmol m}^{-3}$, respectively. Mean riverine PO_4 concentrations were 2.7 ± 0.7
 777 mmol m^{-3} and $2.3 \pm 0.7 \text{ mmol m}^{-3}$, respectively, and mean riverine Si(OH)_4 concentrations were $118 \pm 23 \text{ mmol m}^{-3}$ and 116
 778 $\pm 21 \text{ mmol m}^{-3}$, respectively. The nutrient concentrations bias between simulations and observations is acceptable concerning
 779 the strong influences of high riverine nutrient loads on the shelf.



780
 781 **Figure 3.** Profile comparisons between model hindcasts and WOD measurements for concentrations of (a)–(c) NO_3 , (d)–(f) PO_4 , and
 782 (g)–(i) Si(OH)_4 . Note that the thick vertical lines in (b), (c), (e), (f), (h), and (i) denote the concentration difference of 0 separating the
 783 positive and negative intervals.

784 3.3 Diatom ratios

785 Both measured and model simulated Si(OH)_4 profiles suggested strong diatom productivity in the photic zone (Fig. 3g). Cruise
 786 observations confirmed that the LaTex phytoplankton community is dominated by the diatom group (Schaeffer et al., 2012;
 787 Chakraborty and Lohrenz, 2015). Regional averages (Fig. C2 in Appendix C), vertical averages (only the surface, middle, and
 788 bottom layers were chosen), and monthly averages were applied to the concentration ratio of diatom and total phytoplankton
 789 according to the sampled locations, sampled layers, and sampled months, respectively, of the cruise studies by Schaeffer et al.

Formatted: English (US)

Formatted: English (US)

Formatted: English (US)

Formatted: English (US)

Deleted: DO

Formatted: Normal

Deleted: profiles

Formatted: English (US)

792 (2012) and Chakraborty and Lohrenz (2015). The modeled ratios well reproduced the measured ones in terms of magnitudes,
 793 monthly variability, and cross-shelf variability (Table 1). During the cruise periods in 2008, the range of modeled diatom
 794 percentage (79% to 99%) matched well with the measurements (79% to 88%) except for June 2008 when underestimations
 795 were found. In 2009, our model results agreed well with the measurements in inner shelf waters but overestimated in the mid-
 796 shelf regions, especially in the summer and fall of 2009. The measured percentages exhibited salient monthly variations with
 797 higher values in winter and spring and low ones in summer and fall. In the cross-shelf direction, the phytoplankton community
 798 shifted from a highly diatom-dominated one in the inner shelf waters to a less diatom-dominated one in the mid-shelf waters,
 799 especially in summer. Such patterns were well captured by our model.

800 **Table 1. Comparison of simulated (mean ± 1SD) and measured (mean ± 1SD in parentheses) diatom percentage of the total**
 801 **phytoplankton. Note that the statistics for the simulated percentages were conducted based on concentration values and averaged**
 802 **over the cruise months and over given regions that cover the cruise sampling locations (Fig. C2). The measured percentages by**
 803 **Schaeffer et al. (2012) (for measurements in 2008) were calculated based on biovolume values, while those by Chakraborty and**
 804 **Lohrenz (2015) (for measurements in 2009) were given by chlorophyll *a* attributed to different phytoplankton groups**

	Diatom/total phytoplankton × 100%	
	Inner shelf	Midshelf
February 2008	99±4 (88±16)	
April 2008	99±2 (71±16)	
May 2008	79±39 (79±22)	
June 2008	29±42(85±10)	
January 2009	60±29 (66±21)	57±14 (47±14)
April 2009	50±33 (59±14)	51±19 (33±29)
July 2009	41±33 (40±13)	33±24 (13±16)
October–November 2009	50±33 (46±14)	38±19(19±17)
March 2010	49±35 (50±14)	52±26 (64±12)

805

806 3.4 SOC and overlying water respiration

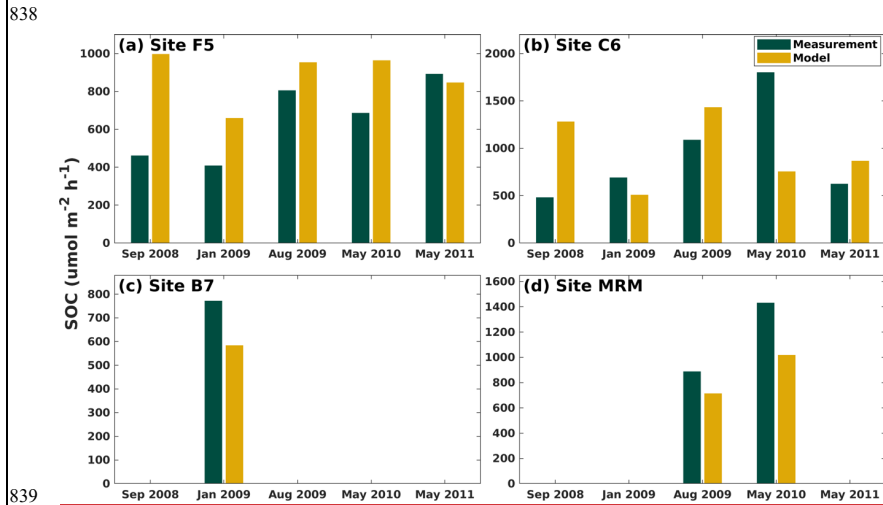
807 McCarthy et al. (2013) provided incubation measurements of the SOC rates and overlying water respiration at five shelf water
 808 sites (Fig. 1 in McCarthy et al., 2013) using sediment and water samples collected during six cruises (i.e., July 2008, September
 809 2008, January 2009, August 2009, May 2010, and May 2011). Modeled SOC rate and SOC/overlying water respiration ratio
 810 were then compared against the measurements. The modeled overlying water respiration rate was approximated by the rate
 811 calculated at the bottom water column considering biochemical processes that occurred at that layer, i.e., phytoplankton
 812 respiration rates, zooplankton metabolism rates, aerobic decomposition rates of PON and DON, and nitrification rate. The

Formatted: English (US)

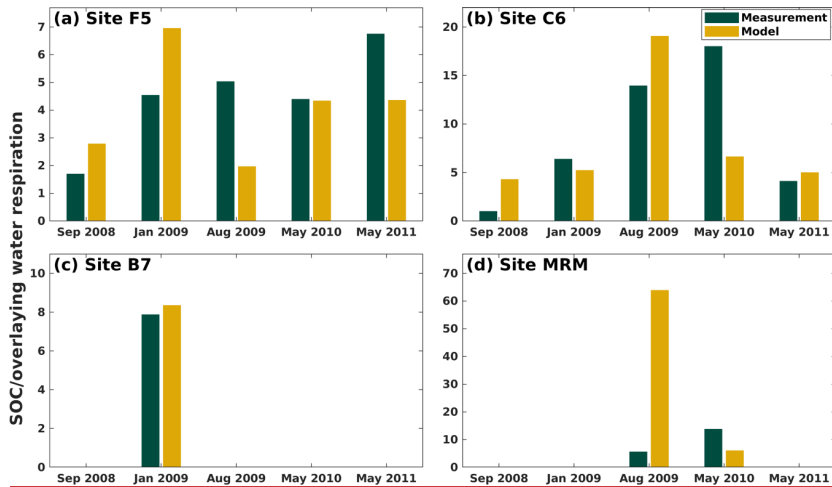
Deleted: DO decreases from the upper to the lower water layers in both simulated and WOD profiles (Figures 4a–4b). Hypoxia was mainly detected in profiles with depth between 10 m and 20 m. Hypoxia was more frequent as shown in the WOD DO profiles, indicating that the model overestimated the observed DO (Figures 4a–4c). The total number of model–measurement relative percentage difference pairs is 901, ~72 % of which are within a range of ±50 %. Our model overestimated/underestimated ~32 %/~19 % of total DO observations by within 20 % and overestimated/underestimated ~21 %/14 % of total DO observations by within 10 %.

In both modeled and NOAA's Shelfwide DO profiles, massive hypoxic events were detected mainly in profiles with depth from 10 to 20 m (Figures 4d–4e). The

827 modeled SOC and ratio of SOC/overlying water respiration were averaged over the cruise months for four shelf sites (i.e.,
 828 F5, C6, B7, and MRM; Fig. 2b). Our model could well capture the SOC magnitude and variability. Both measured and modeled
 829 ratios of SOC/ overlying water respiration were found greater than 1, highlighting the importance of SOC in bottom DO
 830 dynamics (Fig. 5). The model generally overestimated the SOC at sites F5 and C6 except for January 2009 and May 2010 at
 831 site C6, and underestimated SOC at sites B7 and MRM (Fig. 4). The modeled ratio agreed with the measurements except for
 832 site MRM in August 2009. Such a bias might result from the prescription of river inputs along the model boundary for diverting
 833 momentum and concentration tracers from the river point sources to the computational grid cells. The scheme could lead to an
 834 overshot of fresh water at the near-mouth grid cells and a short residence time for organic matter in the water column and an
 835 underestimation of the overlying water respiration rate. As the model results were averaged over an entire month but not over
 836 the exact cruise date due to the lack of cruise information in McCarthy et al. (2013), we considered model-simulated SOC and
 837 ratio of SOC/overlying water respiration acceptable.



839
 840 Figure 4. Comparison of modeled and measured SOC (unit: $\mu\text{mol m}^{-2} \text{h}^{-1}$) at four LaTex shelf sites (Fig. 2b). Note that the
 841 measurements are provided by McCarthy et al.'s (2013) incubation study.



842 **Figure 5. Comparison of modeled and measured (McCarthy et al., 2013) ratios of SOC/overlying water respiration at four LaTex**
 843 **shelf sites.**

845 3.5 DO profiles

846 Both simulated and observed DO profiles were averaged every 2 m from the surface to 50 m depth (Fig. 6a, 6c, and 6e). The
 847 observed DO vertical structures, such as the “zigzag” shape in the WOD profiles and “C” shape in the shelf-wide and SEAMAP
 848 profiles, were well captured by the model. The 10–90 percentile of modeled DO overlap the measured ones. Probability
 849 histograms of relative bias between the model and measurements reveal that the model overestimated the measured DO (Fig.
 850 6b, 6d, and 6f). There were 45% (27%) of the WOD DO samples were overestimated (underestimated) by 50%. When
 851 compared to the shelf-wide cruise measurements, the probability histogram of the relative bias showed a bell-shaped
 852 distribution with a peak around zero. 28%, 44%, and 66% of observations were misestimated by $\pm 10\%$, $\pm 20\%$, and $\pm 50\%$,
 853 respectively (Fig. 6d). Our model seemed to agree well with SEAMAP data. There were 36% (20%), 50% (26%), and 61%
 854 (31%) of records being overestimated (underestimated) by 10%, 20%, and 50%, respectively (Fig. 6f).

Deleted: DO relative percentage differences between simulations and observations shows

Formatted: English (US)

Formatted: English (US)

Deleted: There were ~30 %, ~

Deleted: ~67

Deleted: being

Deleted: within

Formatted: English (US)

Formatted: English (US)

Formatted: English (US)

Formatted: English (US)

Deleted: Figure 4f). Model results showed a good agreement with the Shelfwide observations.

Due to the

Deleted: discontinuity before 2012 and after 2018 provided by WOD and Shelfwide cruises, summer DO profiles measurements by SEAMAP were used for DO validation as well (Figures 4g–4i). Our model well captured the magnitude and vertical structures of observed DO in each summer, although slight overestimations existed.

Deleted: ~52 %, ~75 %, ~93 % of total relative difference pairs dropping within a range of $\pm 10\%$, $\pm 20\%$, and $\pm 50\%$

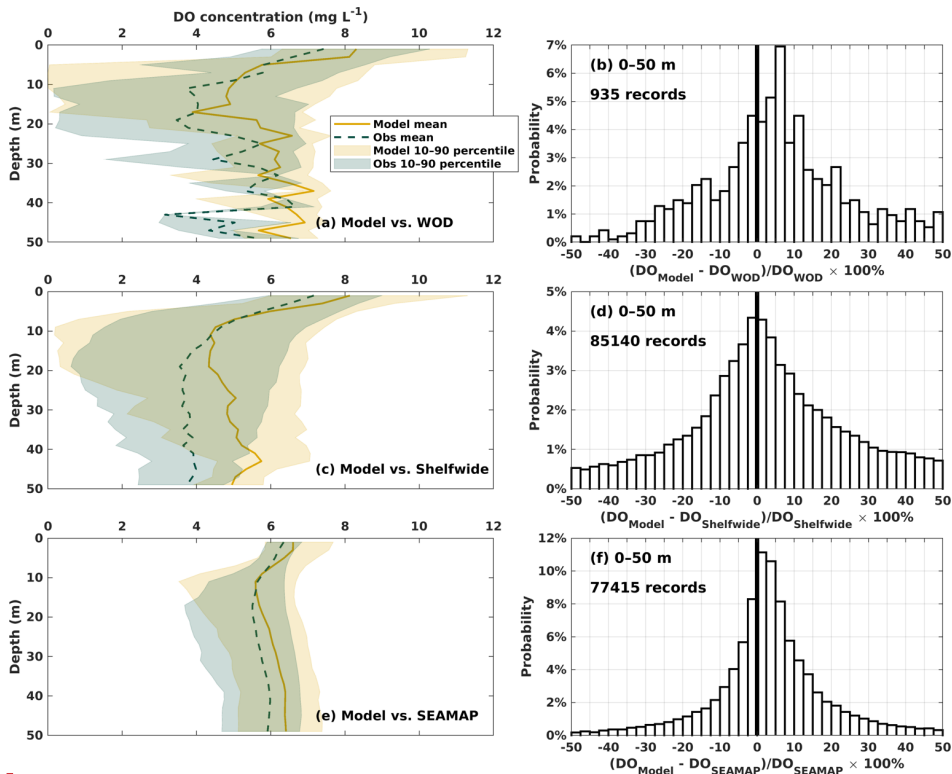
Formatted: English (US)

Formatted: English (US)

Deleted: .

Formatted: English (US)

Formatted: English (US)



874
 875 **Figure 6.** Comparisons of DO profiles between model hindcasts and measurements by (a–b) WOD, (c–d) NOAA’s shelf-wide cruises,
 876 and (e–f) SEAMAP. Probability histograms of relative percentage differences between modeled and observed DO are in the right
 877 column. The thick vertical lines in the histograms denote the percentage difference of 0.

878 **3.6 Spatial distributions of bottom DO and temporal variability of hypoxic area**

879 As the annual NOAA shelf-wide cruises were conducted from the east shelf to the west in the summer, model simulated bottom
 880 DO was resampled following the cruise periods. For example, if the westmost location of the cruise is 90°W on day 1, the
 881 simulated bottom DO concentration over the east of 90°W on that day is extracted. On the following day, if the westmost
 882 location of the cruise is 91°W, the simulation between 91°W and 90°W on day 2 is extracted, and so forth. All the extract frames
 883 were blended to reconstruct the spatial distribution of simulated bottom DO concentration during the summer cruise period.
 884 Simulated results outside the LaTex shelf and over the deep (>50 m) and shallow (<6 m) water regions were excluded since

Deleted: ¶ [146]

Deleted: 4

Deleted: c

Formatted: English (US)

Formatted: English (US)

Formatted: English (US)

Formatted: English (US)

Deleted: NOAA’s summer Shelfwide cruises, and (g–h) [147]

Deleted: . The solid black contour lines in the profile [148]

Formatted: English (US)

Formatted: English (US)

Formatted: English (US)

Deleted: 3.4 Hypoxic thickness, spatial

Deleted: ,

Formatted: English (US)

Formatted: English (US)

Deleted: Previous studies pointed out that hypoxic volu... [149]

Formatted: English (US)

Deleted: periods covered by the Shelfwide cruises during each

Deleted: .

Formatted: English (US)

Formatted: English (US)

Deleted: Shelf

Deleted: 100

Deleted: 10

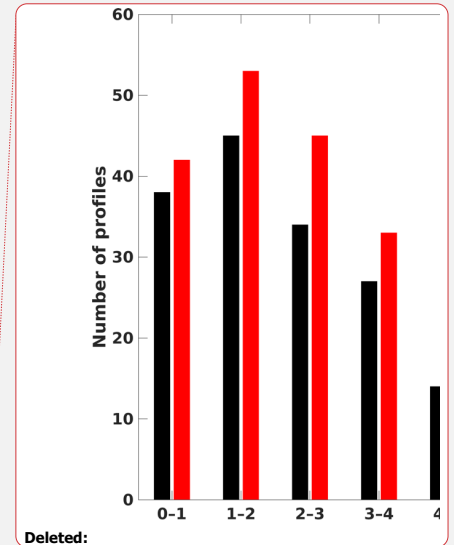
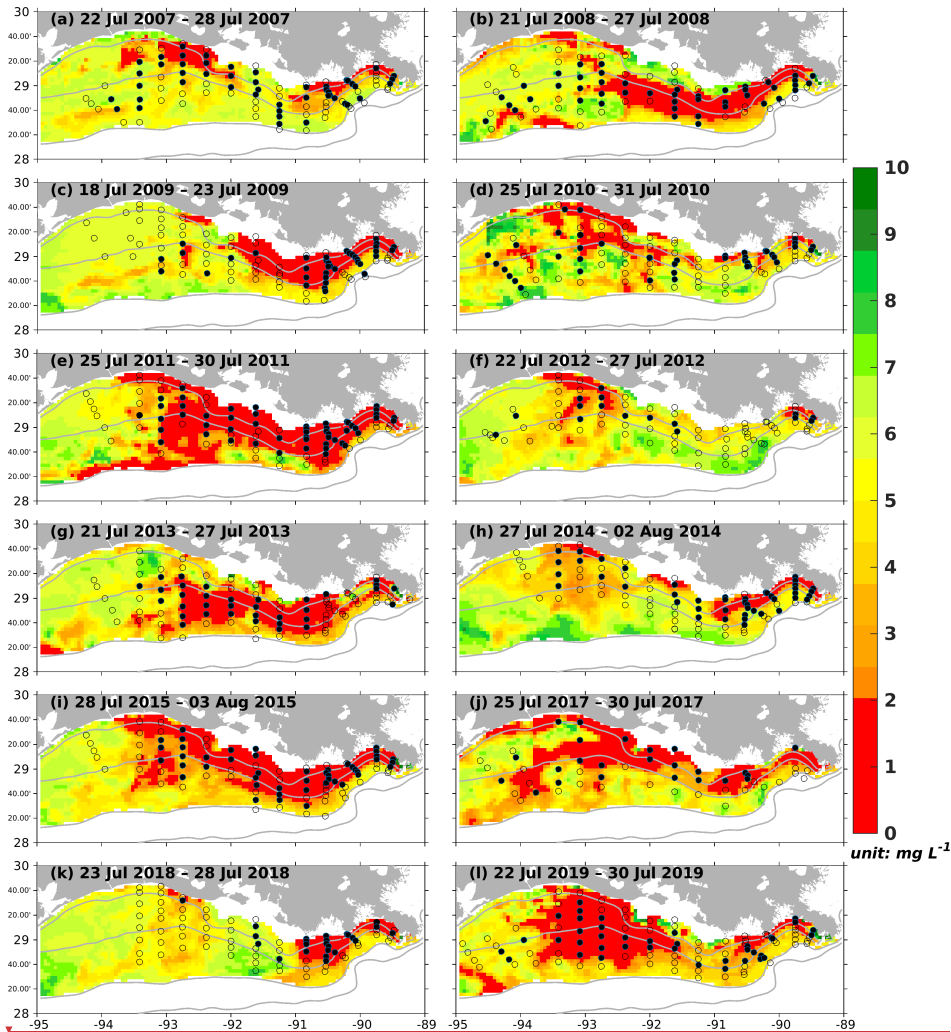
Formatted: English (US)

Formatted: English (US)

Formatted: English (US)

920 observations were unavailable over these regions. Numerical results showed a good agreement with the observations in terms
 921 of interannual variability and spatial extent of bottom hypoxic waters (Fig. 7). The spatial distribution of the hypoxic regions
 922 varied over different summers. For example, the hypoxic area was small and was primarily restricted in nearshore (<20 m)
 923 regions during the summers of 2007, 2009, 2010, 2012, 2014, and 2018. The size of the hypoxic zone, was more prominent
 924 and extended offshore in 2008, 2011, 2013, and 2019. The spatial dispersion of hypoxic waters occurred mostly over the west
 925 of the LaTex shelf, where bathymetry gradients were gentle. Over the eastern shelf, the hypoxic water was mostly constrained
 926 within a narrow belt. In the meantime, the western and eastern hypoxic water was not always merged but were separated at
 927 around 91 °W (e.g., 2007, 2010, 2012, 2014, 2017, and 2018). These results suggested that the hypoxia development on the
 928 LaTex shelf was complex and generally followed the bathymetry and distances from the major river mouths.
 929
 930 The daily time series of the size of the hypoxic zone was calculated over the LaTex shelf (6–50 m; Fig. 8). There was a good
 931 agreement between simulated hypoxia zone size and that captured by the shelf-wide cruises in terms of variability and
 932 magnitude. The overall R^2 was found as 0.47 and varied yearly (Table 2). The 5-year running R^2 increased from 0.02 for the
 933 first 5-year period (2007–2010) to 0.91 for the last 5-year period (2015–2020, excluding 2016). The poor performance before
 934 2010 could be attributed to the coarse resolution of the atmospheric forcings (~ 35 km) provided by CFSR. Since 2011, CFSRv2
 935 provided forcings with a higher resolution of 22 km. Notable underestimations were found in 2007, 2010, 2012, and 2014 with
 936 a root-mean-squared error (RMSE) of 9988 km², while minor underestimations were simulated in 2008, 2017, 2018, and 2020
 937 (RMSE=4862 km²). The model tended to slightly overestimate the measurements in other summers of interest (i.e., 2009,
 938 2011, 2013, 2015, and 2019; RMSE=2132 km²). Nevertheless, those biases were acceptable considering the relative sporadic
 939 converges of cruise data.

- Deleted: show
- Formatted ... [150]
- Deleted: Figure 6). Except for the 2013 summer, no hyp ... [151]
- Formatted ... [152]
- Deleted: varies
- Deleted: extent
- Deleted: mostly
- Formatted ... [153]
- Formatted ... [154]
- Formatted ... [155]
- Deleted: (Figures 6a–6b)
- Deleted: (Figures 6k–6i). However,
- Deleted: extent
- Deleted: much larger with a
- Formatted ... [156]
- Formatted ... [157]
- Formatted ... [158]
- Formatted ... [159]
- Deleted: outreach
- Deleted: (Figures 6c–6d) and 2017 (Figures 6i–6j) but a ... [161]
- Deleted: 2015 (Figures 6g–6h).
- Deleted: occurs
- Formatted ... [160]
- Formatted ... [162]
- Formatted ... [163]
- Formatted ... [164]
- Deleted: Shelf
- Deleted: are
- Deleted: is
- Formatted ... [165]
- Formatted ... [166]
- Formatted ... [167]
- Deleted: are
- Deleted: are
- Formatted ... [168]
- Formatted ... [169]
- Deleted: 2015
- Deleted: suggest
- Formatted ... [170]
- Formatted ... [171]
- Deleted: Shelf can be split according to
- Deleted: (Figure 8d). The above features were found in ... [173]
- Formatted ... [172]
- Formatted ... [174]
- Deleted: hypoxic area was calculated over the LaTex Sh ... [175]
- Deleted: underestimate the measurements in 2008, 2010 ... [177]
- Deleted: .
- Formatted ... [176]
- Formatted ... [178]
- Deleted: are
- Formatted ... [179]
- Formatted ... [180]
- Deleted: cruises
- Formatted ... [181]



Deleted:

Deleted: 5. Frequency distribution of hypoxia thickness obtained from NOAA's Shelfwide cruises measurements and model results during the Shelfwide

Deleted: investigation periods from 2012 to 2018 (exc... [182])

Deleted: from model results (left panels)

Deleted: Shelfwide

Deleted: right panels).

Formatted: English (US)

Formatted: English (US)

Formatted: English (US)

Formatted: English (US)

Formatted: English (US)

Formatted: English (US)

Deleted: while the solid black lines represent isolines of DO concentration of 2 mg L⁻¹

Formatted: English (US)

1015

1016 Figure 7. Modeled summer bottom DO concentration (colored patches) and NOAA's summer shelf-wide hypoxia observations (black
 1017 dots and open circles). The black dots and the open circles are indicators of observed bottom hypoxia and normoxia, respectively.
 1018 The solid grey lines indicate bathymetry of 10, 20, 50, and 100 m, respectively.

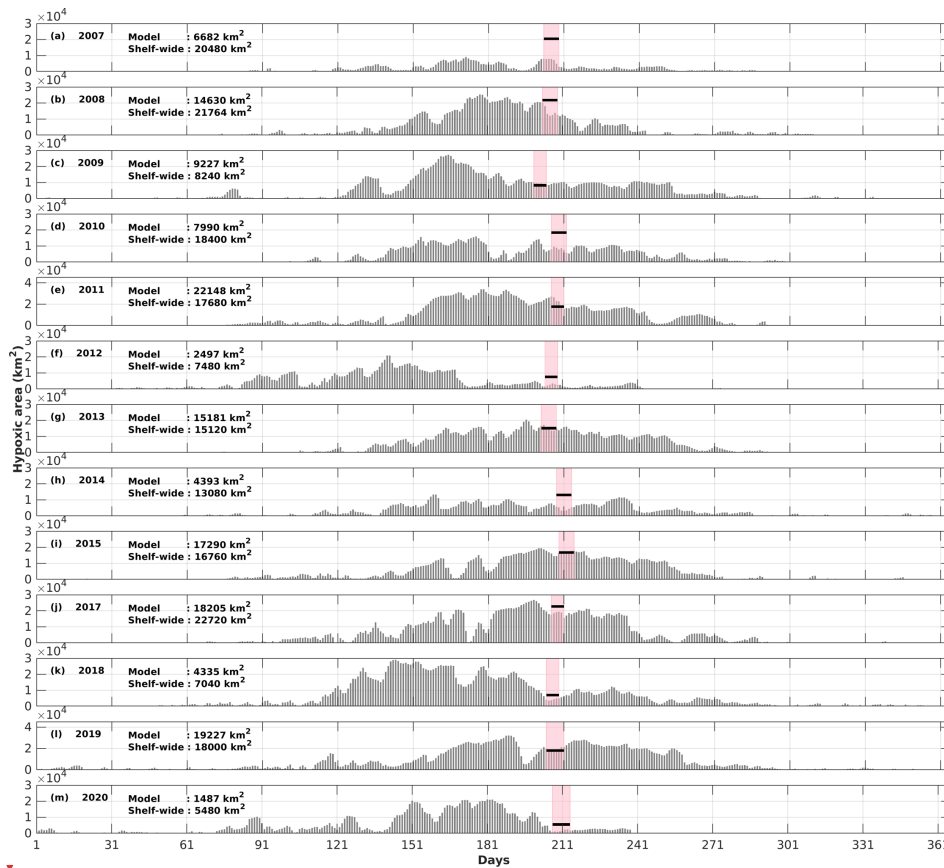
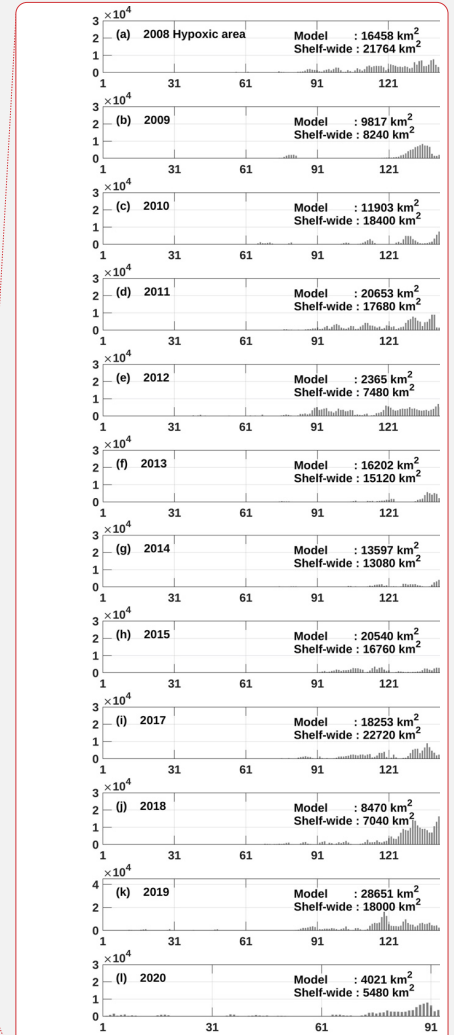


Figure 8. Comparison of the hypoxic area (in km²) between model simulations and shelf-wide cruise observations from 2007 to 2020 (except 2016). The pink patches denote the cruises periods while the solid black lines represent the measured hypoxic area.



Deleted:

Deleted: 7

Deleted: Shelfwide cruises

Deleted: 2008

Formatted: English (US)

Formatted: English (US)

Formatted: English (US)

Formatted: English (US)

1047 **Table 2. The overall (2007–2020) and 5-year running R^2 of summer hypoxic area between model simulations and shelf-wide**
 1048 **measurements. Note that the comparison in the year 2016 was excluded due to the lack of measurement.**

Year ranges	R^2	Year ranges	R^2
2007–2020 (overall)	0.47	2011–2015	0.82
2007–2011	0.02	2012–2017	0.75
2008–2012	0.39	2013–2018	0.71
2009–2013	0.41	2014–2019	0.73
2010–2014	0.44	2015–2020	0.91

1050 4 Results and discussion

1051 4.1 Factors controlling subregion bottom DO variability

1052 Fennel et al. (2016)(Fennel et al., 2016) divided the inner shelf (<50 m water depth) into six subregions (Fig. 9a) largely
 1053 following the bathymetry and distances from the major river mouths: from east to west, two west-Mississippi regions (6–20 m
 1054 nearshore and 20–50 m offshore regions, similar hereinafter), two mid-Atchafalaya regions, and two west-Atchafalaya regions.
 1055 Focusing on the bottom DO concentration balance, we calculated five hydrodynamic-related terms (i.e., the local rate of
 1056 changes in bottom DO, horizontal advection of bottom DO, horizontal diffusion of bottom DO, vertical advection of bottom
 1057 DO, and vertical diffusion of bottom DO) and two biochemical-related terms (i.e., biochemical-induced changes in DO at the
 1058 bottom water column, and SOC). The biochemistry at the bottom water column includes processes of phytoplankton
 1059 photosynthesis, phytoplankton respiration, zooplankton metabolism, aerobic decomposition of PON and DON, and
 1060 nitrification. The summation of these seven terms contributes directly to the total changes in bottom DO concentration. The
 1061 contribution of a given term was estimated by the percentage of the corresponding absolute value over the summation of all
 1062 the absolute terms. We then averaged the absolute percentages over the entire LaTex shelf (water depth 6–50 m) and over the
 1063 six subregions, respectively.

1064
 1065 Monthly climatology illustrated that the variability of bottom DO on the LaTex shelf was mostly controlled by four processes:
 1066 horizontal advection, vertical advection, vertical diffusion, and SOC (Fig. 9b). The sum of the percentages of contributions
 1067 from these four terms (absolute values) was more than 80%. The contributions of the two advection terms exhibited a salient
 1068 seasonal pattern with the maximum in spring and winter and the minimum in summer. The contribution of SOC showed an
 1069 opposite pattern and reached its peak (34%) in summer. It was interesting to note that no salient seasonal pattern was found in
 1070 the percentage of contribution from the vertical diffusion term, which maintained around 20% over a year. The vertical
 1071 diffusion of DO was determined by both vertical DO gradient and vertical stratification. The robust contribution of vertical

Formatted: English (US)

Deleted: Characteristics of

Deleted: in LaTeX Shelf

Formatted: English (US)

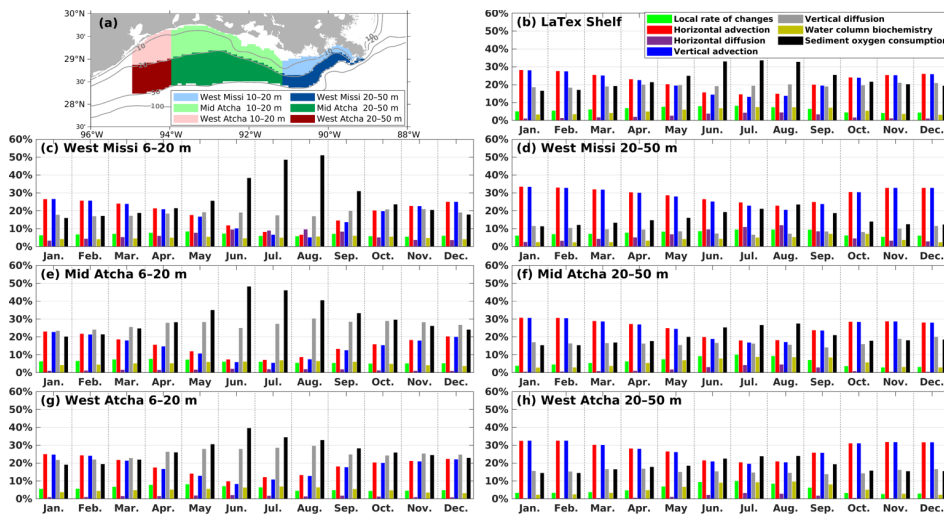
Formatted: English (US)

Deleted: The above analysis suggests that the shelf can be split according to bathymetry and distances from the major river mouths for mechanism study. Therefore, also referring to Fennel et al. (2016), the shelf within 50 m isobath was divided into six subregions for the below analysis (Figure 8d). According to the distances to the two main river systems (i.e., the Mississippi and the Atchafalaya Rivers), from east to west the LaTex Shelf was split into two west-Mississippi regions (10–20 m nearshore and 20–50 m offshore regions, similar hereinafter), two mid-Atchafalaya regions, and two west-Atchafalaya regions. Over the entire shelf, multiyear mean (2007–2020) of bottom DO concentration ranges from 3 to 7 mg L⁻¹ with a regional mean of 5.6 mg L⁻¹ (Figure 8a). A remarkable southwestward gradient manifests the impacts from river plumes and Louisiana coastal currents. Linear long-term trends (Figure 8b) and standard deviations (STDs, Figure 8c) were obtained at every computational grid based on the daily bottom DO concentration results. The bottom DO concentration exhibits an overall negative long-term trend with a maximum decrease rate of 0.15 mg L⁻¹ yr⁻¹ identified in the mid-Atchafalaya nearshore region (Figure 8b). The STDs of detrended bottom DO concentration show an uneven spatial distribution over the shelf (Figure 8c). The STDs are greater than 2 mg L⁻¹ mostly in nearshore regions. The maximum STDs were found at the west-Mississippi and mid-Atchafalaya nearshore regions where multi-year averages are the minimum among the six subregions.

Daily climatology (spatially averaged over the color shaded area in Figure 8d, same hereinafter) of bottom DO concentration and hypoxic area are negatively correlated over a year (Figure 8e). The bottom DO concentration starts to decrease dramatically at the beginning of May followed by a trough of ~3 mg L⁻¹ in July and August and a fast rebound in September. Correspondingly, the hypoxic area increases remarkably in early May followed by a peak of ~17,200 km² in July and August and a dramatic shrinkage in September. May, June, July, and August are the most affected months by hypoxic events. Monthly climatology results show different evolution patterns of bottom hypoxia in the west and east shelf (Figures 9a, 9c, 9e, and 9g). Bottom DO concentrations reach below the hypoxic threshold of 2 mg L⁻¹ in May over the mid-Atchafalaya nearshore region. Low DO area then extends offshore reaching the 20 m isobath in June. In July, mid-Atchafalaya nearshore hypoxic waters propagate south-eastward while the west-Mississippi nearshore waters start to become massively hypoxic. In August, the west hypoxic waters reach more south-eastward than in July merging with the east hypoxic waters. A longitudinally elongated hypoxia belt within the 50 m isobath is eventually

diffusion highlighted the importance of stratification on bottom DO variability throughout the year. The importance of DO advection and SOC on bottom DO balance was also documented by Ruiz Xomchuk et al. (2021), where, however, vertical diffusion was proposed as a minor contributor. Such a disagreement could result from the water layers investigated. Vertical diffusion of DO across the layer 10 m above the bottom was discussed in Ruiz Xomchuk et al. (2021), while here we estimated vertical diffusion of DO across the bottom layer.

The contributions of the four terms on the bottom DO varied in different subregions. In the nearshore regions (6–20 m; Fig. 9c, 9e, and 9g), SOC played a much more important role than the other three terms in modulating the summer bottom DO concentration. The maximum contribution from SOC was 33%–51% while the contributions of two advection terms were only ~10% or even lower. In contrast, over the offshore regions (20–50 m; Fig. 9d, 9f, and 9h), the contribution of SOC decreased notably to 19%–27% in summer and was comparable to the other three hydrodynamic-related terms (18%–26% for the horizontal advection, 17%–25% for the vertical advection, and 7%–16% for the vertical diffusion). During other months, the bottom DO was mostly modulated by the advection processes in the offshore regions. Similar to the regional mean over the entire shelf, the contribution of vertical diffusion maintained almost the same level over a year in both nearshore and offshore regions. The vertical diffusion term contributed more to the total changes in bottom DO in the nearshore regions than in the offshore regions.



138 **Figure 9. (a) Subregions defined by Fennel et al. (2016). Times series of monthly climatology (spatially averaged) of percentages of**
139 **contribution (absolute values) from different hydrodynamic-related and biochemical-related terms over (b) the entire LaTex shelf,**
140 **(c) west-Mississippi nearshore region (6–20 m), (d) west-Mississippi offshore region (20–50 m), (e) mid-Atchafalaya nearshore**
141 **region, (f) mid-Atchafalaya offshore region, (g) west-Atchafalaya nearshore region, and (h) west-Atchafalaya offshore region.**

143 4.2 Stratification and Bottom DO Advection/Diffusion

144 Sedimentary biochemical and hydrodynamics were found almost equally important in modulating the summer bottom DO in
145 the nearshore regions (33%–51% vs 28%–55%). Nevertheless, in the offshore regions, contributions from hydrodynamics
146 (51%–59%) outcompeted the impacts from SOC (19%–27%), which was consistent with the findings by Yu et al. (2015) and
147 Mattern et al. (2013). Previous studies showed that water stratification regulated the oxygen replenishment and hypoxia
148 dynamics in the LaTex shelf (Hetland and DiMarco, 2008; Bianchi et al., 2010; Fennel et al., 2011, 2013, 2016; Justić and
149 Wang, 2014; Wang and Justić, 2009; Feng et al., 2014; Yu et al., 2015; Laurent et al., 2018). Water stratification can serve as
150 an important index for the bottom DO advection and vertical diffusion processes and can be evaluated by the calculation of
151 potential energy anomaly (PEA in J m^{-3}).

$$152 PEA = \frac{1}{H} \int_{-h}^{\eta} (\rho_s - \rho) g z dz, \quad (12)$$

153 Where, ρ is water density profile over water column of depth $H = h + \eta$, h is the location of the bed, η is water surface
154 elevation, g is the gravitational acceleration (9.8 m s^{-2}), z is the vertical axis, ρ_s is the depth-integrated water density given by

$$155 \rho_s = \frac{1}{H} \int_{-h}^{\eta} \rho dz \quad (\text{Simpson and Hunter, 1974; Simpson et al., 1978; Simpson, 1981; Simpson and Bowers, 1981}).$$

156 PEA represents the amount of energy per volume required to homogenize the entire water column. A greater PEA value represents a more
157 stratified water column. We then compared the PEA with the absolute bottom DO advection and vertical diffusion of DO
158 across the bottom layer. It was worth mentioning that the absolute bottom DO advection represents the exchanges of DO at
159 the bottom layer due to advective processes, and that vertical diffusion of DO across the bottom layer was found almost positive
160 in the 15-year simulations (99.99% of simulated records). In other words, the vertical diffusion replenished DO to the bottom
161 layer most of the time on the shelf.

163 Significant negative linear correlations were found between the PEA and the two absolute advection terms of bottom DO (Fig.
164 10a and 10c; $r=-0.73$ between PEA and horizontal advection and $r=-0.76$ between PEA and vertical advection), indicating that
165 the enhanced water stratification in summer usually leads to less DO exchanges due to advection at the bottom layer. Scatter
166 plots and the simple linear regression also showed a strong linear relationship between water stratification and absolute bottom
167 DO advection. The impacts of biochemical processes on the bottom DO advection could not be neglected as biogeochemistry
168 contributed directly to the local DO changes while DO advection was determined by both mean flow and spatial gradients of
169 DO. This can also explain why the linear correlations between PEA and absolute bottom DO advection were not y close to -1.
170 In contrast to the advection terms, bottom DO flux due to vertical diffusion was found positively and moderately correlated to
171 the PEA (Fig. 10e, $r=0.46$). As the water column stability was enhanced in early summer, vertical diffusion of DO through the

Deleted: (e) Daily climatology (spatially averaged over the LaTex Shelf of 10–50 m) of hypoxic area and bottom DO concentration. The solid grey lines in (a)–(d) indicate bathymetry of 10, 20, 50, and 100 m. The solid black lines in (a), (b), and (c) represent the corresponding regionally averaged values of 5.6 mg L^{-1} , $-0.067 \text{ mg L}^{-1} \text{ yr}^{-1}$, and 1.9 mg L^{-1} , respectively

Formatted: English (US) ... [184]

Formatted: English (US)

Deleted: For a given grid point, hypoxia percentage frequencies for May, June, July, and August were given based on occurrences of hypoxic events over the total length of days of the corresponding months (e.g., 434 days for May from 2007 to 2020) (Figures 9b, 9d, 9f, and 9h). The evolution of high hypoxia frequency ($\geq 50\%$) coverage behaves similarly to the evolution of hypoxic extent. The mid-Atchafalaya nearshore region is the most frequently affected domain by hypoxia in June, while the west-Mississippi nearshore region has the most hypoxia events in August. In July, both the two regions encounter high hypoxia occurrences with averaged percentages of 56% and 63%, respectively. More hypoxia events were simulated over the west-Mississippi offshore and mid-Atchafalaya offshore regions in July and August (frequency $\geq 20\%$) than in other summer months.

The above results indicate that the evolution of bottom DO concentration in different subregions has its own characteristics. Bottom DO concentration in the west-Mississippi nearshore ... [185]

Deleted: detected in the summer months. We further cal ... [186]

Deleted: timepoints of bottom DO troughs. The bottom ... [187]

Formatted: English (US)

Formatted: English (US)

Deleted: regulates

Formatted: English (US)

Formatted: English (US)

Deleted: Shelf

Formatted: English (US) ... [188]

Deleted: Water column stratification measures the ... [189]

Deleted: was obtained for quantifying water stratification ... [190]

Formatted: English (US)

Formatted: English (US)

Formatted: English (US) ... [191]

Deleted: where

Formatted: English (US)

Formatted: English (US) ... [192]

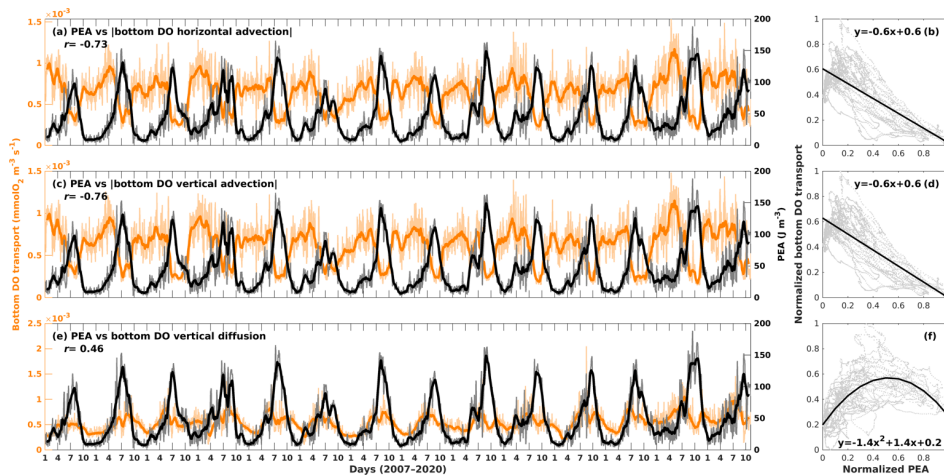
Deleted: Proposed by Simpson and Hunter (1974), PEA ... [194]

Formatted: English (US) ... [193]

Formatted: English (US) ... [195]

Deleted: In nearshore regions, PEA increases from May ... [196]

452 pycnocline would be suppressed (Bianchi et al., 2010; Rabalais and Turner, 2019), while in the lower water column, downward
 453 diffusion of DO to the bottom layer would be generally reinforced because of noticeable upward DO concentration gradients
 454 between the bottom and the above water layers. Such gradients resulted from the increasing SOC and decreasing DO exchanges
 455 by advection in early summer. However, as the strongly stratified water columns persisted, continuous DO removals due to
 456 SOC and decreasing DO supply from the upper layers drew down the DO level at both the bottom and the above layers. A
 457 lower vertical gradient of DO concentration and a weakened downward DO diffusion to the bottom layer was expected (e.g.,
 458 summer in 2011, 2015, and 2019 in Fig. 10e). The scatter plot and the quadratic regression (Fig. 10f) highlighted such non-
 459 linear responses.



462 **Figure 10. Comparison of daily time series (spatially averaged over the entire LaTex shelf, Fig. 2b) of PEA and the dominated bottom**
 463 **DO transport terms (i.e., (a) absolute horizontal advection, (c) absolute vertical advection, and (e) vertical diffusion. The symbol |**
 464 **represents the absolute operator. The light and bold lines shown represent original daily records and 31-day running smooth records,**
 465 **respectively. Linear correlations between the smooth records were also provided. Scatter plots and regression curves of the**
 466 **normalized smooth records (b) between PEA and absolute horizontal advection, (d) between PEA and absolute vertical advection,**
 467 **and (f) between PEA and vertical diffusion. The normalization method applied scales the records within a range from 0 to 1**
 468 **according to the corresponding minimums and maximums.**

470 4.3 Riverine nutrient reductions

471 Since 2001, the Mississippi River/Gulf of Mexico Hypoxia Task Force has set up a goal of controlling the size of mid-summer
 472 hypoxic zone below 5000 km² in a 5-year running average (Mississippi River/Gulf of Mexico Watershed Nutrient Task Force,

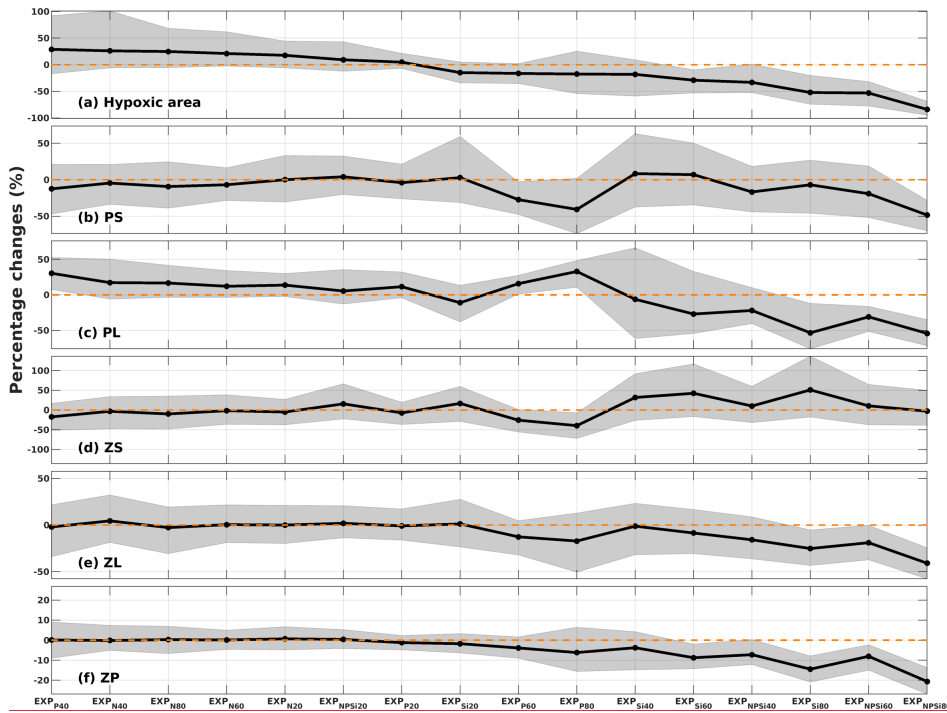
2001; 2008) by reducing riverine nutrient loads. Fennel and Laurent (2018) suggested that a reduction of $63 \pm 18\%$ (referred to as the 2000–2016 average) in total nitrogen loads or a dual reduction of $48 \pm 21\%$ in total nitrogen and phosphorus loads could be necessary to fulfill the hypoxia reduction goal. Statistic models (Scavia et al., 2013; Obenour et al., 2015; Turner et al., 2012; Laurent and Fennel, 2019) suggested a nutrient reduction of 52%–58% related to the 1980–1996 average would be enough to fulfill the goal. Nonetheless, inorganic nutrient types considered in these statistic models were nitrogen-based (i.e., ammonia and nitrite+nitrate) and phosphorus-based (i.e., phosphate) nutrients. The lower trophic community embedded in existing models was simplified with one phytoplankton functional group and one zooplankton functional group (e.g., Fennel et al., 2006, 2011, 2013; Fennel and Laurent, 2018; Justić and Wang, 2014). When applied to the LaTex shelf where diatom dominates the phytoplankton community, these models assume that the silicate supply in the shelf is excessive and the competition among different phytoplankton groups is not important to the DO variability. In this section, we aimed to explore the sensitivity of bottom DO to the riverine nutrient discharge with different combinations, the corresponding changes in plankton biomass, the complexity of the lower trophic community, and its implication for hypoxia reduction.

Table 3. Riverine inorganic nutrient reduction percentages for different sensitivity experiments. Note that all the runs listed were initialized on 1 August 2017 and were conducted from 1 August 2017 to 26 August 2020.

	Riverine inorganic nutrients reduction percentages (%)		
	N	P	Si
EXPcontrol	0	0	0
EXPN20	20	0	0
EXPN40	40	0	0
EXPN60	60	0	0
EXPN80	80	0	0
EXPP20	0	20	0
EXPP40	0	40	0
EXPP60	0	60	0
EXPP80	0	80	0
EXPSi20	0	0	20
EXPSi40	0	0	40
EXPSi60	0	0	60
EXPSi80	0	0	80
EXPNPSi20	20	20	20
EXPNPSi40	40	40	40
EXPNPSi60	60	60	60
EXPNPSi80	80	80	80

A total of 16 sensitivity experiments were set up with different combinations of the riverine inorganic nutrient concentration and river freshwater discharges remained the same as in the control run. To remove numerical bias introduced by initial conditions and to reduce computational efforts, both control run and sensitivity experiments were initialized on 1 August 2017 and were conducted from 1 August 2017 to 26 August 2020. Initial conditions were derived from the 15-year hindcast. Analysis and comparisons were conducted based on simulations from 1 January 2018 to 26 August 2020. In summer, SOC is the

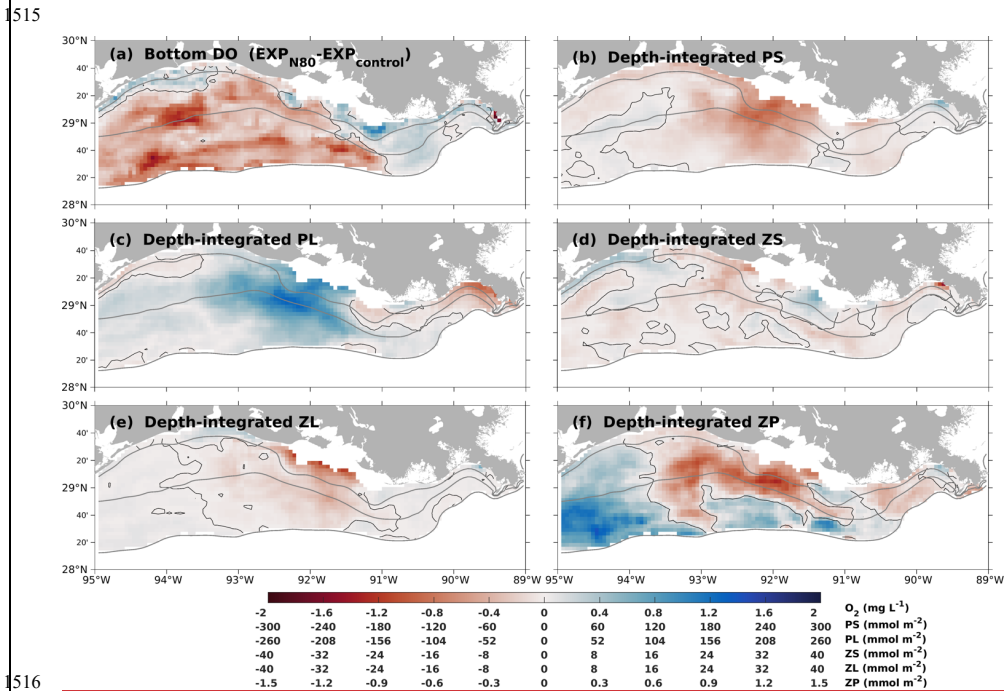
493 prevailing factor in bottom DO changes (Fig. 9) over the shelf. When the hydrodynamics remain the same, changes in the size
 494 of hypoxia water are a result of the changes in the riverine nutrient inputs. The hypoxia averaged through the 2018–2020
 495 summer shelf-wide cruises from the control run, and sensitivity experiments were shown in Fig. 11. To illustrate the complexity
 496 of the lower trophic community regarding decreased nutrient loads as well their contribution to the hypoxia development,
 497 simulated plankton (i.e., PS, PL, ZS, ZL, and ZP) concentration of the sensitivity experiments was also shown.



498 **Figure 11. Percentage differences of multi-yearly summer mean (spatially averaged over the LaTex shelf of 6–50 m) of (a) hypoxic**
 499 **area during the shelf-wide cruises, (b) PS, (c) PL, (d) ZS, (e) ZL, and (f) ZP between the 16 sensitivity runs and the control run. The**
 500 **solid black curves indicate the multi-yearly summer means, while the grey region denotes the ranges of the 10–90 percentiles. The**
 501 **dashed orange lines indicate the 0% of changes. Note that the statistics shown are sorted according to the mean percentage changes**
 502 **in the hypoxic area.**

504 As a more complex plankton community was embedded than in previous modeling studies, we found that a sole nutrient
 505 reduction in nitrogen would not guarantee decreases in the hypoxic area (Fig. 11a); on the contrary, it would generally lead to
 506 an increase in the hypoxic zone. The averaged PS concentration would decrease by ~5% due to the reduced nitrogen supply.

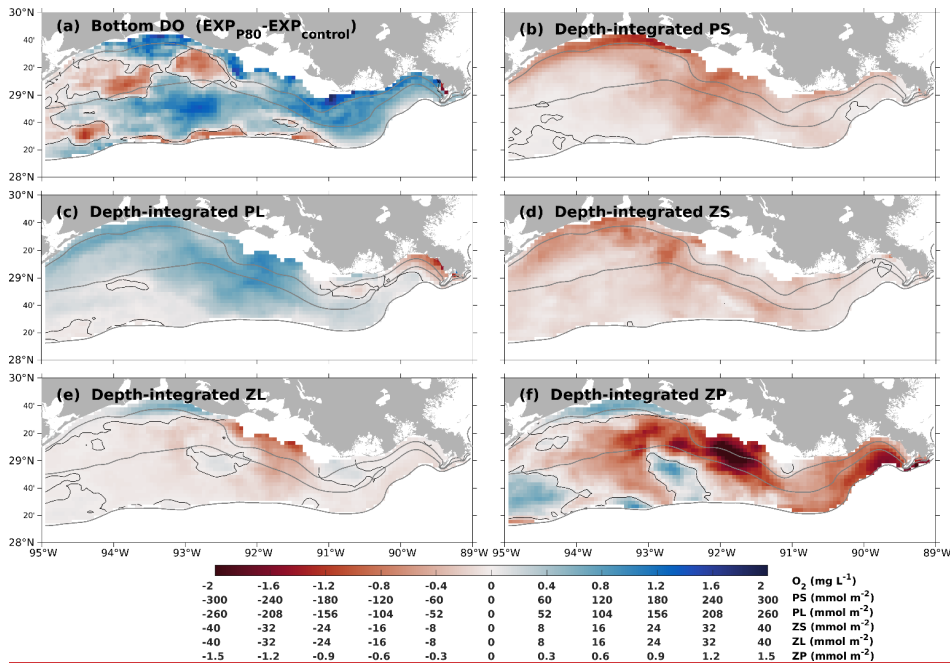
507 However, the average PL concentration would increase by ~15%. Zooplankton concentration would not change much. It could
 508 also be seen in the spatial patterns of concentration differences (e.g., EXP_{N80}, Fig. 12). The decrease (increase) in bottom DO
 509 over the west (east) shelf would be consistent with the increasing (decreasing) PL concentration. The competition between
 510 different phytoplankton groups would lead to different responses of phytoplankton concentration to the changing nutrient
 511 environments. In the meantime, the responses of the secondary production to the changing nutrient supply could be less
 512 straightforward than the primary production due to the complex energy flows associated with grazing and predation processes.
 513 Thus, it is necessary to consider the complexity of the lower-trophic community as an important proxy for the impacts of
 514 nutrient reduction strategies on shelf hypoxia.



517 **Figure 12. Multi-yearly (2018–2020) summer (period covered by mid-summer shelf-wide cruise) mean of model simulations**
 518 **differences between EXP_{N80} and EXP_{control} for (a) bottom DO concentration (mg L⁻¹) and depth-integrated concentration (mmol m⁻²)**
 519 **of different plankton groups (i.e., (b) PS, (c) PL, (d) ZS, (e) ZL, and (f) ZP).**

520 Sensitivity studies on phosphorus reduction also highlighted the importance of plankton competition in hypoxic area
 521 distribution. A sole 60% reduction of phosphorus could reduce the shelf hypoxic area by ~16% (Fig. 11). Such a change could

522 be attributed to a remarkable shrinkage of the PS community and the resulting decreases in secondary productivity (e.g., EXP_{P80};
 523 Fig. 13b, 13d–13f). This result is consistent with that in Laurent and Fennel (2014), which indicates a decrease of 13% in the
 524 hypoxic area when the riverine phosphorus supply is halved. Nevertheless, the correlation between phosphorus cut and
 525 reduction of hypoxia area was found not linear- the hypoxic zone was expected to increase with a low (EXP_{P20}) or moderate
 526 (EXP_{P40}) reduction in phosphorus, mainly owing to the competition between PS and PL (Fig 11). One should also note that
 527 the DO over the shelf would not evenly respond to the reduced phosphorus loads. The bottom DO could decrease on the west
 528 shelf (nearshore; Fig. 13a) in response to an 80% phosphorus cut because the increases in PL concentration could exceed the
 529 decreases in other plankton biomass.

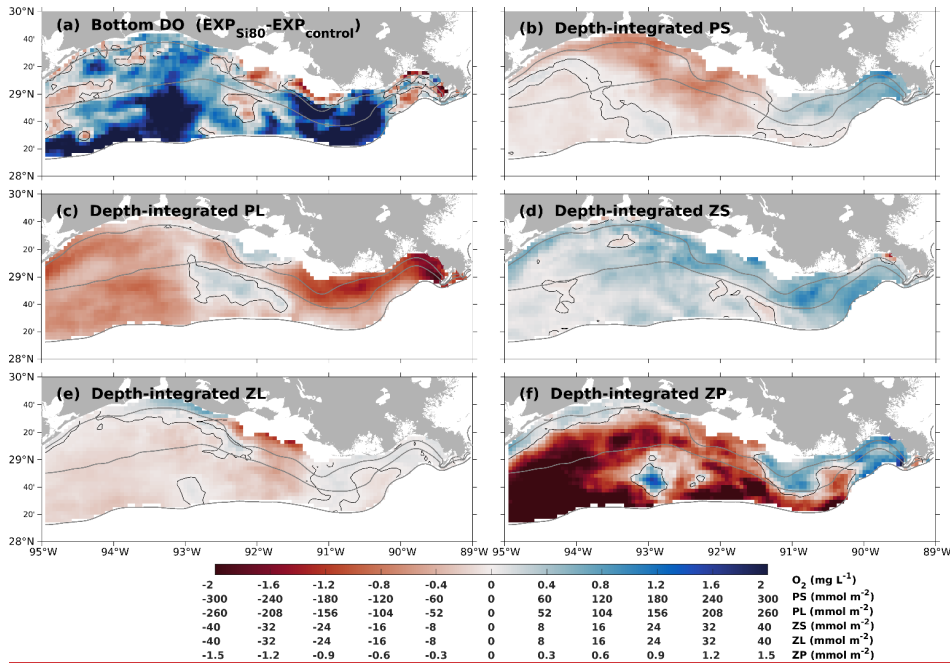


530
 531 **Figure 13. Same as Figure 12, but between EXP_{P80} and EXP_{control}.**

532
 533 The hypoxic area would exhibit an acute reduction when riverine silicon supply was limited (Fig. 11), which was attributed to
 534 the corresponding declines in PL and resulting ZL and ZP concentrations (Fig. 11 and Fig. 14). When riverine silicon supply
 535 was reduced by 80%, the hypoxic area would be expected to decrease by 50% (to 8126 km²). Compared with the control run,

536 the bottom DO of EXP_{Si80} would exhibit an overall increase corresponding to the PL (diatom) reduction. As diatom is the
 537 dominant phytoplankton group in the LaTex shelf, there is no surprise that a remarkable decrease in PL would lead to a
 538 pronounced reduction in hypoxic area and an increase in bottom DO. Nevertheless, elevated DO was not simulated all over
 539 the shelf. For example, we found DO would be decreased near the Mississippi River mouth, where PL was reduced while other
 540 plankton groups were increased.

541



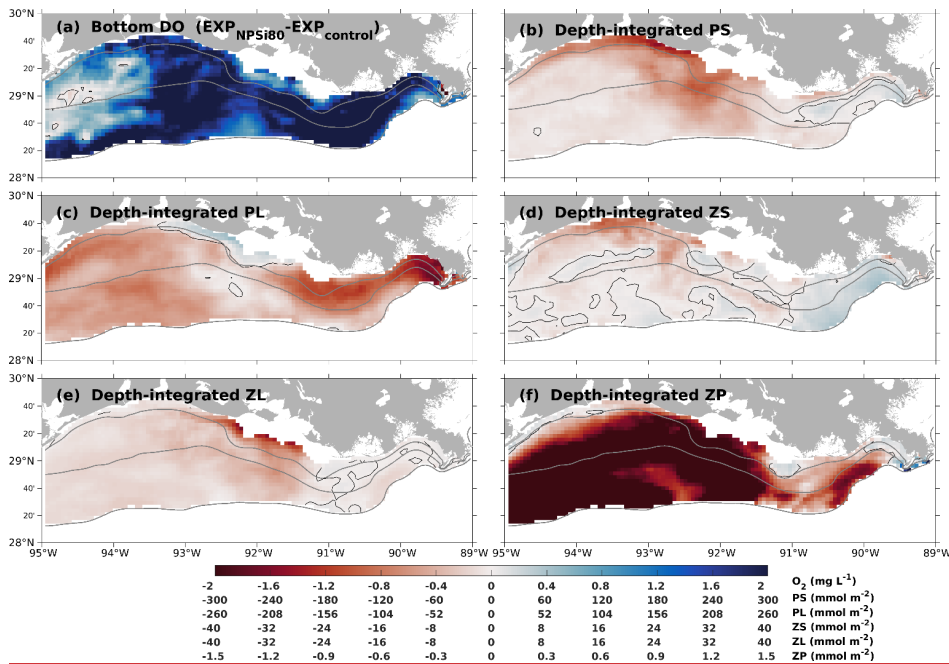
542

543 **Figure 14.** Same as Figure 12, but between EXP_{Si80} and EXP_{control}.

544

545 The PS and PL could perform differently in response to the nutrient reductions. Unlike a sole reduction of silicon, sole
 546 reductions of nitrogen or phosphorus loads tended to suppress PS growth but in contrast, lead to an increase in PL concentration
 547 due to less competition (Fig. 11–14). Such different responses in the primary production would induce different changes in the
 548 secondary productions and together would lead to uncertainties in the directions of SOC changes and thus the size of the
 549 hypoxic area. So far model simulations showed that a sole silicon reduction could be the best for reducing hypoxia. We further

550 tested the sensitivity of hypoxic area changes to triple reduction strategies. The 3-year mean hypoxic area would decrease by
 551 53% (to 8223 km²) and 84% (to 2999 km²) when all nutrient supplies were reduced simultaneously by 60% and 80%,
 552 respectively (Fig. 11). Thus, it is expected that the 3-year mean hypoxic area can reach the hypoxia goal of 5000 km² if all
 553 nutrients are reduced by nearly 80%. The spatial distribution of the differences between EXP_{NPSi80} and the control run suggested
 554 a massive and sharp increase in bottom DO over the shelf attributed to the massive decrease in both primary and secondary
 555 productions (Fig. 15). One should also note that similar to the sole reduction cases, a reduction in all three nutrient loads could
 556 also result in an increase in hypoxic area (e.g., the hypoxic area increased by 9% in EXP_{NPSi20}; Fig. 11) due to the competition
 557 among different plankton groups. Uncertainties introduced by lower-trophic community complexity are responsible for such
 558 nonlinear responses of biomass and bottom DO to nutrient reductions. To meet the hypoxia goal, the recommended percentage
 559 on nutrient loads reduction indicated by previous model studies tended to be less than the suggested percentage by our
 560 simulations (~80%). In addition, a complex plankton community enables a longer resident time or more efficient recycling of
 561 nutrients in the system than the simple models. These results shed lights on the needs of a comprehensive evaluation of DO's
 562 response regarding the proposed Hypoxia Task Force nutrient reduction plan.



563

564 Figure 15. Same as Figure 12, but between EXP_{NPS80} and EXP_{control}.

565 **5 Conclusions**

566 A three-dimensional coupled hydrodynamic-biogeochemical model (NEMURO) was modified and applied to the Gulf of
567 Mexico to study the bottom DO variability in the LaTex Shelf. In addition to nitrogen and silicon, a phosphorous flow was
568 embedded into the NEMURO model to account for the impacts of phosphorous limitation on hypoxia development. Built on
569 the SOC scheme of the instantaneous remineralization developed by Fennel et al. (2006), a pool of sedimentary PON was
570 added to account for temporal delays in SOC to the peak of plankton blooms. The model can well reproduce the vertical
571 profiles of inorganic nutrient concentration (i.e., nitrate, phosphate, and silicate), the ratio of diatom/total phytoplankton, SOC,
572 and the ratio of SOC/overlying water respiration. The model's robustness in DO simulation was affirmed via 1) comparison
573 of the DO profiles against cruise observations from three different databases, 2) comparison of spatial distributions of bottom
574 DO, and 3) time series of the hypoxic area against the shelf-wide cruises observations.

575
576 A 15-year coupled physical-biogeochemical hindcast was achieved covering the period of 2006-2020. Three DO transport
577 terms (i.e., horizontal advection, vertical advection, and vertical diffusion) and a biochemical term (i.e., SOC) were found as
578 the most influential factors modulating the bottom DO dynamics in the LaTex shelf. They jointly contributed ~80% of the
579 variability in bottom DO throughout the year. Specifically, the contribution of SOC (34%) outcompetes other factors in
580 summer. In different subregions of the shelf, the contributions of the four terms vary with depth and distance from the
581 Mississippi River mouth. In the nearshore regions, SOC plays a much more important role in modulating the summer bottom
582 DO concentration with a maximum contribution of 33%–51%; while in the offshore regions, its contribution decreases notably
583 to 19%–27% in summer, which is comparable to the contributions of the other three hydrodynamic-induced terms (18%–26%
584 for the horizontal advection, 17%–25% for the vertical advection, and 7%–16% for the vertical diffusion).

585
586 If the advection and vertical diffusion are considered jointly as a hydrodynamic term, the impacts of SOC (33%–51%) and
587 hydrodynamics (28%–55%) are almost equally important in modulating the summer bottom DO in the nearshore regions,
588 while in the offshore areas, contributions from hydrodynamics (51%–59%) outcompete the SOC impacts (19%–27%). The
589 strong linear correlations between PEA and the advection terms suggest that increased water stability in summer leads to
590 weaker DO exchanges from advection processes. Nevertheless, the relationship between PEA and vertical diffusion of DO
591 across the bottom layer appears to be non-linear. As PEA starts to increase in early summer, the bottom DO starts to drop,
592 resulting in strong vertical DO gradients at the bottom layer and enhanced vertical diffusion. As the strong water column
593 stratification persists in mid and late summer, vertical diffusion of DO tends to be suppressed due to the weaker DO gradient
594 resulting from the continuous DO consumption and the decreasing DO supply from the upper layers.

Formatted: English (US)

Deleted: ¶

Formatted: English (US)

Deleted: bottom DO variability. The NEMURO was applied and modified since the model parameterizes a more sophisticated lower-trophic ecosystem especially including a diatom functional group, which is the dominant species of the nGoM phytoplankton community. An additional

Deleted:).

Deleted: sets of cruises studies

Deleted: the frequency distribution of hypoxia thickness,

Deleted: Shelfwide

Deleted: A 15 year model hindcast was achieved covering the period of 2006-2020. Multiyear mean, long-term trends, and STDs of bottom DO concentration on the LaTex Shelf all highlight the impacts from two major river plumes (i.e., the Mississippi and the Atchafalaya Rivers) and Louisiana coastal currents. May, June, July, and August are the months most affected by hypoxic events (bottom DO concentration $\leq 2 \text{ mg L}^{-1}$). However, the developments of hypoxia are different in different subregions. Based on the monthly climatology, the mid-Atchafalaya nearshore (10–20 m) region was first detected hypoxic in May while hypoxic water was not found in the west-Mississippi nearshore region until June. The west hypoxic water expands offshore and eastward in June and July and finally merges with the east hypoxic water in August.¶

¶ The evolution of hypoxia in the LaTex Shelf (<50 m) is highly affected by SOC and water stratification (quantified by PEA). Qualitative analysis suggests that their impacts on bottom DO vary in different shelf regimes. GBM analysis provides a quantitative assessment of the relative importance of PEA and SOC on bottom DO variability in different subregions. SOC is the main regulator in nearshore (10–20 m) regions while the PEA is the prevailing factor in the offshore (20–50 m) regions. Nevertheless, the variability of bottom DO concentration is weaker in the hydrodynamic-dominated regions than in the regions with stronger impacts of sedimentary biochemical processes. The hypoxic volume is significantly related to the hypoxic area ($r=0.94, p<0.001$) which is mostly modulated by stratification and sedimentary biochemical processes. However, hypoxic volume increases nonlinearly as the area reaches beyond 20,000 km² illustrating a quadratic relationship very close to the previous relationship discovered by Scavia et al. (2019). Such results indicate that the hypoxic volume mostly resulting from the low bottom DO concentration can be possibly predicted using the hypoxic area alone.¶

.....Page Break.....

1640 We further examined the sensitivity of summer bottom DO to riverine nutrient reductions. Our sensitivity experiments
1641 highlighted the importance of the complexity of the lower-trophic community in bottom DO's response to the changing nutrient
1642 loads. Sole nutrient reductions in total nitrogen do not guarantee a hypoxic area decrease. Reduced nitrogen load can stimulate
1643 the competition between PS and PL and uncertainties to secondary productivity. Sole phosphorous reductions can, in general,
1644 reduce hypoxic area as PS and associated decreases in secondary productivity are reduced. A silicon reduction is more effective
1645 in reducing the hypoxic zone than the other two nutrients exhibited by the reductions in PL, ZS, and ZP concentration. One
1646 should also note that changes in the bottom DO are not evenly distributed over the shelf. A triple reduction strategy for all
1647 nutrients performs the best in reducing shelf hypoxic areas. When riverine nitrogen, phosphorous, and silicon loads are reduced
1648 by ~80% simultaneously, the hypoxia reduction goal of 5000 km² is likely to be achieved.

1649
1650 **Code/Data availability:** Model data is available at the LSU mass storage system and details are on the webpage of the Coupled
1651 Ocean Modeling Group at LSU (<https://faculty.lsu.edu/zxue/>). Data requests can be sent to the corresponding author via this
1652 webpage.

Formatted: English (US)

1653
1654 **Author contribution:** Z. George Xue designed the experiments and Yanda Ou carried them out. Yanda Ou developed the
1655 model code and performed the simulations. Yanda Ou and Z. George Xue prepared the manuscript.

1656
1657 **Competing interests:** The authors declare that they have no conflict of interest.

1658
1659 **Acknowledgment:** Research support was provided through the Bureau of Ocean Energy Management (M17AC00019,
1660 M20AC10001). We thank Dr. Jerome Fiechter at UC Santa Cruz for sharing his NEMURO model codes and Dr. Katja Fennel
1661 at Dalhousie University for discussing model parameterization. The computational resource was provided by the High-
1662 Performance Computing Facility (clusters SuperMIC and QueenBee3) at Louisiana State University.

Deleted: . Computational support

Formatted: English (US)

666 **Appendix A: Expressions of processes terms modified in this study**

667 Detailed descriptions of related terms and parameters are listed in Appendix B.

668 **A1 Update gross primary production of PS and PL due to the additional phosphate limitation**

669 $GppPSn = GppNPS + GppAPS,$ (A1)

670 $GppPLn = GppNPL + GppAPL,$ (A2)

671 where,

672 $GppNPS = PSn V_{maxS} \exp(K_{GppS} TMP) \left[1 - \exp\left(-\frac{\alpha_{PS}}{V_{maxS}} I_{PS}\right)\right] \exp\left(-\frac{\beta_{PS}}{V_{maxS}} I_{PS}\right) NutlimPS RnewS,$ (A3) Formatted ... [197]

673 $GppAPS = PSn V_{maxS} \exp(K_{GppS} TMP) \left[1 - \exp\left(-\frac{\alpha_{PS}}{V_{maxS}} I_{PS}\right)\right] \exp\left(-\frac{\beta_{PS}}{V_{maxS}} I_{PS}\right) NutlimPS (1 - RnewS),$ (A4) Formatted ... [198]

674 $GppNPL = PLn V_{maxL} \exp(K_{GppL} TMP) \left[1 - \exp\left(-\frac{\alpha_{PL}}{V_{maxL}} I_{PL}\right)\right] \exp\left(-\frac{\beta_{PL}}{V_{maxL}} I_{PL}\right) NutlimPL RnewL,$ (A5) Formatted ... [199]

675 $GppAPL = PLn V_{maxL} \exp(K_{GppL} TMP) \left[1 - \exp\left(-\frac{\alpha_{PL}}{V_{maxL}} I_{PL}\right)\right] \exp\left(-\frac{\beta_{PL}}{V_{maxL}} I_{PL}\right) NutlimPL (1 - RnewL),$ (A6) Formatted ... [200]

676

677 $RnewS = \frac{NO_3}{(NO_3 + K_{NO_3S}) \left(1 + \frac{NH_4}{K_{NH_4S}}\right)} \frac{1}{\frac{NO_3}{(NO_3 + K_{NO_3S}) \left(1 + \frac{NH_4}{K_{NH_4S}}\right)} + \frac{NH_4}{NH_4 + K_{NH_4S}}},$ (A7) Formatted ... [201]

678 $RnewL = \frac{NO_3}{(NO_3 + K_{NO_3L}) \left(1 + \frac{NH_4}{K_{NH_4L}}\right)} \frac{1}{\frac{NO_3}{(NO_3 + K_{NO_3L}) \left(1 + \frac{NH_4}{K_{NH_4L}}\right)} + \frac{NH_4}{NH_4 + K_{NH_4L}}},$ (A8) Formatted ... [202]

679 $NutlimPS = \min\left(\frac{NO_3}{(NO_3 + K_{NO_3S}) \left(1 + \frac{NH_4}{K_{NH_4S}}\right)} + \frac{NH_4}{NH_4 + K_{NH_4S}} \frac{PO_4}{PO_4 + K_{PO_4S}}\right),$ (A9) Formatted ... [203]

680 $NutlimPL = \min\left(\frac{NO_3}{(NO_3 + K_{NO_3L}) \left(1 + \frac{NH_4}{K_{NH_4L}}\right)} + \frac{NH_4}{NH_4 + K_{NH_4L}} \frac{PO_4}{PO_4 + K_{PO_4L}} \frac{SiOH_4}{SiOH_4 + K_{SiOH_4L}}\right),$ (A10) Formatted ... [204]

681 $I_{PS} = PAR \text{ frac} \exp\{z \text{ AttSW} + \text{AttPS} \int_0^z [PSn(\zeta) + PLn(\zeta)] d\zeta\},$ (A11) Formatted ... [205]

682 $I_{PL} = PAR \text{ frac} \exp\{z \text{ AttSW} + \text{AttPL} \int_0^z [PSn(\zeta) + PLn(\zeta)] d\zeta\},$ (A12) Formatted ... [206]

683 **A2 Update aerobic decomposition from PON to NH₄ and from DON to NH₄ due to introduction of oxygen dependency**

684 $DecP2N = PON VP2N_0 \exp(K_{P2N} TMP) r,$ (A13) Formatted ... [207]

685 $DecD2N = PON VD2N_0 \exp(K_{D2N} TMP) r,$ (A14) Formatted ... [208]

686 where,

687 $r = \max\left[\frac{\max(0, O_{xyg} - O_{xyg_{th}})}{K_{O_{xyg}} + O_{xyg} - \theta_{xyg_{th}}}, 0\right],$ (A15) Formatted ... [209]

688 **A3 Update water column nitrification due to introduction of oxygen dependency and light limitation**

689 $Nit = Nit_0 \exp(K_{Nit}, TMP) LgtlimN r_e$ (A16) Formatted [210]

690 where,

691 $LgtlimN = 1 - \max\left(0, \frac{I_N - I_0}{I_{Ncrit} - I_0}\right)$ (A17) Formatted [211]

692 $I_N = PAR \frac{frac}{exp} \left\{ z AttSW + \max(AttPS, AttPL) \int_0^z [PSn(\zeta) + PLn(\zeta)] d\zeta \right\}$ (A18) Formatted [212]

693 **A4 Additional SOC term:**

694 $SOC = 8.3865 PON_{sed} VP2N_0 \exp(K_{P2N}, TMP)$ (A19) Formatted [213]

695 **Appendix B: Descriptions of terms and parameters**

696 **Table B1. Descriptions of state variables**

Terms	Description	Unit
NH_4	Ammonium concentration	mmolN m ⁻³
NO_3	Nitrate concentration	mmolN m ⁻³
PO_4	Phosphate concentration	mmolP m ⁻³
DOP	Dissolved organic phosphorous concentration	mmolP m ⁻³
POP	Particulate organic phosphorous concentration	mmolP m ⁻³
$SiOH_4$	Silicate concentration	mmolSi m ⁻³
PSn	Small phytoplankton biomass concentration measured in nitrogen	mmolN m ⁻³
PLn	Large phytoplankton biomass concentration measured in nitrogen	mmolN m ⁻³
$Oxyg$	Dissolved oxygen concentration	mmolO ₂ m ⁻³

697 Formatted: English (US)
 698 **Table B2 Descriptions of related terms involved in the phosphorus cycle and nutrient limitation. Superscripts ^{***} and ⁺⁺ denote**
 699 **that the mathematic expressions of corresponding terms are the same as those in Kishi et al. (2007) and Shropshire et al. (2020),**
 700 **respectively. Expressions of terms with no superscript are updated and reported in Appendix A.** Deleted: Superscript
Formatted [214]

Terms	Description	Unit
$DecP2N$	Decomposition rate from PON to NH ₄	mmolN m ⁻³ day ⁻¹
$DecD2N$	Decomposition rate from DON to NH ₄	mmolN m ⁻³ day ⁻¹
$DecP2D^{++}$	Decomposition rate from PON to DON	mmolN m ⁻³ day ⁻¹
$EgeZLn^+$	Large zooplankton egestion rate measured in nitrogen	mmolN m ⁻³ day ⁻¹
$EgeZPn^{++}$	Predatory zooplankton egestion rate measured in nitrogen	mmolN m ⁻³ day ⁻¹

<i>EgeZSn</i> ⁺	Small zooplankton egestion rate measured in nitrogen	mmolN m ⁻³ day ⁻¹
<i>ExcPSn</i> ⁺	Small phytoplankton extracellular excretion rate to DON and is measured in nitrogen	mmolN m ⁻³ day ⁻¹
<i>ExcPLn</i> ⁺	Large phytoplankton extracellular excretion rate to DON and is measured in nitrogen	mmolN m ⁻³ day ⁻¹
<i>ExcZSn</i> ⁺	Small zooplankton excretion rate to NH ₄ and is measured in nitrogen	mmolN m ⁻³ day ⁻¹
<i>ExcZLn</i> ⁺	Large zooplankton excretion rate to NH ₄ and is measured in nitrogen	mmolN m ⁻³ day ⁻¹
<i>ExcZPn</i> ⁺	Predatory zooplankton excretion rate to NH ₄ and is measured in nitrogen	mmolN m ⁻³ day ⁻¹
<i>GppNPS</i>	Small phytoplankton nitrate-induced gross primary production rate measured in nitrogen	mmolN m ⁻³ day ⁻¹
<i>GppAPS</i>	Small phytoplankton ammonium-induced gross primary production rate measured in nitrogen	mmolN m ⁻³ day ⁻¹
<i>GppPSn</i>	Small phytoplankton gross primary production rate measured in nitrogen	mmolN m ⁻³ day ⁻¹
<i>GppNPL</i>	Large phytoplankton nitrate-induced gross primary production rate measured in nitrogen	mmolN m ⁻³ day ⁻¹
<i>GppAPL</i>	Large phytoplankton ammonium-induced gross primary production rate measured in nitrogen	mmolN m ⁻³ day ⁻¹
<i>GppPLn</i>	Large phytoplankton gross primary production rate measured in nitrogen	mmolN m ⁻³ day ⁻¹
<i>MorPSn</i> ⁺	Small phytoplankton mortality rate measured in nitrogen	mmolN m ⁻³ day ⁻¹
<i>MorPLn</i> ⁺	Large phytoplankton mortality rate measured in nitrogen	mmolN m ⁻³ day ⁻¹
<i>MorZSn</i> ⁺	Small zooplankton mortality rate measured in nitrogen	mmolN m ⁻³ day ⁻¹
<i>MorZLn</i> ⁺	Large zooplankton mortality rate measured in nitrogen	mmolN m ⁻³ day ⁻¹
<i>MorZPn</i> ⁺	Predatory zooplankton mortality rate measured in nitrogen	mmolN m ⁻³ day ⁻¹
<i>Nit</i>	Nitrification rate	mmolN m ⁻³ day ⁻¹
<i>ResPSn</i> ⁺	Small phytoplankton respiration rate measured in nitrogen	mmolN m ⁻³ day ⁻¹
<i>ResPLn</i> ⁺	Large phytoplankton respiration rate measured in nitrogen	mmolN m ⁻³ day ⁻¹
<i>SOC</i>	Sediment oxygen consumption rate	mmolO ₂ m ⁻² day ⁻¹

703

704

Table B3 Descriptions of other variables

Terms	Description	Unit
I_{PS}	Photosynthetically available radiation for small phytoplankton	W m ⁻²
I_{PL}	Photosynthetically available radiation for large phytoplankton	W m ⁻²
I_N	Maximum photosynthetically available radiation	W m ⁻²
$LgtlimN$	Light inhibition on nitrification rate	no dimension
$NutlimPS$	Nutrient limitation term for small phytoplankton	no dimension
$NutlimPL$	Nutrient limitation term for large phytoplankton	no dimension
PAR	Net short-wave radiation on water surface	W m ⁻²
r	Oxygen inhibition on nitrification and aerobic decomposition rates	no dimension
$RnewS$	The f-ratio of small phytoplankton which is defined by the ratio of nitrate uptake to total uptake of nitrate and ammonium	no dimension
$RnewL$	The f-ratio of large phytoplankton which is defined by the ratio of nitrate uptake to total uptake of nitrate and ammonium	no dimension
$Thickness_{bot}$	Thickness of the bottom water layer	m
TMP	Water temperature	°C
z, ζ	Vertical coordinate which is negative below sea surface	m

705
706
707
708

Table B4. Descriptions and values of all model parameters. Superscripts “S”, “L”, “F06”, and “F13” denote that the corresponding parameters follow Shropshire et al. (2020), Laurent et al. (2012), Fennel et al. (2006), and Fennel et al. (2013), respectively. Superscript “*” indicates the corresponding parameters are from this study.

Formatted: English (US)

Formatted: English (US)

Parameter	Description	Units	Values
Small phytoplankton			
V_{maxS}	Small phytoplankton maximum photosynthetic rate at 0 °C	day ⁻¹	0.4 ^S
K_{NO_3S}	Small Phytoplankton half saturation constant for nitrate	mmolN m ⁻³	0.5 ^S
K_{NH_4S}	Small Phytoplankton half saturation constant for ammonium	mmolN m ⁻³	0.1 ^S
K_{PO_4S}	Small Phytoplankton half saturation constant for phosphate	mmolP m ⁻³	0.5 ^L
α_{PS}	Small phytoplankton photochemical reaction coefficient, initial slope of P-I curve	m ² W ⁻¹ day ⁻¹	0.1 ^S

Deleted: 4

Formatted: Superscript

Deleted: 5

Deleted: 1

Deleted: 5

Deleted: 1

β_{PS}	Small phytoplankton photoinhibition coefficient	$m^2 W^{-1} day^{-1}$	0,00045 ^S	Deleted: 00045
Res_{PS0}	Small phytoplankton respiration rate at 0 °C	day^{-1}	0,03 ^S	Deleted: 03
Mor_{PS0}	Small phytoplankton mortality rate at 0 °C	$m^3 mmolN^{-1} day^{-1}$	0,002 ^S	Deleted: 002
γ_S	Ratio of extracellular excretion to photosynthesis for small phytoplankton	no dimension	0,135 ^S	Deleted: 135
K_{GPPS}	Small phytoplankton coefficient for photosynthetic rate	$^{\circ}C^{-1}$	0,0693 ^S	Deleted: 0693
K_{ResPS}	Small phytoplankton coefficient for respiration	$^{\circ}C^{-1}$	0,0519 ^S	Deleted: 0519
K_{MorPS}	Small phytoplankton coefficient for mortality	$^{\circ}C^{-1}$	0,0693 ^S	Deleted: 0693
Large phytoplankton				
V_{maxL}	Large phytoplankton photosynthetic rate at 0 °C	day^{-1}	0,8 ^S	Deleted: 8
K_{NO_3L}	Large Phytoplankton constant for nitrate	$mmolN m^{-3}$	3,0 ^S	Deleted: 0
K_{NH_4L}	Large Phytoplankton constant for ammonium	$mmolN m^{-3}$	0,3 ^S	Deleted: 3
K_{PO_4L}	Large Phytoplankton constant for phosphate	$mmolP m^{-3}$	0,5 ^L	Deleted: 5
K_{SiOH_4L}	Large Phytoplankton constant for silicate	$mmolSi m^{-3}$	6,0 ^S	Deleted: 0
α_{PL}	Large phytoplankton reaction coefficient, initial slope of P-I curve	$m^2 W^{-1} day^{-1}$	0,1 ^S	Deleted: 1
β_{PL}	Large phytoplankton photoinhibition coefficient	$m^2 W^{-1} day^{-1}$	0,00045 ^S	Deleted: 00045
Res_{PL0}	Large phytoplankton respiration rate at 0 °C	day^{-1}	0,03 ^S	Deleted: 03
Mor_{PL0}	Large phytoplankton mortality rate at 0 °C	$m^3 mmolN^{-1} day^{-1}$	0,001 ^S	Deleted: 001

γ_L	Ratio of extracellular excretion to photosynthesis for large phytoplankton	no dimension	0.135 ^S	Deleted: 135
K_{GppL}	Large phytoplankton coefficient for photosynthetic rate	temperature °C ⁻¹	0.0693 ^S	Deleted: 0693
K_{MorPL}	Large phytoplankton coefficient for mortality	temperature °C ⁻¹	0.0693 ^S	Deleted: 0693
K_{ResPL}	Large phytoplankton coefficient for respiration	temperature °C ⁻¹	0.0693 ^S	Deleted: 0693
Small zooplankton				
GR_{maxSPs}	Small zooplankton maximum grazing rate on small phytoplankton at 0 °C	day ⁻¹	0.6 ^S	Deleted: 6
λ_S	Ivlev constant of small zooplankton	m ³ mmolN ⁻¹	1.4 ^S	Deleted: 4
$PSZS$	Small zooplankton threshold value for grazing on small phytoplankton	mmolN m ⁻³	0.043 ^S	Deleted: 043
α_{ZS}	Assimilation efficiency of small zooplankton	no dimension	0.7 ^S	Deleted: 7
β_{ZS}	Growth efficiency of small zooplankton	no dimension	0.3 ^S	Deleted: 3
Mor_{ZSO}	Small zooplankton mortality rate at 0 °C	m ³ mmolN ⁻¹ day ⁻¹	0.022 ^S	Deleted: 022
K_{Gras}	Small zooplankton temperature coefficient for grazing	°C ⁻¹	0.0693 ^S	Deleted: 0693
K_{MorZS}	Small zooplankton temperature coefficient for mortality	°C ⁻¹	0.0693 ^S	Deleted: 0693
Large zooplankton				
GR_{maxLps}	Large zooplankton maximum grazing rate on small phytoplankton at 0 °C	day ⁻¹	0 ^S	Deleted: 0
GR_{maxLpl}	Large zooplankton maximum grazing rate on large phytoplankton at 0 °C	day ⁻¹	0.3 ^S	Deleted: 3
GR_{maxLzs}	Large zooplankton maximum grazing rate on small zooplankton at 0 °C	day ⁻¹	0.3 ^S	Deleted: 3
λ_L	Ivlev constant of large zooplankton	m ³ mmolN ⁻¹	1.4 ^S	Deleted: 4
$PLZL$	Large zooplankton threshold value for grazing on large phytoplankton	mmolN m ⁻³	0.040 ^S	Deleted: 040

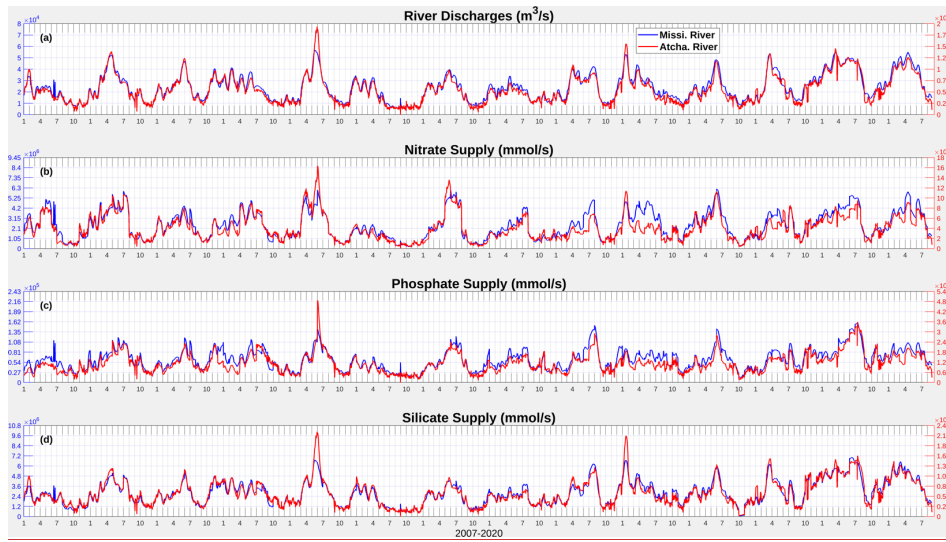
$ZS2ZL$	Large zooplankton threshold value for grazing on small zooplankton	mmolN m ⁻³	0,040 ^S	Deleted: 040
α_{ZL}	Assimilation efficiency of large zooplankton	no dimension	0,7 ^S	Deleted: 7
β_{ZL}	Growth efficiency of large zooplankton	no dimension	0,3 ^S	Deleted: 3
Mor_{ZL0}	Large zooplankton mortality rate at 0 °C	m ³ mmolN ⁻¹ day ⁻¹	0,022 ^S	Deleted: 022
K_{GraL}	Large zooplankton temperature coefficient for grazing	°C ⁻¹	0,0693 ^S	Deleted: 0693
K_{MorZL}	Large zooplankton temperature coefficient for mortality	°C ⁻¹	0,0693 ^S	Deleted: 0693
Predatory zooplankton				
GR_{maxPpl}	Predatory zooplankton maximum grazing rate on large phytoplankton at 0 °C	day ⁻¹	0,1 ^S	Deleted: 1
GR_{maxPzs}	Predatory zooplankton maximum grazing rate on small zooplankton at 0 °C	day ⁻¹	0,1 ^S	Deleted: 1
GR_{maxPzl}	Predatory zooplankton maximum grazing rate on large zooplankton at 0 °C	day ⁻¹	0,3 ^S	Deleted: 3
λ_p	Ivlev constant of predatory zooplankton	m ³ mmolN ⁻¹	1,4 ^S	Deleted: 4
$PL2ZP$	Predatory zooplankton threshold value for grazing on large phytoplankton	mmolN m ⁻³	0,040 ^S	Deleted: 040
$ZS2ZP$	Predatory zooplankton threshold value for grazing on small zooplankton	mmolN m ⁻³	0,040 ^S	Deleted: 040
$ZL2ZP$	Predatory zooplankton threshold value for grazing on large zooplankton	mmolN m ⁻³	0,040 ^S	Deleted: 040
α_{ZP}	Assimilation efficiency of predatory zooplankton	no dimension	0,7 ^S	Deleted: 7
β_{ZP}	Growth efficiency of predatory zooplankton	no dimension	0,3 ^S	Deleted: 3
Mor_{ZP0}	Predatory zooplankton mortality rate at 0 °C	m ³ mmolN ⁻¹ day ⁻¹	0,12 ^S	Deleted: 12
K_{GraP}	Predatory zooplankton temperature coefficient for grazing	°C ⁻¹	0,0693 ^S	Deleted: 0693

K_{MorZP}	Predatory zooplankton temperature coefficient for mortality	$^{\circ}\text{C}^{-1}$	0.0693 ^S	Deleted: 0693
ψ_{PL}	Grazing inhibition coefficient of predatory zooplankton grazing on large phytoplankton	$\text{m}^3 \text{mmolN}^{-1}$	4.605 ^S	Deleted: 605
ψ_{ZS}	Grazing inhibition coefficient of predatory zooplankton grazing on small zooplankton	$\text{m}^3 \text{mmolN}^{-1}$	3.01 ^S	Deleted: 01
Light				
$AttSW$	Light attenuation due to seawater	m^{-1}	0.03 ^S	Deleted: 03
$AttPS$	Light attenuation due to small phytoplankton, self-shading coefficient	$\text{m}^2 \text{mmolN}^{-1}$	0.03 ^S	Deleted: 03
$AttPL$	Light attenuation due to large phytoplankton, self-shading coefficient	$\text{m}^2 \text{mmolN}^{-1}$	0.03 ^S	Deleted: 03
$frac$	Fraction of shortwave radiation that is photosynthetically active	no dimension	0.43 ^S	Deleted: 43
I_0	Threshold of light inhibition of nitrification	W m^{-2}	0.0095 ^{F06}	Deleted: 0095
k_I	Light intensity at which light inhibition of nitrification is half-saturated	W m^{-2}	0.1 ^{F06}	Deleted: 1
Water column nitrification and aerobic decomposition				
Nit_0	Nitrification rate at 0 $^{\circ}\text{C}$	day^{-1}	0.003 ^S	Deleted: 003
$VP2N_0$	Decomposition rate at 0 $^{\circ}\text{C}$ (PON \rightarrow NH ₄)	day^{-1}	0.01 ^S	Deleted: 01
$VP2D_0$	Decomposition rate at 0 $^{\circ}\text{C}$ (PON \rightarrow DON)	day^{-1}	0.05 ^S	Deleted: 05
$VD2N_0$	Decomposition rate at 0 $^{\circ}\text{C}$ (DON \rightarrow NH ₄)	day^{-1}	0.02 ^S	Deleted: 02
$VO2S_0$	Decomposition rate at 0 $^{\circ}\text{C}$ (Opal \rightarrow Si(OH) ₄)	day^{-1}	0.01 ^S	Deleted: 01
K_{Nit}	Temperature coefficient for nitrification	$^{\circ}\text{C}^{-1}$	0.0693 ^S	Deleted: 0693
K_{P2D}	Temperature coefficient for decomposition (PON \rightarrow DON)	$^{\circ}\text{C}^{-1}$	0.0693 ^S	Deleted: 0693
K_{P2N}	Temperature coefficient for decomposition (PON \rightarrow NH ₄)	$^{\circ}\text{C}^{-1}$	0.0693 ^S	Deleted: 0693
K_{D2N}	Temperature coefficient for decomposition (DON \rightarrow NH ₄)	$^{\circ}\text{C}^{-1}$	0.0693 ^S	Deleted: 0693

K_{O_2S}	Temperature coefficient for decomposition (Opal→Si(OH) ₄)	°C ⁻¹	0.0693 ^S	Deleted: 0693
Other parameters				
$K_{O_{xyg}}$	Oxygen concentration at which inhibition of nitrification and aerobic respiration are half-saturated	mmolO ₂ m ⁻³	3.0 ^{F13}	Deleted: 0
$O_{xyg_{th}}$	Oxygen concentration threshold below which no aerobic respiration or nitrification occurs	mmolO ₂ m ⁻³	6.0 ^{F13}	Deleted: 0
R_{PO4N}	P: N ratio	mmolP mmolN ⁻¹	1/16 ^L	Deleted: 16
R_{SiN}	Si: N ratio	mmolSi mmolN ⁻¹	1 ^S	Deleted: 1
r_{OxNO_3}	Stoichiometric ratios corresponding to the oxygen produced per mol of nitrate assimilated during photosynthesis	mmolO ₂ mmolNO ₃ ⁻¹	138/16 ^{F13}	Deleted: 16
r_{OxNH_4}	Stoichiometric ratios corresponding to the oxygen produced per mol of ammonium assimilated during photosynthesis	mmolO ₂ mmolNH ₄ ⁻¹	106/16 ^{F13}	Deleted: 16
$setVPON$	Sinking velocity of PON	m day ⁻¹	-5 ^S	Deleted: 15
$setVOpal$	Sinking velocity of Opal	m day ⁻¹	-5 ^S	Deleted: 15

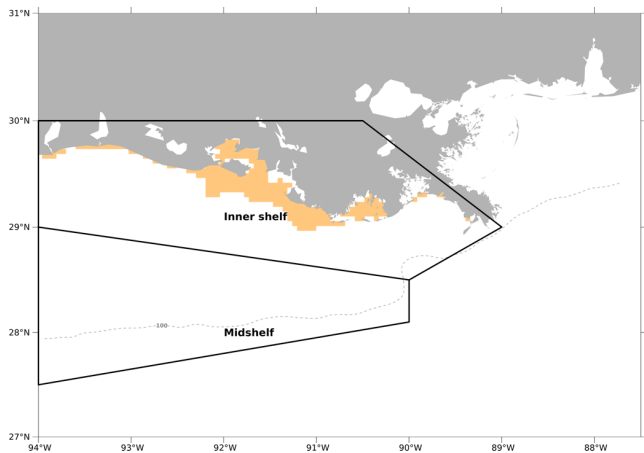
1782

792 **Appendix C: Supporting figures**



793
794 **Figure C1. Daily time series (2007–2020) of river discharges of freshwater, nitrate, phosphate, and silicate from the Mississippi and**
795 **Atchafalava rivers.**

796



1797
1798 **Figure C2.** The model computational meshes over which the regionally averaged diatom ratios were conducted for validation
1799 purposes. The orange-patched region covers roughly the study regions in Schaeffer et al. (2012), while the regions restricted by two
1800 black polygons are two regions (i.e., inner shelf and mid shelf) where samples were collected in Chakraborty and Lohrenz's (2015)
1801 study.

Formatted: English (US)

1803 References

1804 [Anglès, S., Jordi, A., Henrichs, D. W., and Campbell, L.: Influence of coastal upwelling and river discharge on the phytoplankton community
1805 composition in the northwestern Gulf of Mexico, Prog. Oceanogr., 173, 26–36, <https://doi.org/10.1016/j.pocean.2019.02.001>, 2019.](#)

Formatted: English (US)

1806 [Baronas, J. J., Hammond, D. E., Berelson, W. M., McManus, J., and Severmann, S.: Germanium-silicon fractionation in a river-influenced
1807 continental margin: The Northern Gulf of Mexico, Geochim. Cosmochim. Acta, 178, 124–142, <https://doi.org/10.1016/j.gca.2016.01.028>,
1808 2016.](#)

1809 [Bianchi, T. S., DiMarco, S. F., Cowan, J. H., Hetland, R. D., Chapman, P., Day, J. W., and Allison, M. A.: The science of hypoxia in the
1810 northern Gulf of Mexico: A review, Sci. Total Environ., 408, 1471–1484, <https://doi.org/10.1016/j.scitotenv.2009.11.047>, 2010.](#)

1811 [Bleck, R.: An oceanic general circulation model framed in hybrid isopycnic-Cartesian coordinates, Ocean Model., 4, 55–88,
1812 \[https://doi.org/10.1016/S1463-5003\\(01\\)00012-9\]\(https://doi.org/10.1016/S1463-5003\(01\)00012-9\), 2002.](#)

1813 [Bleck, R. and Boudra, D. B.: Initial testing of a numerical ocean circulation model using a hybrid \(quasi-isopycnic\) vertical coordinate, J.
1814 Phys. Oceanogr., 11, 755–770, \[https://doi.org/https://doi.org/10.1175/1520-0485\\(1981\\)011<0755:TOANO>2.0.CO;2\]\(https://doi.org/https://doi.org/10.1175/1520-0485\(1981\)011<0755:TOANO>2.0.CO;2\), 1981.](#)

1815 [Boyer, T. P., Baranova, O. K., Coleman, C., Garcia, H. E., Grodsky, A., Locarnini, R. A., Mishonov, A. V., Paver, C. R., Reagan, J. R.,
1816 Seidov, D., Smolyar, I. V., Weathers, K. W., and Zweng, M. M.: World Ocean Database 2018, Technical., edited by: Mishonov, A. V.,
1817 NOAA Atlas NESDIS 87, 2018.](#)

1818 [Chakraborty, S. and Lohrenz, S. E.: Phytoplankton community structure in the river-influenced continental margin of the northern Gulf of](#)

819 Mexico, *Mar. Ecol. Prog. Ser.*, 521, 31–47, <https://doi.org/10.3354/meps11107>, 2015.

820 Chakraborty, S., Lohrenz, S. E., and Gundersen, K.: Photophysiological and light absorption properties of phytoplankton communities in
821 the river-dominated margin of the northern Gulf of Mexico, *J. Geophys. Res. Ocean.*, 122, 4922–4938,
822 <https://doi.org/10.1002/2016JC012092>, 2017.

823 Chapman, D. C.: Numerical treatment of cross-shelf open boundaries in a barotropic coastal ocean model, [https://doi.org/10.1175/1520-0485\(1985\)015<1060:ntocso>2.0.co;2](https://doi.org/10.1175/1520-0485(1985)015<1060:ntocso>2.0.co;2), 1985.

824

825 Cummings, J. A.: Operational multivariate ocean data assimilation, *Q. J. R. Meteorol. Soc.*, 131, 3583–3604,
826 <https://doi.org/10.1256/qj.05.105>, 2005.

827 Cummings, J. A. and Smedstad, O. M.: Variational Data Assimilation for the Global Ocean, in: *Data Assimilation for Atmospheric, Oceanic and Hydrologic Applications*, vol. II, edited by: Park, S. K. and Xu, L., Springer Berlin Heidelberg, 303–343, https://doi.org/10.1007/978-3-642-35088-7_13, 2013.

828

829

830 Feng, Y., Fennel, K., Jackson, G. A., DiMarco, S. F., and Hetland, R. D.: A model study of the response of hypoxia to upwelling-favorable
831 wind on the northern Gulf of Mexico shelf, *J. Mar. Syst.*, 131, 63–73, <https://doi.org/10.1016/j.jmarsys.2013.11.009>, 2014.

832 Fennel, K. and Laurent, A.: N and P as ultimate and proximate limiting nutrients in the northern Gulf of Mexico: Implications for hypoxia
833 reduction strategies, *J. Geophys. Res. Ocean.*, 115, 3121–3131, <https://doi.org/10.5194/bg-15-3121-2018>, 2018.

834 Fennel, K. and Testa, J. M.: Biogeochemical Controls on Coastal Hypoxia, *Ann. Rev. Mar. Sci.*, 11, 105–130,
835 <https://doi.org/10.1146/annurev-marine-010318-095138>, 2019.

836 Fennel, K., Wilkin, J., Levin, J., Moisan, J., O'Reilly, J., and Haidvogel, D.: Nitrogen cycling in the Middle Atlantic Bight: Results from a
837 three-dimensional model and implications for the North Atlantic nitrogen budget, *Global Biogeochem. Cycles*, 20, 1–14,
838 <https://doi.org/10.1029/2005GB002456>, 2006.

839 Fennel, K., Hetland, R., Feng, Y., and Dimarco, S.: A coupled physical-biological model of the Northern Gulf of Mexico shelf: Model
840 description, validation and analysis of phytoplankton variability, *J. Geophys. Res. Ocean.*, 118, 1881–1899, <https://doi.org/10.5194/bg-8-1881-2011>, 2011.

841 Fennel, K., Hu, J., Laurent, A., Marta-Almeida, M., and Hetland, R.: Sensitivity of hypoxia predictions for the northern Gulf of Mexico to
842 sediment oxygen consumption and model nesting, *J. Geophys. Res. Ocean.*, 118, 990–1002, <https://doi.org/10.1002/jgrc.20077>, 2013.

843 Fennel, K., Laurent, A., Hetland, R., Justic, D., Ko, D. S., Lehrter, J., Murrell, M., Wang, L., Yu, L., and Zhang, W.: Effects of model physics
844 on hypoxia simulations for the northern Gulf of Mexico: A model intercomparison, *J. Geophys. Res. Ocean.*, 121, 5731–5750,
845 <https://doi.org/10.1002/2015JC011516>, 2016.

846 Fiechter, J. and Moore, A. M.: Interannual spring bloom variability and Ekman pumping in the coastal Gulf of Alaska, *J. Geophys. Res. Ocean.*, 114, 1–19, <https://doi.org/10.1029/2008JC005140>, 2009.

847

848 Flather, R. A.: A tidal model of the northwest European continental shelf, *Mem. la Soc. R. Sci. Liege*, 6, 141–164, 1976.

849 Fox, D. N., Teague, W. J., Barron, C. N., Carnes, M. R., and Lee, C. M.: The Modular Ocean Data Assimilation System (MODAS), *J. Atmos. Ocean. Technol.*, 19, 240–252, [https://doi.org/10.1175/1520-0426\(2002\)019<0240:TMODAS>2.0.CO;2](https://doi.org/10.1175/1520-0426(2002)019<0240:TMODAS>2.0.CO;2), 2002.

850

851 Garcia, H. E., Weathers, K., Paver, C. R., Smolyar, I., Boyer, T. P., Locarnini, R. A., Zweng, M. M., Mishonov, A. V., Baranova, O. K.,
852 Seidov, D., and Reagan, J. R.: *World Ocean Atlas 2018, Volume 3: Dissolved Oxygen, Apparent Oxygen Utilization, and Oxygen Saturation*,
853 Technical., edited by: Mishonov, A. V., NOAA Atlas NESDIS 83, 38 pp., 2018.

854 Gomez, F. A., Lee, S. K., Liu, Y., Hernandez, F. J., Muller-Karger, F. E., and Lamkin, J. T.: Seasonal patterns in phytoplankton biomass
855 across the northern and deep Gulf of Mexico: A numerical model study, *J. Geophys. Res. Ocean.*, 115, 3561–3576, <https://doi.org/10.5194/bg-15-3561-2018>, 2018.

856 Große, F., Fennel, K., and Laurent, A.: Quantifying the Relative Importance of Riverine and Open-Ocean Nitrogen Sources for Hypoxia
857 Formation in the Northern Gulf of Mexico, *J. Geophys. Res. Ocean.*, 114, 5451–5467, <https://doi.org/10.1029/2019jc015230>, 2019.

Deleted: , *J. Phys. Oceanogr.*, 15, 1060–1075,

Deleted: Conley, D. J., Paerl, H. W., Howarth, R. W., Boesch, D. F., Seitzinger, S. P., Havens, K. E., Lancelot, C., and Likens, G. E.: Controlling Eutrophication: Nitrogen and Phosphorus, *Science*, 323, 1014–1015, <https://doi.org/10.1126/science.1167755>, 2009.†

Deleted: *Biogeosciences*,

Deleted: *Biogeosciences*,

Deleted: Friedman, J. H.: Greedy function approximation: A gradient boosting machine, *Ann. Stat.*, 29, 1189–1232, <https://doi.org/10.1214/aos/1013203451>, 2001.†

Deleted: -

Deleted: *Biogeosciences*,

Deleted: 1–34

Deleted: Greenwell, B., Boehmke, B., Cunningham, J., and Developers, G.: gbm: Generalized boosted regression models, <https://github.com/gbm-developers/gbm>, 2020.†

874 Haidvogel, D. B., Arango, H. G., Hedstrom, K., Beckmann, A., Malanotte-Rizzoli, P., and Shchepetkin, A. F.: Model evaluation experiments
875 in the North Atlantic Basin: Simulations in nonlinear terrain-following coordinates, *Dyn. Atmos. Ocean.*, 32, 239–281,
876 [https://doi.org/10.1016/S0377-0265\(00\)00049-X](https://doi.org/10.1016/S0377-0265(00)00049-X), 2000.

877 Helber, R. W., Townsend, T. L., Barron, C. N., Dastugue, J. M., and Carnes, M. R.: Validation Test Report for the Improved Synthetic
878 Ocean Profile (ISOP) System, Part I: Synthetic Profile Methods and Algorithm, 2013.

879 Hetland, R. D. and DiMarco, S. F.: How does the character of oxygen demand control the structure of hypoxia on the Texas-Louisiana
880 continental shelf?, *J. Mar. Syst.*, 70, 49–62, <https://doi.org/10.1016/j.jmarsys.2007.03.002>, 2008.

881 Justić, D. and Wang, L.: Assessing temporal and spatial variability of hypoxia over the inner Louisiana-upper Texas shelf: Application of
882 an unstructured-grid three-dimensional coupled hydrodynamic-water quality model, *Cont. Shelf Res.*, 72, 163–179,
883 <https://doi.org/10.1016/j.csr.2013.08.006>, 2014.

884 [Justić, D., Rabalais, N. N., and Turner, R. E.: Simulated responses of the Gulf of Mexico hypoxia to variations in climate and anthropogenic
885 nutrient loading, *J. Mar. Syst.*, 42, 115–126, \[https://doi.org/10.1016/S0924-7963\\(03\\)00070-8\]\(https://doi.org/10.1016/S0924-7963\(03\)00070-8\), 2003.](#)

886 [Justić, D., Bierman, V. J. J., Scavia, D., and Hetland, R. D.: Forecasting Gulf's Hypoxia: The Next 50 Years?, 30, 791–801, 2007.](#)

887 Kishi, M. J., Kashiwai, M., Ware, D. M., Megrey, B. A., Eslinger, D. L., Werner, F. E., Noguchi-Aita, M., Azumaya, T., Fujii, M.,
888 Hashimoto, S., Huang, D., Iizumi, H., Ishida, Y., Kang, S., Kantakov, G. A., Kim, H. cheol, Komatsu, K., Navrotsky, V. V., Smith, S. L.,
889 Tadokoro, K., Tsuda, A., Yamamura, O., Yamanaka, Y., Yokouchi, K., Yoshie, N., Zhang, J., Zuenko, Y. I., and Zvalinsky, V. I.: NEMURO-
890 a lower trophic level model for the North Pacific marine ecosystem, *Ecol. Modell.*, 202, 12–25,
891 <https://doi.org/10.1016/j.ecolmodel.2006.08.021>, 2007.

892 Laurent, A. and Fennel, K.: Simulated reduction of hypoxia in the northern Gulf of Mexico due to phosphorus limitation, *Elem. Sci. Anthr.*,
893 2, 1–12, <https://doi.org/10.12952/journal.elementa.000022>, 2014.

894 [Laurent, A. and Fennel, K.: Time-Evolving, Spatially Explicit Forecasts of the Northern Gulf of Mexico Hypoxic Zone, *Environ. Sci.
895 Technol.*, 53, 14449–14458, <https://doi.org/10.1021/acs.est.9b05790>, 2019.](#)

896 Laurent, A., Fennel, K., Hu, J., and Hetland, R.: Simulating the effects of phosphorus limitation in the Mississippi and Atchafalaya river
897 plumes, 9, 4707–4723, <https://doi.org/10.5194/bg-9-4707-2012>, 2012.

898 Laurent, A., Fennel, K., Wilson, R., Lehrter, J., and Devereux, R.: Parameterization of biogeochemical sediment-water fluxes using in situ
899 measurements and a diagenetic model, 13, 77–94, <https://doi.org/10.5194/bg-13-77-2016>, 2016.

900 Laurent, A., Fennel, K., Ko, D. S., and Lehrter, J.: Climate change projected to exacerbate impacts of coastal Eutrophication in the Northern
901 Gulf of Mexico, *J. Geophys. Res. Ocean.*, 123, 3408–3426, <https://doi.org/10.1002/2017JC013583>, 2018.

902 Li, Q. P., Franks, P. J. S., Landry, M. R., Goericke, R., and Taylor, A. G.: Modeling phytoplankton growth rates and chlorophyll to carbon
903 ratios in California coastal and pelagic ecosystems, *J. Geophys. Res. Biogeosciences*, 115, 1–12, <https://doi.org/10.1029/2009JG001111>,
904 2010.

905 Marchesiello, P., McWilliams, J. C., and Shchepetkin, A.: Open boundary conditions for long-term integration of regional oceanic models,
906 *Ocean Model.*, 3, 1–20, [https://doi.org/10.1016/S1463-5003\(00\)00013-5](https://doi.org/10.1016/S1463-5003(00)00013-5), 2001.

907 Mattern, J. P., Fennel, K., and Dowd, M.: Sensitivity and uncertainty analysis of model hypoxia estimates for the Texas-Louisiana shelf, *J.
908 Geophys. Res. Ocean.*, 118, 1316–1332, <https://doi.org/10.1002/jgrc.20130>, 2013.

909 McCarthy, M. J., Carini, S. A., Liu, Z., Ostrom, N. E., and Gardner, W. S.: Oxygen consumption in the water column and sediments of the
910 northern Gulf of Mexico hypoxic zone, *Estuar. Coast. Shelf Sci.*, 123, 46–53, <https://doi.org/10.1016/j.ecss.2013.02.019>, 2013.

911 [Mississippi River/Gulf of Mexico Watershed Nutrient Task Force: Action Plan for Reducing, Mitigating, and Controlling Hypoxia in the
912 Northern Gulf of Mexico, Washington, DC., 2001.](#)

913 [Mississippi River/Gulf of Mexico Watershed Nutrient Task Force: Gulf Hypoxia Action Plan 2008 for Reducing, Mitigating, and Controlling](#)

Deleted: Elementa: Science of the Anthropocene,

Deleted: Biogeosciences,

Deleted: Michaelis, L. and Menten, M. L.: Die Kinetik der
invertinwirkung, *Biochem. Z.*, 49, 333–369, 1913.¶

1918 [Hypoxia in the Northern Gulf of Mexico and Improving Water Quality in the Mississippi River Basin, Washington, DC., 2008.](#)

1919 Moriarty, J. M., Harris, C. K., Friedrichs, M. A. M., Fennel, K., and Xu, K.: Impact of Seabed Resuspension on Oxygen and Nitrogen
1920 Dynamics in the Northern Gulf of Mexico: A Numerical Modeling Study, *J. Geophys. Res. Ocean.*, 123, 7237–7263,
1921 <https://doi.org/10.1029/2018JC013950>, 2018.

1922 Murrell, M. C. and Lehrter, J. C.: Sediment and Lower Water Column Oxygen Consumption in the Seasonally Hypoxic Region of the
1923 Louisiana Continental Shelf, *PLoS ONE*, 16, 1–12, <https://doi.org/10.1007/s12237-010-9351-9>, 2011.

1924 [Obenour, D. R., Michalak, A. M., and Scavia, D.: Assessing biophysical controls on Gulf of Mexico hypoxia through probabilistic modeling, Ecol. Appl., 25, 492–505, https://doi.org/10.1890/13-2257.1, 2015.](#)

1925

1926 Olson, R. J.: Differential photoinhibition of marine nitrifying bacteria: a possible mechanism for the formation of the primary nitrite
1927 maximum, *J. Mar. Res.*, 39, 227–238, 1981.

1928 Parker, R. A.: Dynamic models for ammonium inhibition of nitrate uptake by phytoplankton, *Ecol. Modell.*, 66, 113–120,
1929 [https://doi.org/10.1016/0304-3800\(93\)90042-Q](https://doi.org/10.1016/0304-3800(93)90042-Q), 1993.

1930 Platt, T., Gallegos, C. L., and Harrison, W. G.: Photoinhibition of photosynthesis in natural assemblages of marine phytoplankton, *J. Mar.*
1931 *Res.*, 38, 687–701, 1980.

1932 Rabalais, N. N. and Baustian, M. M.: Historical Shifts in Benthic Infaunal Diversity in the Northern Gulf of Mexico since the Appearance
1933 of Seasonally Severe Hypoxia, *PLoS ONE*, 15, 1–12, <https://doi.org/10.3390/d12020049>, 2020.

1934 Rabalais, N. N. and Turner, R. E.: Gulf of Mexico Hypoxia: Past, Present, and Future, *Limnol. Oceanogr. Bull.*, 28, 117–124,
1935 <https://doi.org/10.1002/lob.10351>, 2019.

1936 Rabalais, N. N., Turner, R. E., and Wiseman, W. J.: Gulf of Mexico hypoxia, a.k.a. “The dead zone,” *Annu. Rev. Ecol. Syst.*, 33, 235–263,
1937 <https://doi.org/10.1146/annurev.ecolsys.33.010802.150513>, 2002.

1938 Rabalais, N. N., Turner, R. E., Sen Gupta, B. K., Boesch, D. F., Chapman, P., and Murrell, M. C.: Hypoxia in the northern Gulf of Mexico:
1939 Does the science support the plan to reduce, mitigate, and control hypoxia?, *PLoS ONE*, 10, 1–12, <https://doi.org/10.1007/BF02841332>, 2007a.

1940 Rabalais, N. N., Turner, R. E., Gupta, B. K. S., Platon, E., and Parsons, M. L.: Sediments tell the history of eutrophication and hypoxia in
1941 the northern Gulf of Mexico, *Ecol. Appl.*, 17, 129–143, <https://doi.org/10.1890/06-0644.1>, 2007b.

1942 Rowe, G. T., Cruz Kaegi, M. E., Morse, J. W., Boland, G. S., and Escobar Briones, E. G.: Sediment community metabolism associated with
1943 continental shelf hypoxia, northern Gulf of Mexico, *PLoS ONE*, 7, 1–12, <https://doi.org/10.1007/BF02692207>, 2002.

1944 [Ruiz Xomchuk, V., Hetland, R. D., and Ou, L.: Small-Scale Variability of Bottom Oxygen in the Northern Gulf of Mexico, https://doi.org/10.1029/2020JC016279, 2021.](#)

1945

1946 Saha, S., Moorthi, S., Pan, H.-L., Wu, X., Wang, J., Nadiga, S., Tripp, P., Kistler, R., Woollen, J., Behringer, D., Liu, H., Stokes, D.,
1947 Grumbine, R., Gayno, G., Wang, J., Hou, Y.-T., Chuang, H.-Y., Juang, H.-M. H., Sela, J., Iredell, M., Treadon, R., Kleist, D., Van Delst,
1948 P., Keyser, D., Derber, J., Ek, M., Meng, J., Wei, H., Yang, R., Lord, S., van den Dool, H., Kumar, A., Wang, W., Long, C., Chelliah, M.,
1949 Xue, Y., Huang, B., Schemm, J.-K., Ebisuzaki, W., Lin, R., Xie, P., Chen, M., Zhou, S., Higgins, W., Zou, C.-Z., Liu, Q., Chen, Y., Han,
1950 Y., Cucurull, L., Reynolds, R. W., Rutledge, G., and Goldberg, M.: NCEP Climate Forecast System Reanalysis (CFSR) 6-hourly Products,
1951 January 1979 to December 2010, <https://doi.org/10.5065/D69K487J>, 2010.

1952 Saha, S., Moorthi, S., Wu, X., Wang, J., Nadiga, S., Tripp, P., Behringer, D., Hou, Y.-T., Chuang, H., Iredell, M., Ek, M., Meng, J., Yang,
1953 R., Mendez, M. P., van den Dool, H., Zhang, Q., Wang, W., Chen, M., and Becker, E.: NCEP Climate Forecast System Version 2 (CFSv2)
1954 6-hourly Products, <https://doi.org/10.5065/D61C1TXF>, 2011.

1955 Scavia, D., [Evans, M. A., and Obenour, D. R.: A scenario and forecast model for gulf of mexico hypoxic area and volume, Environ. Sci. Technol., 47, 10423–10428, https://doi.org/10.1021/es4025035, 2013.](#)

1956

1957 Schaeffer, B. A., Kurtz, J. C., and Hein, M. K.: Phytoplankton community composition in nearshore coastal waters of Louisiana, *Mar. Pollut.*

Deleted: Estuaries and Coasts,

Deleted: Diversity,

Deleted: Estuaries and Coasts,

Deleted: Estuaries,

Deleted: Justić, D.,

Deleted: .. Craig, J. K., and Wang, L.: Hypoxic volume is more responsive than...

Deleted: to nutrient load reductions in the northern Gulf of Mexico - And it matters to fish and fisheries

Deleted: Res. Lett., 14

Deleted: 1088/1748-9326/aaF938, 2019

- 1969 Bull., 64, 1705–1712, <https://doi.org/10.1016/j.marpolbul.2012.03.017>, 2012.
- 1970 Seitzinger, S. P. and Giblin, A. E.: Estimating denitrification in North Atlantic continental shelf sediments, in: Nitrogen Cycling in the North
1971 Atlantic Ocean and its Watersheds, edited by: Howarth, R. W., Springer Dordrecht, 235–260, https://doi.org/10.1007/978-94-009-1776-7_7,
1972 1996.
- 1973 Shepetchkin, A. F. and McWilliams, J. C.: The regional oceanic modeling system (ROMS): A split-explicit, free-surface, topography-
1974 following-coordinate oceanic model, *Ocean Model.*, 9, 347–404, <https://doi.org/10.1016/j.ocemod.2004.08.002>, 2005.
- 1975 Shepetchkin, A. F. and McWilliams, J. C.: Correction and commentary for “Ocean forecasting in terrain-following coordinates: Formulation
1976 and skill assessment of the regional ocean modeling system” by Haidvogel et al., *J. Comp. Phys.* 227, pp. 3595-3624, *J. Comput. Phys.*, 228,
1977 8985–9000, <https://doi.org/10.1016/j.jcp.2009.09.002>, 2009.
- 1978 Shropshire, T., Morey, S., Chassignet, E., Bozec, A., Coles, V., Landry, M., Swalethorp, R., Zapfe, G., and Stukel, M.: Quantifying
1979 spatiotemporal variability in zooplankton dynamics in the Gulf of Mexico with a physical-biogeochemical model, *J. Geophys. Res.*, 117, 3385–3407,
1980 <https://doi.org/10.5194/bg-17-3385-2020>, 2020.
- 1981 Simpson, J. H.: The shelf-sea fronts: implications of their existence and behaviour, *Philos. Trans. R. Soc. London. Ser. A, Math. Phys. Sci.*,
1982 302, 531–546, <https://doi.org/10.1098/rsta.1981.0181>, 1981.
- 1983 Simpson, J. H. and Bowers, D.: Models of stratification and frontal movement in shelf seas, *Deep Sea Res. Part A, Oceanogr. Res. Pap.*, 28,
1984 727–738, [https://doi.org/10.1016/0198-0149\(81\)90132-1](https://doi.org/10.1016/0198-0149(81)90132-1), 1981.
- 1985 Simpson, J. H. and Hunter, J. R.: Fronts in the Irish Sea, *Nature*, 250, 404–406, <https://doi.org/10.1038/250404a0>, 1974.
- 1986 Simpson, J. H., Allen, C. M., and Morris, N. C. G.: Fronts on the Continental Shelf, *J. Geophys. Res.*, 83, 4607–4614,
1987 <https://doi.org/10.1029/JC083iC09p04607>, 1978.
- 1988 ~~Sylvan, J. B., Quigg, A., Tozzi, S., and Ammerman, J. W.: Eutrophication-induced phosphorus limitation in the Mississippi River plume:
1989 Evidence from fast repetition rate fluorometry, *Limnol. Oceanogr.*, 52, 2679–2685, <https://doi.org/10.4319/lo.2007.52.6.2679>, 2007.~~
- 1990 ~~Turner, R. E., Rabalais, N. N., and Justić, D.: Predicting summer hypoxia in the northern Gulf of Mexico: Redux, *Mar. Pollut. Bull.*, 64,
1991 319–324, <https://doi.org/10.1016/j.marpolbul.2011.11.008>, 2012.~~
- 1992 Wang, L. and Justić, D.: A modeling study of the physical processes affecting the development of seasonal hypoxia over the inner Louisiana-
1993 Texas shelf: Circulation and stratification, *Cont. Shelf Res.*, 29, 1464–1476, <https://doi.org/10.1016/j.csr.2009.03.014>, 2009.
- 1994 Wanninkhof, R.: Relationship Between Wind Speed and Gas Exchange Over the Ocean, *J. Geophys. Res.*, 97, 7373–7382,
1995 <https://doi.org/10.1029/92JC00188>, 1992.
- 1996 Warner, J. C., Geyer, W. R., and Lerczak, J. A.: Numerical modeling of an estuary: A comprehensive skill assessment, *J. Geophys. Res. C*
1997 *Ocean.*, 110, 1–13, <https://doi.org/10.1029/2004JC002691>, 2005.
- 1998 Warner, J. C., Armstrong, B., He, R., and Zambon, J. B.: Development of a Coupled Ocean-Atmosphere-Wave-Sediment Transport
1999 (COAWST) Modeling System, *Ocean Model.*, 35, 230–244, <https://doi.org/10.1016/j.ocemod.2010.07.010>, 2010.
- 2000 Warner, J. C., Defne, Z., Haas, K., and Arango, H. G.: A wetting and drying scheme for ROMS, *Comput. Geosci.*, 58, 54–61,
2001 <https://doi.org/10.1016/j.cageo.2013.05.004>, 2013.
- 2002 Wawrik, B. and Paul, J. H.: Phytoplankton community structure and productivity along the axis of the Mississippi River plume in
2003 oligotrophic Gulf of Mexico waters, *Aquat. Microb. Ecol.*, 35, 185–196, <https://doi.org/10.3354/ame035185>, 2004.
- 2004 Yu, L., Fennel, K., and Laurent, A.: A modeling study of physical controls on hypoxia generation in the northern Gulf of Mexico, *J. Geophys.*
2005 *Res. Ocean.*, 120, 5019–5039, <https://doi.org/10.1002/2014JC010634>, 2015.
- 2006 Zang, Z., Xue, Z. G., Bao, S., Chen, Q., Walker, N. D., Haag, A. S., Ge, Q., and Yao, Z.: Numerical study of sediment dynamics during
2007 hurricane Gustav, *Ocean Model.*, 126, 29–42, <https://doi.org/10.1016/j.ocemod.2018.04.002>, 2018.

Deleted: Biogeosciences,

Deleted: Tao,

Deleted: Tian, H., Ren, W., Yang, J., Yang, Q., He, R., Cai, W

Deleted: Lohrenz, S.: Increasing

Deleted: river discharge throughout the 21st century influenced by changes in climate, land use, and atmospheric CO₂, *Geophys. Res. Lett.*, 41, 4978–4986

Deleted: 1002/2014GL060361, 2014

2016 Zang, Z., Xue, Z. G., Xu, K., Bentley, S. J., Chen, Q., D'Sa, E. J., and Ge, Q.: A Two Decadal (1993–2012) Numerical Assessment of
2017 Sediment Dynamics in the Northern Gulf of Mexico, *J. Geophys. Res.*, 114, 938, <https://doi.org/10.3390/w11050938>, 2019.

Deleted: Water,

2018 Zang, Z., Xue, Z. G., Xu, K., Ozdemir, C. E., Chen, Q., Bentley, S. J., and Sahin, C.: A Numerical Investigation of Wave-Supported Gravity
2019 Flow During Cold Fronts Over the Atchafalaya Shelf, *J. Geophys. Res. Ocean.*, 125, 1–24, <https://doi.org/10.1029/2019JC015269>, 2020.

Deleted: .

2020 ▲

Formatted: English (US)

Page 1: [1] Formatted Yanda Ou 9/2/22 1:28:00 PM

English (US)

Page 1: [2] Formatted Yanda Ou 9/2/22 1:28:00 PM

English (US)

Page 1: [3] Formatted Yanda Ou 9/2/22 1:28:00 PM

English (US)

Page 1: [4] Formatted Yanda Ou 9/2/22 1:28:00 PM

English (US)

Page 1: [5] Formatted Yanda Ou 9/2/22 1:28:00 PM

English (US)

Page 1: [6] Formatted Yanda Ou 9/2/22 1:28:00 PM

English (US)

Page 1: [7] Formatted Yanda Ou 9/2/22 1:28:00 PM

English (US)

Page 1: [8] Formatted Yanda Ou 9/2/22 1:28:00 PM

English (US)

Page 1: [9] Formatted Yanda Ou 9/2/22 1:28:00 PM

English (US)

Page 1: [9] Formatted Yanda Ou 9/2/22 1:28:00 PM

English (US)

Page 1: [9] Formatted Yanda Ou 9/2/22 1:28:00 PM

English (US)

Page 1: [10] Formatted Yanda Ou 9/2/22 1:28:00 PM

English (US)

Page 1: [11] Formatted Yanda Ou 9/2/22 1:28:00 PM

English (US)

Page 1: [12] Formatted Yanda Ou 9/2/22 1:28:00 PM

English (US)

Page 1: [13] Formatted Yanda Ou 9/2/22 1:28:00 PM

English (US)

Page 1: [14] Formatted Yanda Ou 9/2/22 1:28:00 PM

English (US)

▲ **Page 1: [16] Formatted** Yanda Ou 9/2/22 1:28:00 PM

English (US)

▲ **Page 1: [17] Deleted** Yanda Ou 9/2/22 1:28:00 PM

▼
▲ **Page 1: [18] Formatted** Yanda Ou 9/2/22 1:28:00 PM

English (US)

▲ **Page 1: [19] Deleted** Yanda Ou 9/2/22 1:28:00 PM

▼
▲ **Page 1: [20] Formatted** Yanda Ou 9/2/22 1:28:00 PM

English (US)

▲ **Page 1: [21] Formatted** Yanda Ou 9/2/22 1:28:00 PM

English (US)

▲ **Page 1: [22] Deleted** Yanda Ou 9/2/22 1:28:00 PM

▼
▲ **Page 1: [23] Formatted** Yanda Ou 9/2/22 1:28:00 PM

English (US)

▲ **Page 1: [24] Formatted** Yanda Ou 9/2/22 1:28:00 PM

English (US)

▲ **Page 1: [25] Formatted** Yanda Ou 9/2/22 1:28:00 PM

English (US)

▲ **Page 1: [26] Formatted** Yanda Ou 9/2/22 1:28:00 PM

English (US)

▲ **Page 1: [27] Formatted** Yanda Ou 9/2/22 1:28:00 PM

English (US)

▲ **Page 1: [28] Deleted** Yanda Ou 9/2/22 1:28:00 PM

▼
▲ **Page 1: [29] Formatted** Yanda Ou 9/2/22 1:28:00 PM

English (US)

▲ **Page 1: [30] Formatted** Yanda Ou 9/2/22 1:28:00 PM

English (US)

▲ **Page 1: [30] Formatted** Yanda Ou 9/2/22 1:28:00 PM

English (US)

English (US)

▲
Page 1: [32] Formatted **Yanda Ou** **9/2/22 1:28:00 PM**

English (US)

▲
Page 1: [32] Formatted **Yanda Ou** **9/2/22 1:28:00 PM**

English (US)

▲
Page 1: [33] Formatted **Yanda Ou** **9/2/22 1:28:00 PM**

English (US)

▲
Page 1: [33] Formatted **Yanda Ou** **9/2/22 1:28:00 PM**

English (US)

▲
Page 1: [33] Formatted **Yanda Ou** **9/2/22 1:28:00 PM**

English (US)

▲
Page 1: [33] Formatted **Yanda Ou** **9/2/22 1:28:00 PM**

English (US)

▲
Page 1: [33] Formatted **Yanda Ou** **9/2/22 1:28:00 PM**

English (US)

▲
Page 1: [34] Formatted **Yanda Ou** **9/2/22 1:28:00 PM**

English (US)

▲
Page 1: [34] Formatted **Yanda Ou** **9/2/22 1:28:00 PM**

English (US)

▲
Page 1: [34] Formatted **Yanda Ou** **9/2/22 1:28:00 PM**

English (US)

▲
Page 1: [34] Formatted **Yanda Ou** **9/2/22 1:28:00 PM**

English (US)

▲
Page 1: [34] Formatted **Yanda Ou** **9/2/22 1:28:00 PM**

English (US)

▲
Page 1: [35] Formatted **Yanda Ou** **9/2/22 1:28:00 PM**

English (US)

▲
Page 2: [36] Formatted **Yanda Ou** **9/2/22 1:28:00 PM**

English (US)

▲
Page 2: [36] Formatted **Yanda Ou** **9/2/22 1:28:00 PM**

English (US)

▲

Page 2: [38] Formatted Yanda Ou 9/2/22 1:28:00 PM

English (US)

Page 2: [38] Formatted Yanda Ou 9/2/22 1:28:00 PM

English (US)

Page 2: [38] Formatted Yanda Ou 9/2/22 1:28:00 PM

English (US)

Page 2: [38] Formatted Yanda Ou 9/2/22 1:28:00 PM

English (US)

Page 2: [39] Deleted Yanda Ou 9/2/22 1:28:00 PM

Page 2: [40] Formatted Yanda Ou 9/2/22 1:28:00 PM

English (US)

Page 2: [40] Formatted Yanda Ou 9/2/22 1:28:00 PM

English (US)

Page 2: [40] Formatted Yanda Ou 9/2/22 1:28:00 PM

English (US)

Page 2: [41] Formatted Yanda Ou 9/2/22 1:28:00 PM

English (US)

Page 2: [42] Formatted Yanda Ou 9/2/22 1:28:00 PM

English (US)

Page 2: [43] Formatted Yanda Ou 9/2/22 1:28:00 PM

English (US)

Page 2: [44] Formatted Yanda Ou 9/2/22 1:28:00 PM

English (US)

Page 2: [45] Formatted Yanda Ou 9/2/22 1:28:00 PM

English (US)

Page 2: [45] Formatted Yanda Ou 9/2/22 1:28:00 PM

English (US)

Page 2: [46] Formatted Yanda Ou 9/2/22 1:28:00 PM

English (US)

Page 2: [46] Formatted Yanda Ou 9/2/22 1:28:00 PM

English (US)

▲ **Page 2: [47] Formatted** Yanda Ou 9/2/22 1:28:00 PM

English (US)

▲ **Page 2: [47] Formatted** Yanda Ou 9/2/22 1:28:00 PM

English (US)

▲ **Page 2: [47] Formatted** Yanda Ou 9/2/22 1:28:00 PM

English (US)

▲ **Page 2: [47] Formatted** Yanda Ou 9/2/22 1:28:00 PM

English (US)

▲ **Page 2: [47] Formatted** Yanda Ou 9/2/22 1:28:00 PM

English (US)

▲ **Page 2: [47] Formatted** Yanda Ou 9/2/22 1:28:00 PM

English (US)

▲ **Page 2: [47] Formatted** Yanda Ou 9/2/22 1:28:00 PM

English (US)

▲ **Page 2: [47] Formatted** Yanda Ou 9/2/22 1:28:00 PM

English (US)

▲ **Page 2: [47] Formatted** Yanda Ou 9/2/22 1:28:00 PM

English (US)

▲ **Page 2: [47] Formatted** Yanda Ou 9/2/22 1:28:00 PM

English (US)

▲ **Page 2: [47] Formatted** Yanda Ou 9/2/22 1:28:00 PM

English (US)

▲ **Page 2: [48] Formatted** Yanda Ou 9/2/22 1:28:00 PM

English (US)

▲ **Page 2: [49] Deleted** Yanda Ou 9/2/22 1:28:00 PM

▼

▲ **Page 2: [50] Formatted** Yanda Ou 9/2/22 1:28:00 PM

English (US)

▲ **Page 2: [50] Formatted** Yanda Ou 9/2/22 1:28:00 PM

English (US)

▲ **Page 2: [50] Formatted** Yanda Ou 9/2/22 1:28:00 PM

English (US)

English (US)

▲
Page 2: [50] Formatted **Yanda Ou** **9/2/22 1:28:00 PM**

English (US)

▲
Page 2: [50] Formatted **Yanda Ou** **9/2/22 1:28:00 PM**

English (US)

▲
Page 2: [50] Formatted **Yanda Ou** **9/2/22 1:28:00 PM**

English (US)

▲
Page 2: [51] Deleted **Yanda Ou** **9/2/22 1:28:00 PM**

▼

▲
Page 2: [52] Formatted **Yanda Ou** **9/2/22 1:28:00 PM**

English (US)

▲
Page 2: [52] Formatted **Yanda Ou** **9/2/22 1:28:00 PM**

English (US)

▲
Page 2: [52] Formatted **Yanda Ou** **9/2/22 1:28:00 PM**

English (US)

▲
Page 2: [52] Formatted **Yanda Ou** **9/2/22 1:28:00 PM**

English (US)

▲
Page 2: [52] Formatted **Yanda Ou** **9/2/22 1:28:00 PM**

English (US)

▲
Page 2: [53] Formatted **Yanda Ou** **9/2/22 1:28:00 PM**

English (US)

▲
Page 2: [54] Formatted **Yanda Ou** **9/2/22 1:28:00 PM**

English (US)

▲
Page 2: [54] Formatted **Yanda Ou** **9/2/22 1:28:00 PM**

English (US)

▲
Page 2: [54] Formatted **Yanda Ou** **9/2/22 1:28:00 PM**

English (US)

▲
Page 2: [55] Formatted **Yanda Ou** **9/2/22 1:28:00 PM**

English (US)

▲
Page 2: [55] Formatted **Yanda Ou** **9/2/22 1:28:00 PM**

English (US)

▲

Page 2: [56] Formatted Yanda Ou 9/2/22 1:28:00 PM

English (US)

Page 2: [56] Formatted Yanda Ou 9/2/22 1:28:00 PM

English (US)

Page 2: [56] Formatted Yanda Ou 9/2/22 1:28:00 PM

English (US)

Page 2: [56] Formatted Yanda Ou 9/2/22 1:28:00 PM

English (US)

Page 2: [56] Formatted Yanda Ou 9/2/22 1:28:00 PM

English (US)

Page 2: [57] Formatted Yanda Ou 9/2/22 1:28:00 PM

English (US)

Page 2: [58] Formatted Yanda Ou 9/2/22 1:28:00 PM

English (US)

Page 2: [59] Formatted Yanda Ou 9/2/22 1:28:00 PM

English (US)

Page 2: [60] Formatted Yanda Ou 9/2/22 1:28:00 PM

English (US)

Page 2: [61] Formatted Yanda Ou 9/2/22 1:28:00 PM

English (US)

Page 2: [62] Deleted Yanda Ou 9/2/22 1:28:00 PM

Page 2: [63] Formatted Yanda Ou 9/2/22 1:28:00 PM

English (US)

Page 2: [63] Formatted Yanda Ou 9/2/22 1:28:00 PM

English (US)

Page 2: [63] Formatted Yanda Ou 9/2/22 1:28:00 PM

English (US)

Page 2: [63] Formatted Yanda Ou 9/2/22 1:28:00 PM

English (US)

Page 2: [63] Formatted Yanda Ou 9/2/22 1:28:00 PM

English (US)

▲
Page 2: [63] Formatted **Yanda Ou** **9/2/22 1:28:00 PM**

English (US)

▲
Page 2: [64] Formatted **Yanda Ou** **9/2/22 1:28:00 PM**

English (US)

▲
Page 2: [64] Formatted **Yanda Ou** **9/2/22 1:28:00 PM**

English (US)

▲
Page 2: [64] Formatted **Yanda Ou** **9/2/22 1:28:00 PM**

English (US)

▲
Page 2: [64] Formatted **Yanda Ou** **9/2/22 1:28:00 PM**

English (US)

▲
Page 2: [64] Formatted **Yanda Ou** **9/2/22 1:28:00 PM**

English (US)

▲
Page 2: [64] Formatted **Yanda Ou** **9/2/22 1:28:00 PM**

English (US)

▲
Page 2: [64] Formatted **Yanda Ou** **9/2/22 1:28:00 PM**

English (US)

▲
Page 2: [65] Formatted **Yanda Ou** **9/2/22 1:28:00 PM**

English (US)

▲
Page 2: [65] Formatted **Yanda Ou** **9/2/22 1:28:00 PM**

English (US)

▲
Page 2: [65] Formatted **Yanda Ou** **9/2/22 1:28:00 PM**

English (US)

▲
Page 2: [65] Formatted **Yanda Ou** **9/2/22 1:28:00 PM**

English (US)

▲
Page 2: [65] Formatted **Yanda Ou** **9/2/22 1:28:00 PM**

English (US)

▲
Page 2: [65] Formatted **Yanda Ou** **9/2/22 1:28:00 PM**

English (US)

▲
Page 2: [65] Formatted **Yanda Ou** **9/2/22 1:28:00 PM**

English (US)

▲
Page 2: [66] Formatted **Yanda Ou** **9/2/22 1:28:00 PM**

English (US)

English (US)

▲
Page 2: [66] Formatted **Yanda Ou** **9/2/22 1:28:00 PM**

English (US)

▲
Page 2: [67] Formatted **Yanda Ou** **9/2/22 1:28:00 PM**

English (US)

▲
Page 2: [67] Formatted **Yanda Ou** **9/2/22 1:28:00 PM**

English (US)

▲
Page 2: [67] Formatted **Yanda Ou** **9/2/22 1:28:00 PM**

English (US)

▲
Page 2: [68] Deleted **Yanda Ou** **9/2/22 1:28:00 PM**

▼
▲
Page 3: [69] Formatted **Yanda Ou** **9/2/22 1:28:00 PM**

English (US)

▲
Page 3: [69] Formatted **Yanda Ou** **9/2/22 1:28:00 PM**

English (US)

▲
Page 3: [69] Formatted **Yanda Ou** **9/2/22 1:28:00 PM**

English (US)

▲
Page 3: [69] Formatted **Yanda Ou** **9/2/22 1:28:00 PM**

English (US)

▲
Page 3: [69] Formatted **Yanda Ou** **9/2/22 1:28:00 PM**

English (US)

▲
Page 3: [69] Formatted **Yanda Ou** **9/2/22 1:28:00 PM**

English (US)

▲
Page 3: [69] Formatted **Yanda Ou** **9/2/22 1:28:00 PM**

English (US)

▲
Page 3: [69] Formatted **Yanda Ou** **9/2/22 1:28:00 PM**

English (US)

▲
Page 3: [69] Formatted **Yanda Ou** **9/2/22 1:28:00 PM**

English (US)

▲
Page 3: [69] Formatted **Yanda Ou** **9/2/22 1:28:00 PM**

English (US)

▲

Page 3: [70] Formatted **Yanda Ou** **9/2/22 1:28:00 PM**

English (US)

Page 3: [70] Formatted **Yanda Ou** **9/2/22 1:28:00 PM**

English (US)

Page 3: [70] Formatted **Yanda Ou** **9/2/22 1:28:00 PM**

English (US)

Page 3: [70] Formatted **Yanda Ou** **9/2/22 1:28:00 PM**

English (US)

Page 3: [70] Formatted **Yanda Ou** **9/2/22 1:28:00 PM**

English (US)

Page 3: [70] Formatted **Yanda Ou** **9/2/22 1:28:00 PM**

English (US)

Page 3: [70] Formatted **Yanda Ou** **9/2/22 1:28:00 PM**

English (US)

Page 3: [70] Formatted **Yanda Ou** **9/2/22 1:28:00 PM**

English (US)

Page 3: [70] Formatted **Yanda Ou** **9/2/22 1:28:00 PM**

English (US)

Page 3: [70] Formatted **Yanda Ou** **9/2/22 1:28:00 PM**

English (US)

Page 3: [70] Formatted **Yanda Ou** **9/2/22 1:28:00 PM**

English (US)

Page 3: [70] Formatted **Yanda Ou** **9/2/22 1:28:00 PM**

English (US)

Page 3: [70] Formatted **Yanda Ou** **9/2/22 1:28:00 PM**

English (US)

Page 3: [70] Formatted **Yanda Ou** **9/2/22 1:28:00 PM**

English (US)

Page 3: [70] Formatted **Yanda Ou** **9/2/22 1:28:00 PM**

English (US)

Page 3: [70] Formatted **Yanda Ou** **9/2/22 1:28:00 PM**

English (US)

▲
Page 3: [70] Formatted Yanda Ou 9/2/22 1:28:00 PM

English (US)

▲
Page 3: [71] Formatted Yanda Ou 9/2/22 1:28:00 PM

English (US)

▲
Page 3: [71] Formatted Yanda Ou 9/2/22 1:28:00 PM

English (US)

▲
Page 3: [72] Formatted Yanda Ou 9/2/22 1:28:00 PM

English (US)

▲
Page 3: [72] Formatted Yanda Ou 9/2/22 1:28:00 PM

English (US)

▲
Page 3: [72] Formatted Yanda Ou 9/2/22 1:28:00 PM

English (US)

▲
Page 3: [72] Formatted Yanda Ou 9/2/22 1:28:00 PM

English (US)

▲
Page 3: [72] Formatted Yanda Ou 9/2/22 1:28:00 PM

English (US)

▲
Page 3: [72] Formatted Yanda Ou 9/2/22 1:28:00 PM

English (US)

▲
Page 3: [73] Formatted Yanda Ou 9/2/22 1:28:00 PM

English (US)

▲
Page 3: [73] Formatted Yanda Ou 9/2/22 1:28:00 PM

English (US)

▲
Page 3: [74] Deleted Yanda Ou 9/2/22 1:28:00 PM

▼
▲
Page 3: [74] Deleted Yanda Ou 9/2/22 1:28:00 PM

▼
▲
Page 3: [75] Formatted Yanda Ou 9/2/22 1:28:00 PM

English (US)

▲
Page 3: [75] Formatted Yanda Ou 9/2/22 1:28:00 PM

English (US)

▲
Page 3: [75] Formatted Yanda Ou 9/2/22 1:28:00 PM

English (US)

English (US)

▲
Page 4: [77] Formatted **Yanda Ou** **9/2/22 1:28:00 PM**

English (US)

▲
Page 4: [78] Formatted **Yanda Ou** **9/2/22 1:28:00 PM**

English (US)

▲
Page 4: [79] Formatted **Yanda Ou** **9/2/22 1:28:00 PM**

English (US)

▲
Page 4: [80] Formatted **Yanda Ou** **9/2/22 1:28:00 PM**

English (US)

▲
Page 4: [80] Formatted **Yanda Ou** **9/2/22 1:28:00 PM**

English (US)

▲
Page 4: [81] Formatted **Yanda Ou** **9/2/22 1:28:00 PM**

English (US)

▲
Page 4: [81] Formatted **Yanda Ou** **9/2/22 1:28:00 PM**

English (US)

▲
Page 4: [81] Formatted **Yanda Ou** **9/2/22 1:28:00 PM**

English (US)

▲
Page 4: [81] Formatted **Yanda Ou** **9/2/22 1:28:00 PM**

English (US)

▲
Page 4: [81] Formatted **Yanda Ou** **9/2/22 1:28:00 PM**

English (US)

▲
Page 4: [81] Formatted **Yanda Ou** **9/2/22 1:28:00 PM**

English (US)

▲
Page 4: [82] Formatted **Yanda Ou** **9/2/22 1:28:00 PM**

English (US)

▲
Page 4: [82] Formatted **Yanda Ou** **9/2/22 1:28:00 PM**

English (US)

▲
Page 4: [82] Formatted **Yanda Ou** **9/2/22 1:28:00 PM**

English (US)

▲
Page 4: [82] Formatted **Yanda Ou** **9/2/22 1:28:00 PM**

English (US)

▲

Page 4: [84] Formatted Yanda Ou 9/2/22 1:28:00 PM

English (US)

Page 4: [85] Formatted Yanda Ou 9/2/22 1:28:00 PM

English (US)

Page 4: [86] Formatted Yanda Ou 9/2/22 1:28:00 PM

English (US)

Page 4: [87] Formatted Yanda Ou 9/2/22 1:28:00 PM

English (US)

Page 4: [88] Formatted Yanda Ou 9/2/22 1:28:00 PM

English (US)

Page 4: [89] Formatted Yanda Ou 9/2/22 1:28:00 PM

English (US)

Page 4: [89] Formatted Yanda Ou 9/2/22 1:28:00 PM

English (US)

Page 4: [90] Formatted Yanda Ou 9/2/22 1:28:00 PM

English (US)

Page 4: [90] Formatted Yanda Ou 9/2/22 1:28:00 PM

English (US)

Page 4: [90] Formatted Yanda Ou 9/2/22 1:28:00 PM

English (US)

Page 4: [91] Formatted Yanda Ou 9/2/22 1:28:00 PM

English (US)

Page 4: [92] Formatted Yanda Ou 9/2/22 1:28:00 PM

English (US)

Page 4: [92] Formatted Yanda Ou 9/2/22 1:28:00 PM

English (US)

Page 4: [93] Formatted Yanda Ou 9/2/22 1:28:00 PM

English (US)

Page 4: [94] Formatted Yanda Ou 9/2/22 1:28:00 PM

English (US)

Page 4: [95] Formatted Yanda Ou 9/2/22 1:28:00 PM

English (US)

▲
Page 4: [96] Formatted Yanda Ou 9/2/22 1:28:00 PM

English (US)

▲
Page 4: [97] Formatted Yanda Ou 9/2/22 1:28:00 PM

English (US)

▲
Page 5: [98] Formatted Yanda Ou 9/2/22 1:28:00 PM

English (US)

▲
Page 5: [98] Formatted Yanda Ou 9/2/22 1:28:00 PM

English (US)

▲
Page 5: [98] Formatted Yanda Ou 9/2/22 1:28:00 PM

English (US)

▲
Page 5: [98] Formatted Yanda Ou 9/2/22 1:28:00 PM

English (US)

▲
Page 5: [98] Formatted Yanda Ou 9/2/22 1:28:00 PM

English (US)

▲
Page 5: [98] Formatted Yanda Ou 9/2/22 1:28:00 PM

English (US)

▲
Page 5: [98] Formatted Yanda Ou 9/2/22 1:28:00 PM

English (US)

▲
Page 5: [98] Formatted Yanda Ou 9/2/22 1:28:00 PM

English (US)

▲
Page 5: [99] Formatted Yanda Ou 9/2/22 1:28:00 PM

English (US)

▲
Page 5: [99] Formatted Yanda Ou 9/2/22 1:28:00 PM

English (US)

▲
Page 5: [99] Formatted Yanda Ou 9/2/22 1:28:00 PM

English (US)

▲
Page 5: [99] Formatted Yanda Ou 9/2/22 1:28:00 PM

English (US)

▲
Page 5: [100] Formatted Yanda Ou 9/2/22 1:28:00 PM

English (US)

▲
Page 5: [100] Formatted Yanda Ou 9/2/22 1:28:00 PM

English (US)

English (US)

▲
Page 5: [100] Formatted Yanda Ou 9/2/22 1:28:00 PM

English (US)

▲
Page 5: [101] Formatted Yanda Ou 9/2/22 1:28:00 PM

English (US)

▲
Page 5: [101] Formatted Yanda Ou 9/2/22 1:28:00 PM

English (US)

▲
Page 5: [101] Formatted Yanda Ou 9/2/22 1:28:00 PM

English (US)

▲
Page 5: [101] Formatted Yanda Ou 9/2/22 1:28:00 PM

English (US)

▲
Page 5: [102] Formatted Yanda Ou 9/2/22 1:28:00 PM

English (US)

▲
Page 5: [102] Formatted Yanda Ou 9/2/22 1:28:00 PM

English (US)

▲
Page 5: [103] Formatted Yanda Ou 9/2/22 1:28:00 PM

English (US)

▲
Page 5: [103] Formatted Yanda Ou 9/2/22 1:28:00 PM

English (US)

▲
Page 5: [103] Formatted Yanda Ou 9/2/22 1:28:00 PM

English (US)

▲
Page 5: [103] Formatted Yanda Ou 9/2/22 1:28:00 PM

English (US)

▲
Page 5: [103] Formatted Yanda Ou 9/2/22 1:28:00 PM

English (US)

▲
Page 5: [103] Formatted Yanda Ou 9/2/22 1:28:00 PM

English (US)

▲
Page 5: [103] Formatted Yanda Ou 9/2/22 1:28:00 PM

English (US)

▲
Page 5: [104] Formatted Yanda Ou 9/2/22 1:28:00 PM

English (US)

▲

Page 5: [105] Formatted Yanda Ou 9/2/22 1:28:00 PM

English (US)

Page 5: [105] Formatted Yanda Ou 9/2/22 1:28:00 PM

English (US)

Page 5: [106] Formatted Yanda Ou 9/2/22 1:28:00 PM

English (US)

Page 5: [106] Formatted Yanda Ou 9/2/22 1:28:00 PM

English (US)

Page 5: [107] Formatted Yanda Ou 9/2/22 1:28:00 PM

English (US)

Page 5: [107] Formatted Yanda Ou 9/2/22 1:28:00 PM

English (US)

Page 5: [107] Formatted Yanda Ou 9/2/22 1:28:00 PM

English (US)

Page 5: [107] Formatted Yanda Ou 9/2/22 1:28:00 PM

English (US)

Page 5: [107] Formatted Yanda Ou 9/2/22 1:28:00 PM

English (US)

Page 5: [107] Formatted Yanda Ou 9/2/22 1:28:00 PM

English (US)

Page 5: [108] Formatted Yanda Ou 9/2/22 1:28:00 PM

English (US)

Page 5: [108] Formatted Yanda Ou 9/2/22 1:28:00 PM

English (US)

Page 5: [108] Formatted Yanda Ou 9/2/22 1:28:00 PM

English (US)

Page 5: [108] Formatted Yanda Ou 9/2/22 1:28:00 PM

English (US)

Page 5: [108] Formatted Yanda Ou 9/2/22 1:28:00 PM

English (US)

Page 5: [108] Formatted Yanda Ou 9/2/22 1:28:00 PM

English (US)

▲
Page 5: [109] Formatted Yanda Ou 9/2/22 1:28:00 PM

English (US)

▲
Page 5: [110] Formatted Yanda Ou 9/2/22 1:28:00 PM

English (US)

▲
Page 5: [110] Formatted Yanda Ou 9/2/22 1:28:00 PM

English (US)

▲
Page 5: [111] Formatted Yanda Ou 9/2/22 1:28:00 PM

English (US)

▲
Page 5: [111] Formatted Yanda Ou 9/2/22 1:28:00 PM

English (US)

▲
Page 6: [112] Formatted Yanda Ou 9/2/22 1:28:00 PM

English (US)

▲
Page 6: [112] Formatted Yanda Ou 9/2/22 1:28:00 PM

English (US)

▲
Page 6: [112] Formatted Yanda Ou 9/2/22 1:28:00 PM

English (US)

▲
Page 6: [112] Formatted Yanda Ou 9/2/22 1:28:00 PM

English (US)

▲
Page 6: [113] Formatted Yanda Ou 9/2/22 1:28:00 PM

English (US)

▲
Page 6: [113] Formatted Yanda Ou 9/2/22 1:28:00 PM

English (US)

▲
Page 6: [113] Formatted Yanda Ou 9/2/22 1:28:00 PM

English (US)

▲
Page 6: [113] Formatted Yanda Ou 9/2/22 1:28:00 PM

English (US)

▲
Page 6: [113] Formatted Yanda Ou 9/2/22 1:28:00 PM

English (US)

▲
Page 6: [113] Formatted Yanda Ou 9/2/22 1:28:00 PM

English (US)

▲
Page 6: [113] Formatted Yanda Ou 9/2/22 1:28:00 PM

English (US)

English (US)

▲
Page 6: [114] Formatted Yanda Ou 9/2/22 1:28:00 PM

English (US)

▲
Page 6: [114] Formatted Yanda Ou 9/2/22 1:28:00 PM

English (US)

▲
Page 6: [114] Formatted Yanda Ou 9/2/22 1:28:00 PM

English (US)

▲
Page 6: [114] Formatted Yanda Ou 9/2/22 1:28:00 PM

English (US)

▲
Page 6: [114] Formatted Yanda Ou 9/2/22 1:28:00 PM

English (US)

▲
Page 6: [114] Formatted Yanda Ou 9/2/22 1:28:00 PM

English (US)

▲
Page 6: [114] Formatted Yanda Ou 9/2/22 1:28:00 PM

English (US)

▲
Page 6: [114] Formatted Yanda Ou 9/2/22 1:28:00 PM

English (US)

▲
Page 6: [114] Formatted Yanda Ou 9/2/22 1:28:00 PM

English (US)

▲
Page 6: [114] Formatted Yanda Ou 9/2/22 1:28:00 PM

English (US)

▲
Page 6: [114] Formatted Yanda Ou 9/2/22 1:28:00 PM

English (US)

▲
Page 6: [115] Formatted Yanda Ou 9/2/22 1:28:00 PM

English (US)

▲
Page 6: [115] Formatted Yanda Ou 9/2/22 1:28:00 PM

English (US)

▲
Page 6: [115] Formatted Yanda Ou 9/2/22 1:28:00 PM

English (US)

▲
Page 6: [115] Formatted Yanda Ou 9/2/22 1:28:00 PM

English (US)

▲

Page 6: [115] Formatted Yanda Ou 9/2/22 1:28:00 PM

English (US)

Page 6: [115] Formatted Yanda Ou 9/2/22 1:28:00 PM

English (US)

Page 6: [115] Formatted Yanda Ou 9/2/22 1:28:00 PM

English (US)

Page 6: [116] Formatted Yanda Ou 9/2/22 1:28:00 PM

English (US)

Page 6: [116] Formatted Yanda Ou 9/2/22 1:28:00 PM

English (US)

Page 6: [116] Formatted Yanda Ou 9/2/22 1:28:00 PM

English (US)

Page 6: [116] Formatted Yanda Ou 9/2/22 1:28:00 PM

English (US)

Page 6: [116] Formatted Yanda Ou 9/2/22 1:28:00 PM

English (US)

Page 6: [116] Formatted Yanda Ou 9/2/22 1:28:00 PM

English (US)

Page 6: [116] Formatted Yanda Ou 9/2/22 1:28:00 PM

English (US)

Page 6: [116] Formatted Yanda Ou 9/2/22 1:28:00 PM

English (US)

Page 6: [116] Formatted Yanda Ou 9/2/22 1:28:00 PM

English (US)

Page 6: [117] Formatted Yanda Ou 9/2/22 1:28:00 PM

English (US)

Page 6: [117] Formatted Yanda Ou 9/2/22 1:28:00 PM

English (US)

Page 6: [117] Formatted Yanda Ou 9/2/22 1:28:00 PM

English (US)

Page 6: [117] Formatted Yanda Ou 9/2/22 1:28:00 PM

English (US)

▲
Page 6: [117] Formatted Yanda Ou 9/2/22 1:28:00 PM

English (US)

▲
Page 6: [117] Formatted Yanda Ou 9/2/22 1:28:00 PM

English (US)

▲
Page 6: [117] Formatted Yanda Ou 9/2/22 1:28:00 PM

English (US)

▲
Page 6: [117] Formatted Yanda Ou 9/2/22 1:28:00 PM

English (US)

▲
Page 6: [118] Formatted Yanda Ou 9/2/22 1:28:00 PM

English (US)

▲
Page 6: [118] Formatted Yanda Ou 9/2/22 1:28:00 PM

English (US)

▲
Page 6: [118] Formatted Yanda Ou 9/2/22 1:28:00 PM

English (US)

▲
Page 6: [119] Formatted Yanda Ou 9/2/22 1:28:00 PM

English (US)

▲
Page 6: [119] Formatted Yanda Ou 9/2/22 1:28:00 PM

English (US)

▲
Page 6: [120] Formatted Yanda Ou 9/2/22 1:28:00 PM

English (US)

▲
Page 6: [120] Formatted Yanda Ou 9/2/22 1:28:00 PM

English (US)

▲
Page 6: [120] Formatted Yanda Ou 9/2/22 1:28:00 PM

English (US)

▲
Page 6: [120] Formatted Yanda Ou 9/2/22 1:28:00 PM

English (US)

▲
Page 6: [120] Formatted Yanda Ou 9/2/22 1:28:00 PM

English (US)

▲
Page 6: [121] Formatted Yanda Ou 9/2/22 1:28:00 PM

English (US)

▲
Page 6: [121] Formatted Yanda Ou 9/2/22 1:28:00 PM

English (US)

English (US)

▲
Page 6: [122] Formatted Yanda Ou 9/2/22 1:28:00 PM

English (US)

▲
Page 6: [122] Formatted Yanda Ou 9/2/22 1:28:00 PM

English (US)

▲
Page 6: [122] Formatted Yanda Ou 9/2/22 1:28:00 PM

English (US)

▲
Page 6: [122] Formatted Yanda Ou 9/2/22 1:28:00 PM

English (US)

▲
Page 6: [123] Formatted Yanda Ou 9/2/22 1:28:00 PM

English (US)

▲
Page 6: [123] Formatted Yanda Ou 9/2/22 1:28:00 PM

English (US)

▲
Page 6: [123] Formatted Yanda Ou 9/2/22 1:28:00 PM

English (US)

▲
Page 6: [124] Formatted Yanda Ou 9/2/22 1:28:00 PM

English (US)

▲
Page 6: [124] Formatted Yanda Ou 9/2/22 1:28:00 PM

English (US)

▲
Page 6: [124] Formatted Yanda Ou 9/2/22 1:28:00 PM

English (US)

▲
Page 6: [125] Formatted Yanda Ou 9/2/22 1:28:00 PM

English (US)

▲
Page 6: [125] Formatted Yanda Ou 9/2/22 1:28:00 PM

English (US)

▲
Page 6: [125] Formatted Yanda Ou 9/2/22 1:28:00 PM

English (US)

▲
Page 6: [125] Formatted Yanda Ou 9/2/22 1:28:00 PM

English (US)

▲
Page 6: [125] Formatted Yanda Ou 9/2/22 1:28:00 PM

English (US)

▲

Page 6: [125] Formatted Yanda Ou 9/2/22 1:28:00 PM

English (US)

Page 6: [126] Formatted Yanda Ou 9/2/22 1:28:00 PM

English (US)

Page 6: [126] Formatted Yanda Ou 9/2/22 1:28:00 PM

English (US)

Page 6: [126] Formatted Yanda Ou 9/2/22 1:28:00 PM

English (US)

Page 6: [126] Formatted Yanda Ou 9/2/22 1:28:00 PM

English (US)

Page 6: [126] Formatted Yanda Ou 9/2/22 1:28:00 PM

English (US)

Page 6: [126] Formatted Yanda Ou 9/2/22 1:28:00 PM

English (US)

Page 6: [126] Formatted Yanda Ou 9/2/22 1:28:00 PM

English (US)

Page 6: [126] Formatted Yanda Ou 9/2/22 1:28:00 PM

English (US)

Page 6: [126] Formatted Yanda Ou 9/2/22 1:28:00 PM

English (US)

Page 6: [126] Formatted Yanda Ou 9/2/22 1:28:00 PM

English (US)

Page 6: [126] Formatted Yanda Ou 9/2/22 1:28:00 PM

English (US)

Page 6: [126] Formatted Yanda Ou 9/2/22 1:28:00 PM

English (US)

Page 6: [126] Formatted Yanda Ou 9/2/22 1:28:00 PM

English (US)

Page 6: [126] Formatted Yanda Ou 9/2/22 1:28:00 PM

English (US)

Page 6: [126] Formatted Yanda Ou 9/2/22 1:28:00 PM

English (US)

▲
Page 6: [127] Formatted Yanda Ou 9/2/22 1:28:00 PM

English (US)

▲
Page 6: [127] Formatted Yanda Ou 9/2/22 1:28:00 PM

English (US)

▲
Page 7: [128] Formatted Yanda Ou 9/2/22 1:28:00 PM

English (US)

▲
Page 7: [128] Formatted Yanda Ou 9/2/22 1:28:00 PM

English (US)

▲
Page 7: [128] Formatted Yanda Ou 9/2/22 1:28:00 PM

English (US)

▲
Page 7: [128] Formatted Yanda Ou 9/2/22 1:28:00 PM

English (US)

▲
Page 7: [128] Formatted Yanda Ou 9/2/22 1:28:00 PM

English (US)

▲
Page 7: [128] Formatted Yanda Ou 9/2/22 1:28:00 PM

English (US)

▲
Page 7: [128] Formatted Yanda Ou 9/2/22 1:28:00 PM

English (US)

▲
Page 7: [128] Formatted Yanda Ou 9/2/22 1:28:00 PM

English (US)

▲
Page 7: [128] Formatted Yanda Ou 9/2/22 1:28:00 PM

English (US)

▲
Page 7: [128] Formatted Yanda Ou 9/2/22 1:28:00 PM

English (US)

▲
Page 7: [128] Formatted Yanda Ou 9/2/22 1:28:00 PM

English (US)

▲
Page 7: [128] Formatted Yanda Ou 9/2/22 1:28:00 PM

English (US)

▲
Page 7: [128] Formatted Yanda Ou 9/2/22 1:28:00 PM

English (US)

▲
Page 7: [128] Formatted Yanda Ou 9/2/22 1:28:00 PM

English (US)

English (US)

▲
Page 7: [128] Formatted Yanda Ou 9/2/22 1:28:00 PM

English (US)

▲
Page 7: [128] Formatted Yanda Ou 9/2/22 1:28:00 PM

English (US)

▲
Page 7: [128] Formatted Yanda Ou 9/2/22 1:28:00 PM

English (US)

▲
Page 7: [128] Formatted Yanda Ou 9/2/22 1:28:00 PM

English (US)

▲
Page 7: [128] Formatted Yanda Ou 9/2/22 1:28:00 PM

English (US)

▲
Page 7: [128] Formatted Yanda Ou 9/2/22 1:28:00 PM

English (US)

▲
Page 7: [128] Formatted Yanda Ou 9/2/22 1:28:00 PM

English (US)

▲
Page 7: [128] Formatted Yanda Ou 9/2/22 1:28:00 PM

English (US)

▲
Page 7: [128] Formatted Yanda Ou 9/2/22 1:28:00 PM

English (US)

▲
Page 7: [128] Formatted Yanda Ou 9/2/22 1:28:00 PM

English (US)

▲
Page 7: [128] Formatted Yanda Ou 9/2/22 1:28:00 PM

English (US)

▲
Page 7: [128] Formatted Yanda Ou 9/2/22 1:28:00 PM

English (US)

▲
Page 7: [129] Formatted Yanda Ou 9/2/22 1:28:00 PM

English (US)

▲
Page 7: [129] Formatted Yanda Ou 9/2/22 1:28:00 PM

English (US)

▲
Page 7: [129] Formatted Yanda Ou 9/2/22 1:28:00 PM

English (US)

▲

Page 7: [129] Formatted Yanda Ou 9/2/22 1:28:00 PM

English (US)

Page 7: [129] Formatted Yanda Ou 9/2/22 1:28:00 PM

English (US)

Page 7: [129] Formatted Yanda Ou 9/2/22 1:28:00 PM

English (US)

Page 7: [129] Formatted Yanda Ou 9/2/22 1:28:00 PM

English (US)

Page 7: [129] Formatted Yanda Ou 9/2/22 1:28:00 PM

English (US)

Page 7: [129] Formatted Yanda Ou 9/2/22 1:28:00 PM

English (US)

Page 7: [129] Formatted Yanda Ou 9/2/22 1:28:00 PM

English (US)

Page 7: [129] Formatted Yanda Ou 9/2/22 1:28:00 PM

English (US)

Page 7: [130] Formatted Yanda Ou 9/2/22 1:28:00 PM

English (US)

Page 7: [130] Formatted Yanda Ou 9/2/22 1:28:00 PM

English (US)

Page 7: [130] Formatted Yanda Ou 9/2/22 1:28:00 PM

English (US)

Page 7: [130] Formatted Yanda Ou 9/2/22 1:28:00 PM

English (US)

Page 7: [130] Formatted Yanda Ou 9/2/22 1:28:00 PM

English (US)

Page 7: [130] Formatted Yanda Ou 9/2/22 1:28:00 PM

English (US)

Page 7: [130] Formatted Yanda Ou 9/2/22 1:28:00 PM

English (US)

Page 7: [130] Formatted Yanda Ou 9/2/22 1:28:00 PM

English (US)

▲
Page 7: [130] Formatted Yanda Ou 9/2/22 1:28:00 PM

English (US)

▲
Page 7: [130] Formatted Yanda Ou 9/2/22 1:28:00 PM

English (US)

▲
Page 7: [130] Formatted Yanda Ou 9/2/22 1:28:00 PM

English (US)

▲
Page 7: [130] Formatted Yanda Ou 9/2/22 1:28:00 PM

English (US)

▲
Page 7: [130] Formatted Yanda Ou 9/2/22 1:28:00 PM

English (US)

▲
Page 7: [130] Formatted Yanda Ou 9/2/22 1:28:00 PM

English (US)

▲
Page 7: [130] Formatted Yanda Ou 9/2/22 1:28:00 PM

English (US)

▲
Page 7: [130] Formatted Yanda Ou 9/2/22 1:28:00 PM

English (US)

▲
Page 7: [130] Formatted Yanda Ou 9/2/22 1:28:00 PM

English (US)

▲
Page 7: [130] Formatted Yanda Ou 9/2/22 1:28:00 PM

English (US)

▲
Page 7: [130] Formatted Yanda Ou 9/2/22 1:28:00 PM

English (US)

▲
Page 7: [130] Formatted Yanda Ou 9/2/22 1:28:00 PM

English (US)

▲
Page 7: [130] Formatted Yanda Ou 9/2/22 1:28:00 PM

English (US)

▲
Page 7: [130] Formatted Yanda Ou 9/2/22 1:28:00 PM

English (US)

▲
Page 7: [130] Formatted Yanda Ou 9/2/22 1:28:00 PM

English (US)

▲
Page 7: [130] Formatted Yanda Ou 9/2/22 1:28:00 PM

English (US)

English (US)

▲
Page 7: [130] Formatted Yanda Ou 9/2/22 1:28:00 PM

English (US)

▲
Page 7: [130] Formatted Yanda Ou 9/2/22 1:28:00 PM

English (US)

▲
Page 7: [130] Formatted Yanda Ou 9/2/22 1:28:00 PM

English (US)

▲
Page 7: [131] Formatted Yanda Ou 9/2/22 1:28:00 PM

English (US)

▲
Page 7: [131] Formatted Yanda Ou 9/2/22 1:28:00 PM

English (US)

▲
Page 7: [131] Formatted Yanda Ou 9/2/22 1:28:00 PM

English (US)

▲
Page 7: [131] Formatted Yanda Ou 9/2/22 1:28:00 PM

English (US)

▲
Page 7: [132] Formatted Yanda Ou 9/2/22 1:28:00 PM

English (US)

▲
Page 7: [132] Formatted Yanda Ou 9/2/22 1:28:00 PM

English (US)

▲
Page 7: [132] Formatted Yanda Ou 9/2/22 1:28:00 PM

English (US)

▲
Page 7: [132] Formatted Yanda Ou 9/2/22 1:28:00 PM

English (US)

▲
Page 7: [132] Formatted Yanda Ou 9/2/22 1:28:00 PM

English (US)

▲
Page 7: [132] Formatted Yanda Ou 9/2/22 1:28:00 PM

English (US)

▲
Page 7: [132] Formatted Yanda Ou 9/2/22 1:28:00 PM

English (US)

▲
Page 7: [132] Formatted Yanda Ou 9/2/22 1:28:00 PM

English (US)

▲

Page 7: [132] Formatted Yanda Ou 9/2/22 1:28:00 PM

English (US)

Page 7: [133] Formatted Yanda Ou 9/2/22 1:28:00 PM

English (US)

Page 7: [133] Formatted Yanda Ou 9/2/22 1:28:00 PM

English (US)

Page 7: [133] Formatted Yanda Ou 9/2/22 1:28:00 PM

English (US)

Page 7: [133] Formatted Yanda Ou 9/2/22 1:28:00 PM

English (US)

Page 7: [133] Formatted Yanda Ou 9/2/22 1:28:00 PM

English (US)

Page 7: [133] Formatted Yanda Ou 9/2/22 1:28:00 PM

English (US)

Page 7: [133] Formatted Yanda Ou 9/2/22 1:28:00 PM

English (US)

Page 7: [133] Formatted Yanda Ou 9/2/22 1:28:00 PM

English (US)

Page 7: [133] Formatted Yanda Ou 9/2/22 1:28:00 PM

English (US)

Page 7: [133] Formatted Yanda Ou 9/2/22 1:28:00 PM

English (US)

Page 7: [134] Formatted Yanda Ou 9/2/22 1:28:00 PM

English (US)

Page 7: [134] Formatted Yanda Ou 9/2/22 1:28:00 PM

English (US)

Page 7: [134] Formatted Yanda Ou 9/2/22 1:28:00 PM

English (US)

Page 7: [134] Formatted Yanda Ou 9/2/22 1:28:00 PM

English (US)

Page 7: [134] Formatted Yanda Ou 9/2/22 1:28:00 PM

English (US)

▲
Page 7: [134] Formatted Yanda Ou 9/2/22 1:28:00 PM

English (US)

▲
Page 7: [134] Formatted Yanda Ou 9/2/22 1:28:00 PM

English (US)

▲
Page 7: [134] Formatted Yanda Ou 9/2/22 1:28:00 PM

English (US)

▲
Page 7: [134] Formatted Yanda Ou 9/2/22 1:28:00 PM

English (US)

▲
Page 7: [135] Formatted Yanda Ou 9/2/22 1:28:00 PM

English (US)

▲
Page 7: [135] Formatted Yanda Ou 9/2/22 1:28:00 PM

English (US)

▲
Page 7: [135] Formatted Yanda Ou 9/2/22 1:28:00 PM

English (US)

▲
Page 7: [135] Formatted Yanda Ou 9/2/22 1:28:00 PM

English (US)

▲
Page 7: [135] Formatted Yanda Ou 9/2/22 1:28:00 PM

English (US)

▲
Page 7: [135] Formatted Yanda Ou 9/2/22 1:28:00 PM

English (US)

▲
Page 7: [135] Formatted Yanda Ou 9/2/22 1:28:00 PM

English (US)

▲
Page 7: [135] Formatted Yanda Ou 9/2/22 1:28:00 PM

English (US)

▲
Page 7: [135] Formatted Yanda Ou 9/2/22 1:28:00 PM

English (US)

▲
Page 7: [136] Formatted Yanda Ou 9/2/22 1:28:00 PM

English (US)

▲
Page 7: [136] Formatted Yanda Ou 9/2/22 1:28:00 PM

English (US)

▲
Page 7: [136] Formatted Yanda Ou 9/2/22 1:28:00 PM

English (US)

English (US)

▲
Page 7: [136] Formatted Yanda Ou 9/2/22 1:28:00 PM

English (US)

▲
Page 7: [136] Formatted Yanda Ou 9/2/22 1:28:00 PM

English (US)

▲
Page 7: [136] Formatted Yanda Ou 9/2/22 1:28:00 PM

English (US)

▲
Page 7: [136] Formatted Yanda Ou 9/2/22 1:28:00 PM

English (US)

▲
Page 7: [136] Formatted Yanda Ou 9/2/22 1:28:00 PM

English (US)

▲
Page 7: [136] Formatted Yanda Ou 9/2/22 1:28:00 PM

English (US)

▲
Page 7: [136] Formatted Yanda Ou 9/2/22 1:28:00 PM

English (US)

▲
Page 7: [136] Formatted Yanda Ou 9/2/22 1:28:00 PM

English (US)

▲
Page 7: [136] Formatted Yanda Ou 9/2/22 1:28:00 PM

English (US)

▲
Page 7: [137] Formatted Yanda Ou 9/2/22 1:28:00 PM

English (US)

▲
Page 7: [137] Formatted Yanda Ou 9/2/22 1:28:00 PM

English (US)

▲
Page 7: [137] Formatted Yanda Ou 9/2/22 1:28:00 PM

English (US)

▲
Page 7: [137] Formatted Yanda Ou 9/2/22 1:28:00 PM

English (US)

▲
Page 7: [137] Formatted Yanda Ou 9/2/22 1:28:00 PM

English (US)

▲
Page 7: [137] Formatted Yanda Ou 9/2/22 1:28:00 PM

English (US)

▲

Page 7: [137] Formatted Yanda Ou 9/2/22 1:28:00 PM

English (US)

Page 7: [137] Formatted Yanda Ou 9/2/22 1:28:00 PM

English (US)

Page 7: [137] Formatted Yanda Ou 9/2/22 1:28:00 PM

English (US)

Page 7: [137] Formatted Yanda Ou 9/2/22 1:28:00 PM

English (US)

Page 7: [137] Formatted Yanda Ou 9/2/22 1:28:00 PM

English (US)

Page 7: [137] Formatted Yanda Ou 9/2/22 1:28:00 PM

English (US)

Page 7: [138] Formatted Yanda Ou 9/2/22 1:28:00 PM

English (US)

Page 7: [138] Formatted Yanda Ou 9/2/22 1:28:00 PM

English (US)

Page 7: [138] Formatted Yanda Ou 9/2/22 1:28:00 PM

English (US)

Page 7: [139] Formatted Yanda Ou 9/2/22 1:28:00 PM

English (US)

Page 7: [139] Formatted Yanda Ou 9/2/22 1:28:00 PM

English (US)

Page 7: [140] Formatted Yanda Ou 9/2/22 1:28:00 PM

English (US)

Page 7: [140] Formatted Yanda Ou 9/2/22 1:28:00 PM

English (US)

Page 7: [140] Formatted Yanda Ou 9/2/22 1:28:00 PM

English (US)

Page 7: [140] Formatted Yanda Ou 9/2/22 1:28:00 PM

English (US)

Page 7: [140] Formatted Yanda Ou 9/2/22 1:28:00 PM

English (US)

▲
Page 7: [140] Formatted Yanda Ou 9/2/22 1:28:00 PM

English (US)

▲
Page 8: [141] Formatted Yanda Ou 9/2/22 1:28:00 PM

English (US)

▲
Page 8: [141] Formatted Yanda Ou 9/2/22 1:28:00 PM

English (US)

▲
Page 8: [141] Formatted Yanda Ou 9/2/22 1:28:00 PM

English (US)

▲
Page 8: [142] Formatted Yanda Ou 9/2/22 1:28:00 PM

English (US)

▲
Page 8: [142] Formatted Yanda Ou 9/2/22 1:28:00 PM

English (US)

▲
Page 8: [143] Formatted Yanda Ou 9/2/22 1:28:00 PM

English (US)

▲
Page 8: [143] Formatted Yanda Ou 9/2/22 1:28:00 PM

English (US)

▲
Page 8: [143] Formatted Yanda Ou 9/2/22 1:28:00 PM

English (US)

▲
Page 8: [143] Formatted Yanda Ou 9/2/22 1:28:00 PM

English (US)

▲
Page 8: [143] Formatted Yanda Ou 9/2/22 1:28:00 PM

English (US)

▲
Page 8: [143] Formatted Yanda Ou 9/2/22 1:28:00 PM

English (US)

▲
Page 8: [143] Formatted Yanda Ou 9/2/22 1:28:00 PM

English (US)

▲
Page 8: [143] Formatted Yanda Ou 9/2/22 1:28:00 PM

English (US)

▲
Page 8: [143] Formatted Yanda Ou 9/2/22 1:28:00 PM

English (US)

▲
Page 8: [143] Formatted Yanda Ou 9/2/22 1:28:00 PM

English (US)

English (US)

▲
Page 8: [143] Formatted Yanda Ou 9/2/22 1:28:00 PM

English (US)

▲
Page 8: [143] Formatted Yanda Ou 9/2/22 1:28:00 PM

English (US)

▲
Page 8: [143] Formatted Yanda Ou 9/2/22 1:28:00 PM

English (US)

▲
Page 8: [143] Formatted Yanda Ou 9/2/22 1:28:00 PM

English (US)

▲
Page 10: [144] Deleted Yanda Ou 9/2/22 1:28:00 PM

✖
Page 11: [145] Deleted Yanda Ou 9/2/22 1:28:00 PM

✖
Page 16: [146] Deleted Yanda Ou 9/2/22 1:28:00 PM

✖
Page 16: [147] Deleted Yanda Ou 9/2/22 1:28:00 PM

▼
▲
Page 16: [148] Deleted Yanda Ou 9/2/22 1:28:00 PM

▼
▲
Page 16: [149] Deleted Yanda Ou 9/2/22 1:28:00 PM

▼
▲
Page 17: [150] Formatted Yanda Ou 9/2/22 1:28:00 PM

English (US)

▲
Page 17: [150] Formatted Yanda Ou 9/2/22 1:28:00 PM

English (US)

▲
Page 17: [151] Deleted Yanda Ou 9/2/22 1:28:00 PM

▼
▲
Page 17: [152] Formatted Yanda Ou 9/2/22 1:28:00 PM

English (US)

▲
Page 17: [153] Formatted Yanda Ou 9/2/22 1:28:00 PM

English (US)

▲
Page 17: [154] Formatted Yanda Ou 9/2/22 1:28:00 PM

English (US)

▲
Page 17: [155] Formatted Yanda Ou 9/2/22 1:28:00 PM

English (US)

English (US)

▲
Page 17: [155] Formatted Yanda Ou 9/2/22 1:28:00 PM

English (US)

▲
Page 17: [156] Formatted Yanda Ou 9/2/22 1:28:00 PM

English (US)

▲
Page 17: [157] Formatted Yanda Ou 9/2/22 1:28:00 PM

English (US)

▲
Page 17: [158] Formatted Yanda Ou 9/2/22 1:28:00 PM

English (US)

▲
Page 17: [159] Formatted Yanda Ou 9/2/22 1:28:00 PM

English (US)

▲
Page 17: [159] Formatted Yanda Ou 9/2/22 1:28:00 PM

English (US)

▲
Page 17: [160] Formatted Yanda Ou 9/2/22 1:28:00 PM

English (US)

▲
Page 17: [160] Formatted Yanda Ou 9/2/22 1:28:00 PM

English (US)

▲
Page 17: [161] Deleted Yanda Ou 9/2/22 1:28:00 PM

▼
▲
Page 17: [162] Formatted Yanda Ou 9/2/22 1:28:00 PM

English (US)

▲
Page 17: [163] Formatted Yanda Ou 9/2/22 1:28:00 PM

English (US)

▲
Page 17: [164] Formatted Yanda Ou 9/2/22 1:28:00 PM

English (US)

▲
Page 17: [165] Formatted Yanda Ou 9/2/22 1:28:00 PM

English (US)

▲
Page 17: [166] Formatted Yanda Ou 9/2/22 1:28:00 PM

English (US)

▲
Page 17: [167] Formatted Yanda Ou 9/2/22 1:28:00 PM

English (US)

▲

Page 17: [169] Formatted **Yanda Ou** **9/2/22 1:28:00 PM**

English (US)

▲
Page 17: [169] Formatted **Yanda Ou** **9/2/22 1:28:00 PM**

English (US)

▲
Page 17: [170] Formatted **Yanda Ou** **9/2/22 1:28:00 PM**

English (US)

▲
Page 17: [171] Formatted **Yanda Ou** **9/2/22 1:28:00 PM**

English (US)

▲
Page 17: [171] Formatted **Yanda Ou** **9/2/22 1:28:00 PM**

English (US)

▲
Page 17: [172] Formatted **Yanda Ou** **9/2/22 1:28:00 PM**

English (US)

▲
Page 17: [173] Deleted **Yanda Ou** **9/2/22 1:28:00 PM**

▼

▲
Page 17: [174] Formatted **Yanda Ou** **9/2/22 1:28:00 PM**

English (US)

▲
Page 17: [175] Deleted **Yanda Ou** **9/2/22 1:28:00 PM**

▼

▲
Page 17: [176] Formatted **Yanda Ou** **9/2/22 1:28:00 PM**

English (US)

▲
Page 17: [177] Deleted **Yanda Ou** **9/2/22 1:28:00 PM**

▼

▲
Page 17: [178] Formatted **Yanda Ou** **9/2/22 1:28:00 PM**

English (US)

▲
Page 17: [178] Formatted **Yanda Ou** **9/2/22 1:28:00 PM**

English (US)

▲
Page 17: [179] Formatted **Yanda Ou** **9/2/22 1:28:00 PM**

English (US)

▲
Page 17: [180] Formatted **Yanda Ou** **9/2/22 1:28:00 PM**

English (US)

▲
Page 17: [181] Formatted **Yanda Ou** **9/2/22 1:28:00 PM**

English (US)

▼
▲
Page 20: [183] Deleted Yanda Ou 9/2/22 1:28:00 PM

▼
▲
Page 22: [184] Formatted Yanda Ou 9/2/22 1:28:00 PM
English (US)

▼
▲
Page 22: [184] Formatted Yanda Ou 9/2/22 1:28:00 PM
English (US)

▼
▲
Page 22: [184] Formatted Yanda Ou 9/2/22 1:28:00 PM
English (US)

▼
▲
Page 22: [185] Deleted Yanda Ou 9/2/22 1:28:00 PM

▼
▲
Page 22: [186] Deleted Yanda Ou 9/2/22 1:28:00 PM

▼
▲
Page 22: [187] Deleted Yanda Ou 9/2/22 1:28:00 PM

▼
▲
Page 22: [188] Formatted Yanda Ou 9/2/22 1:28:00 PM
English (US)

▼
▲
Page 22: [188] Formatted Yanda Ou 9/2/22 1:28:00 PM
English (US)

▼
▲
Page 22: [188] Formatted Yanda Ou 9/2/22 1:28:00 PM
English (US)

▼
▲
Page 22: [188] Formatted Yanda Ou 9/2/22 1:28:00 PM
English (US)

▼
▲
Page 22: [188] Formatted Yanda Ou 9/2/22 1:28:00 PM
English (US)

▼
▲
Page 22: [188] Formatted Yanda Ou 9/2/22 1:28:00 PM
English (US)

▼
▲
Page 22: [188] Formatted Yanda Ou 9/2/22 1:28:00 PM
English (US)

▼
▲
Page 22: [188] Formatted Yanda Ou 9/2/22 1:28:00 PM
English (US)

▼
▲
Page 22: [188] Formatted Yanda Ou 9/2/22 1:28:00 PM
English (US)

▼
▲
Page 22: [188] Formatted Yanda Ou 9/2/22 1:28:00 PM

Page 22: [188] Formatted Yanda Ou 9/2/22 1:28:00 PM

English (US)

▲
Page 22: [188] Formatted Yanda Ou 9/2/22 1:28:00 PM

English (US)

▲
Page 22: [188] Formatted Yanda Ou 9/2/22 1:28:00 PM

English (US)

▲
Page 22: [188] Formatted Yanda Ou 9/2/22 1:28:00 PM

English (US)

▲
Page 22: [188] Formatted Yanda Ou 9/2/22 1:28:00 PM

English (US)

▲
Page 22: [188] Formatted Yanda Ou 9/2/22 1:28:00 PM

English (US)

▲
Page 22: [188] Formatted Yanda Ou 9/2/22 1:28:00 PM

English (US)

▲
Page 22: [188] Formatted Yanda Ou 9/2/22 1:28:00 PM

English (US)

▲
Page 22: [188] Formatted Yanda Ou 9/2/22 1:28:00 PM

English (US)

▲
Page 22: [189] Deleted Yanda Ou 9/2/22 1:28:00 PM

▼

▲
Page 22: [190] Deleted Yanda Ou 9/2/22 1:28:00 PM

▼

▲
Page 22: [191] Formatted Yanda Ou 9/2/22 1:28:00 PM

English (US)

▲
Page 22: [191] Formatted Yanda Ou 9/2/22 1:28:00 PM

English (US)

▲
Page 22: [191] Formatted Yanda Ou 9/2/22 1:28:00 PM

English (US)

▲
Page 22: [191] Formatted Yanda Ou 9/2/22 1:28:00 PM

English (US)

▲
Page 22: [191] Formatted Yanda Ou 9/2/22 1:28:00 PM

English (US)

▲
Page 22: [191] Formatted **Yanda Ou** **9/2/22 1:28:00 PM**

English (US)

▲
Page 22: [191] Formatted **Yanda Ou** **9/2/22 1:28:00 PM**

English (US)

▲
Page 22: [192] Formatted **Yanda Ou** **9/2/22 1:28:00 PM**

English (US)

▲
Page 22: [192] Formatted **Yanda Ou** **9/2/22 1:28:00 PM**

English (US)

▲
Page 22: [193] Formatted **Yanda Ou** **9/2/22 1:28:00 PM**

English (US)

▲
Page 22: [193] Formatted **Yanda Ou** **9/2/22 1:28:00 PM**

English (US)

▲
Page 22: [193] Formatted **Yanda Ou** **9/2/22 1:28:00 PM**

English (US)

▲
Page 22: [193] Formatted **Yanda Ou** **9/2/22 1:28:00 PM**

English (US)

▲
Page 22: [193] Formatted **Yanda Ou** **9/2/22 1:28:00 PM**

English (US)

▲
Page 22: [193] Formatted **Yanda Ou** **9/2/22 1:28:00 PM**

English (US)

▲
Page 22: [193] Formatted **Yanda Ou** **9/2/22 1:28:00 PM**

English (US)

▲
Page 22: [193] Formatted **Yanda Ou** **9/2/22 1:28:00 PM**

English (US)

▲
Page 22: [193] Formatted **Yanda Ou** **9/2/22 1:28:00 PM**

English (US)

▲
Page 22: [193] Formatted **Yanda Ou** **9/2/22 1:28:00 PM**

English (US)

▲
Page 22: [193] Formatted **Yanda Ou** **9/2/22 1:28:00 PM**

English (US)

▲
Page 22: [193] Formatted **Yanda Ou** **9/2/22 1:28:00 PM**

English (US)

English (US)

▲ **Page 22: [193] Formatted** Yanda Ou 9/2/22 1:28:00 PM

English (US)

▲ **Page 22: [193] Formatted** Yanda Ou 9/2/22 1:28:00 PM

English (US)

▲ **Page 22: [193] Formatted** Yanda Ou 9/2/22 1:28:00 PM

English (US)

▲ **Page 22: [194] Deleted** Yanda Ou 9/2/22 1:28:00 PM

▼

▲ **Page 22: [195] Formatted** Yanda Ou 9/2/22 1:28:00 PM

English (US)

▲ **Page 22: [195] Formatted** Yanda Ou 9/2/22 1:28:00 PM

English (US)

▲ **Page 22: [196] Deleted** Yanda Ou 9/2/22 1:28:00 PM

▼ **Page 32: [197] Formatted** Yanda Ou 9/2/22 1:28:00 PM

English (US)

▲ **Page 32: [197] Formatted** Yanda Ou 9/2/22 1:28:00 PM

English (US)

▲ **Page 32: [197] Formatted** Yanda Ou 9/2/22 1:28:00 PM

English (US)

▲ **Page 32: [197] Formatted** Yanda Ou 9/2/22 1:28:00 PM

English (US)

▲ **Page 32: [197] Formatted** Yanda Ou 9/2/22 1:28:00 PM

English (US)

▲ **Page 32: [197] Formatted** Yanda Ou 9/2/22 1:28:00 PM

English (US)

▲ **Page 32: [197] Formatted** Yanda Ou 9/2/22 1:28:00 PM

English (US)

▲ **Page 32: [197] Formatted** Yanda Ou 9/2/22 1:28:00 PM

English (US)

▲ **Page 32: [197] Formatted** Yanda Ou 9/2/22 1:28:00 PM

English (US)

English (US)

▲
Page 32: [197] Formatted **Yanda Ou** **9/2/22 1:28:00 PM**

English (US)

▲
Page 32: [197] Formatted **Yanda Ou** **9/2/22 1:28:00 PM**

English (US)

▲
Page 32: [197] Formatted **Yanda Ou** **9/2/22 1:28:00 PM**

English (US)

▲
Page 32: [197] Formatted **Yanda Ou** **9/2/22 1:28:00 PM**

English (US)

▲
Page 32: [197] Formatted **Yanda Ou** **9/2/22 1:28:00 PM**

English (US)

▲
Page 32: [197] Formatted **Yanda Ou** **9/2/22 1:28:00 PM**

English (US)

▲
Page 32: [197] Formatted **Yanda Ou** **9/2/22 1:28:00 PM**

English (US)

▲
Page 32: [197] Formatted **Yanda Ou** **9/2/22 1:28:00 PM**

English (US)

▲
Page 32: [197] Formatted **Yanda Ou** **9/2/22 1:28:00 PM**

English (US)

▲
Page 32: [197] Formatted **Yanda Ou** **9/2/22 1:28:00 PM**

English (US)

▲
Page 32: [197] Formatted **Yanda Ou** **9/2/22 1:28:00 PM**

English (US)

▲
Page 32: [197] Formatted **Yanda Ou** **9/2/22 1:28:00 PM**

English (US)

▲
Page 32: [198] Formatted **Yanda Ou** **9/2/22 1:28:00 PM**

English (US)

▲
Page 32: [198] Formatted **Yanda Ou** **9/2/22 1:28:00 PM**

English (US)

▲
Page 32: [198] Formatted **Yanda Ou** **9/2/22 1:28:00 PM**

English (US)

▲

Page 32: [198] Formatted **Yanda Ou** **9/2/22 1:28:00 PM**

English (US)

Page 32: [198] Formatted **Yanda Ou** **9/2/22 1:28:00 PM**

English (US)

Page 32: [198] Formatted **Yanda Ou** **9/2/22 1:28:00 PM**

English (US)

Page 32: [198] Formatted **Yanda Ou** **9/2/22 1:28:00 PM**

English (US)

Page 32: [198] Formatted **Yanda Ou** **9/2/22 1:28:00 PM**

English (US)

Page 32: [198] Formatted **Yanda Ou** **9/2/22 1:28:00 PM**

English (US)

Page 32: [198] Formatted **Yanda Ou** **9/2/22 1:28:00 PM**

English (US)

Page 32: [198] Formatted **Yanda Ou** **9/2/22 1:28:00 PM**

English (US)

Page 32: [198] Formatted **Yanda Ou** **9/2/22 1:28:00 PM**

English (US)

Page 32: [198] Formatted **Yanda Ou** **9/2/22 1:28:00 PM**

English (US)

Page 32: [198] Formatted **Yanda Ou** **9/2/22 1:28:00 PM**

English (US)

Page 32: [198] Formatted **Yanda Ou** **9/2/22 1:28:00 PM**

English (US)

Page 32: [198] Formatted **Yanda Ou** **9/2/22 1:28:00 PM**

English (US)

Page 32: [198] Formatted **Yanda Ou** **9/2/22 1:28:00 PM**

English (US)

Page 32: [198] Formatted **Yanda Ou** **9/2/22 1:28:00 PM**

English (US)

Page 32: [198] Formatted **Yanda Ou** **9/2/22 1:28:00 PM**

English (US)

▲
Page 32: [198] Formatted **Yanda Ou** **9/2/22 1:28:00 PM**

English (US)

▲
Page 32: [199] Formatted **Yanda Ou** **9/2/22 1:28:00 PM**

English (US)

▲
Page 32: [199] Formatted **Yanda Ou** **9/2/22 1:28:00 PM**

English (US)

▲
Page 32: [199] Formatted **Yanda Ou** **9/2/22 1:28:00 PM**

English (US)

▲
Page 32: [199] Formatted **Yanda Ou** **9/2/22 1:28:00 PM**

English (US)

▲
Page 32: [199] Formatted **Yanda Ou** **9/2/22 1:28:00 PM**

English (US)

▲
Page 32: [199] Formatted **Yanda Ou** **9/2/22 1:28:00 PM**

English (US)

▲
Page 32: [199] Formatted **Yanda Ou** **9/2/22 1:28:00 PM**

English (US)

▲
Page 32: [199] Formatted **Yanda Ou** **9/2/22 1:28:00 PM**

English (US)

▲
Page 32: [199] Formatted **Yanda Ou** **9/2/22 1:28:00 PM**

English (US)

▲
Page 32: [199] Formatted **Yanda Ou** **9/2/22 1:28:00 PM**

English (US)

▲
Page 32: [199] Formatted **Yanda Ou** **9/2/22 1:28:00 PM**

English (US)

▲
Page 32: [199] Formatted **Yanda Ou** **9/2/22 1:28:00 PM**

English (US)

▲
Page 32: [199] Formatted **Yanda Ou** **9/2/22 1:28:00 PM**

English (US)

▲
Page 32: [199] Formatted **Yanda Ou** **9/2/22 1:28:00 PM**

English (US)

▲
Page 32: [199] Formatted **Yanda Ou** **9/2/22 1:28:00 PM**

English (US)

English (US)

▲
Page 32: [199] Formatted **Yanda Ou** **9/2/22 1:28:00 PM**

English (US)

▲
Page 32: [199] Formatted **Yanda Ou** **9/2/22 1:28:00 PM**

English (US)

▲
Page 32: [199] Formatted **Yanda Ou** **9/2/22 1:28:00 PM**

English (US)

▲
Page 32: [199] Formatted **Yanda Ou** **9/2/22 1:28:00 PM**

English (US)

▲
Page 32: [199] Formatted **Yanda Ou** **9/2/22 1:28:00 PM**

English (US)

▲
Page 32: [199] Formatted **Yanda Ou** **9/2/22 1:28:00 PM**

English (US)

▲
Page 32: [199] Formatted **Yanda Ou** **9/2/22 1:28:00 PM**

English (US)

▲
Page 32: [200] Formatted **Yanda Ou** **9/2/22 1:28:00 PM**

English (US)

▲
Page 32: [200] Formatted **Yanda Ou** **9/2/22 1:28:00 PM**

English (US)

▲
Page 32: [200] Formatted **Yanda Ou** **9/2/22 1:28:00 PM**

English (US)

▲
Page 32: [200] Formatted **Yanda Ou** **9/2/22 1:28:00 PM**

English (US)

▲
Page 32: [200] Formatted **Yanda Ou** **9/2/22 1:28:00 PM**

English (US)

▲
Page 32: [200] Formatted **Yanda Ou** **9/2/22 1:28:00 PM**

English (US)

▲
Page 32: [200] Formatted **Yanda Ou** **9/2/22 1:28:00 PM**

English (US)

▲
Page 32: [200] Formatted **Yanda Ou** **9/2/22 1:28:00 PM**

English (US)

▲

Page 32: [200] Formatted **Yanda Ou** **9/2/22 1:28:00 PM**

English (US)

Page 32: [200] Formatted **Yanda Ou** **9/2/22 1:28:00 PM**

English (US)

Page 32: [200] Formatted **Yanda Ou** **9/2/22 1:28:00 PM**

English (US)

Page 32: [200] Formatted **Yanda Ou** **9/2/22 1:28:00 PM**

English (US)

Page 32: [200] Formatted **Yanda Ou** **9/2/22 1:28:00 PM**

English (US)

Page 32: [200] Formatted **Yanda Ou** **9/2/22 1:28:00 PM**

English (US)

Page 32: [200] Formatted **Yanda Ou** **9/2/22 1:28:00 PM**

English (US)

Page 32: [200] Formatted **Yanda Ou** **9/2/22 1:28:00 PM**

English (US)

Page 32: [200] Formatted **Yanda Ou** **9/2/22 1:28:00 PM**

English (US)

Page 32: [200] Formatted **Yanda Ou** **9/2/22 1:28:00 PM**

English (US)

Page 32: [200] Formatted **Yanda Ou** **9/2/22 1:28:00 PM**

English (US)

Page 32: [200] Formatted **Yanda Ou** **9/2/22 1:28:00 PM**

English (US)

Page 32: [200] Formatted **Yanda Ou** **9/2/22 1:28:00 PM**

English (US)

Page 32: [200] Formatted **Yanda Ou** **9/2/22 1:28:00 PM**

English (US)

Page 32: [200] Formatted **Yanda Ou** **9/2/22 1:28:00 PM**

English (US)

Page 32: [200] Formatted **Yanda Ou** **9/2/22 1:28:00 PM**

English (US)

▲
Page 32: [201] Formatted **Yanda Ou** **9/2/22 1:28:00 PM**

English (US)

▲
Page 32: [201] Formatted **Yanda Ou** **9/2/22 1:28:00 PM**

English (US)

▲
Page 32: [201] Formatted **Yanda Ou** **9/2/22 1:28:00 PM**

English (US)

▲
Page 32: [201] Formatted **Yanda Ou** **9/2/22 1:28:00 PM**

English (US)

▲
Page 32: [201] Formatted **Yanda Ou** **9/2/22 1:28:00 PM**

English (US)

▲
Page 32: [201] Formatted **Yanda Ou** **9/2/22 1:28:00 PM**

English (US)

▲
Page 32: [201] Formatted **Yanda Ou** **9/2/22 1:28:00 PM**

English (US)

▲
Page 32: [201] Formatted **Yanda Ou** **9/2/22 1:28:00 PM**

English (US)

▲
Page 32: [201] Formatted **Yanda Ou** **9/2/22 1:28:00 PM**

English (US)

▲
Page 32: [201] Formatted **Yanda Ou** **9/2/22 1:28:00 PM**

English (US)

▲
Page 32: [201] Formatted **Yanda Ou** **9/2/22 1:28:00 PM**

English (US)

▲
Page 32: [201] Formatted **Yanda Ou** **9/2/22 1:28:00 PM**

English (US)

▲
Page 32: [201] Formatted **Yanda Ou** **9/2/22 1:28:00 PM**

English (US)

▲
Page 32: [201] Formatted **Yanda Ou** **9/2/22 1:28:00 PM**

English (US)

▲
Page 32: [201] Formatted **Yanda Ou** **9/2/22 1:28:00 PM**

English (US)

▲
Page 32: [201] Formatted **Yanda Ou** **9/2/22 1:28:00 PM**

English (US)

English (US)

▲
Page 32: [201] Formatted **Yanda Ou** **9/2/22 1:28:00 PM**

English (US)

▲
Page 32: [201] Formatted **Yanda Ou** **9/2/22 1:28:00 PM**

English (US)

▲
Page 32: [201] Formatted **Yanda Ou** **9/2/22 1:28:00 PM**

English (US)

▲
Page 32: [201] Formatted **Yanda Ou** **9/2/22 1:28:00 PM**

English (US)

▲
Page 32: [201] Formatted **Yanda Ou** **9/2/22 1:28:00 PM**

English (US)

▲
Page 32: [201] Formatted **Yanda Ou** **9/2/22 1:28:00 PM**

English (US)

▲
Page 32: [201] Formatted **Yanda Ou** **9/2/22 1:28:00 PM**

English (US)

▲
Page 32: [201] Formatted **Yanda Ou** **9/2/22 1:28:00 PM**

English (US)

▲
Page 32: [201] Formatted **Yanda Ou** **9/2/22 1:28:00 PM**

English (US)

▲
Page 32: [201] Formatted **Yanda Ou** **9/2/22 1:28:00 PM**

English (US)

▲
Page 32: [201] Formatted **Yanda Ou** **9/2/22 1:28:00 PM**

English (US)

▲
Page 32: [201] Formatted **Yanda Ou** **9/2/22 1:28:00 PM**

English (US)

▲
Page 32: [201] Formatted **Yanda Ou** **9/2/22 1:28:00 PM**

English (US)

▲
Page 32: [201] Formatted **Yanda Ou** **9/2/22 1:28:00 PM**

English (US)

▲
Page 32: [201] Formatted **Yanda Ou** **9/2/22 1:28:00 PM**

English (US)

▲

Page 32: [201] Formatted **Yanda Ou** **9/2/22 1:28:00 PM**

English (US)

Page 32: [201] Formatted **Yanda Ou** **9/2/22 1:28:00 PM**

English (US)

Page 32: [201] Formatted **Yanda Ou** **9/2/22 1:28:00 PM**

English (US)

Page 32: [201] Formatted **Yanda Ou** **9/2/22 1:28:00 PM**

English (US)

Page 32: [201] Formatted **Yanda Ou** **9/2/22 1:28:00 PM**

English (US)

Page 32: [201] Formatted **Yanda Ou** **9/2/22 1:28:00 PM**

English (US)

Page 32: [201] Formatted **Yanda Ou** **9/2/22 1:28:00 PM**

English (US)

Page 32: [201] Formatted **Yanda Ou** **9/2/22 1:28:00 PM**

English (US)

Page 32: [201] Formatted **Yanda Ou** **9/2/22 1:28:00 PM**

English (US)

Page 32: [201] Formatted **Yanda Ou** **9/2/22 1:28:00 PM**

English (US)

Page 32: [201] Formatted **Yanda Ou** **9/2/22 1:28:00 PM**

English (US)

Page 32: [202] Formatted **Yanda Ou** **9/2/22 1:28:00 PM**

English (US)

Page 32: [202] Formatted **Yanda Ou** **9/2/22 1:28:00 PM**

English (US)

Page 32: [202] Formatted **Yanda Ou** **9/2/22 1:28:00 PM**

English (US)

Page 32: [202] Formatted **Yanda Ou** **9/2/22 1:28:00 PM**

English (US)

Page 32: [202] Formatted **Yanda Ou** **9/2/22 1:28:00 PM**

English (US)

▲
Page 32: [202] Formatted **Yanda Ou** **9/2/22 1:28:00 PM**

English (US)

▲
Page 32: [202] Formatted **Yanda Ou** **9/2/22 1:28:00 PM**

English (US)

▲
Page 32: [202] Formatted **Yanda Ou** **9/2/22 1:28:00 PM**

English (US)

▲
Page 32: [202] Formatted **Yanda Ou** **9/2/22 1:28:00 PM**

English (US)

▲
Page 32: [202] Formatted **Yanda Ou** **9/2/22 1:28:00 PM**

English (US)

▲
Page 32: [202] Formatted **Yanda Ou** **9/2/22 1:28:00 PM**

English (US)

▲
Page 32: [202] Formatted **Yanda Ou** **9/2/22 1:28:00 PM**

English (US)

▲
Page 32: [202] Formatted **Yanda Ou** **9/2/22 1:28:00 PM**

English (US)

▲
Page 32: [202] Formatted **Yanda Ou** **9/2/22 1:28:00 PM**

English (US)

▲
Page 32: [202] Formatted **Yanda Ou** **9/2/22 1:28:00 PM**

English (US)

▲
Page 32: [202] Formatted **Yanda Ou** **9/2/22 1:28:00 PM**

English (US)

▲
Page 32: [202] Formatted **Yanda Ou** **9/2/22 1:28:00 PM**

English (US)

▲
Page 32: [202] Formatted **Yanda Ou** **9/2/22 1:28:00 PM**

English (US)

▲
Page 32: [202] Formatted **Yanda Ou** **9/2/22 1:28:00 PM**

English (US)

▲
Page 32: [202] Formatted **Yanda Ou** **9/2/22 1:28:00 PM**

English (US)

▲
Page 32: [202] Formatted **Yanda Ou** **9/2/22 1:28:00 PM**

English (US)

English (US)

▲
Page 32: [202] Formatted **Yanda Ou** **9/2/22 1:28:00 PM**

English (US)

▲
Page 32: [202] Formatted **Yanda Ou** **9/2/22 1:28:00 PM**

English (US)

▲
Page 32: [202] Formatted **Yanda Ou** **9/2/22 1:28:00 PM**

English (US)

▲
Page 32: [202] Formatted **Yanda Ou** **9/2/22 1:28:00 PM**

English (US)

▲
Page 32: [202] Formatted **Yanda Ou** **9/2/22 1:28:00 PM**

English (US)

▲
Page 32: [202] Formatted **Yanda Ou** **9/2/22 1:28:00 PM**

English (US)

▲
Page 32: [202] Formatted **Yanda Ou** **9/2/22 1:28:00 PM**

English (US)

▲
Page 32: [202] Formatted **Yanda Ou** **9/2/22 1:28:00 PM**

English (US)

▲
Page 32: [202] Formatted **Yanda Ou** **9/2/22 1:28:00 PM**

English (US)

▲
Page 32: [202] Formatted **Yanda Ou** **9/2/22 1:28:00 PM**

English (US)

▲
Page 32: [202] Formatted **Yanda Ou** **9/2/22 1:28:00 PM**

English (US)

▲
Page 32: [202] Formatted **Yanda Ou** **9/2/22 1:28:00 PM**

English (US)

▲
Page 32: [202] Formatted **Yanda Ou** **9/2/22 1:28:00 PM**

English (US)

▲
Page 32: [202] Formatted **Yanda Ou** **9/2/22 1:28:00 PM**

English (US)

▲
Page 32: [202] Formatted **Yanda Ou** **9/2/22 1:28:00 PM**

English (US)

▲

Page 32: [202] Formatted **Yanda Ou** **9/2/22 1:28:00 PM**

English (US)

Page 32: [202] Formatted **Yanda Ou** **9/2/22 1:28:00 PM**

English (US)

Page 32: [202] Formatted **Yanda Ou** **9/2/22 1:28:00 PM**

English (US)

Page 32: [202] Formatted **Yanda Ou** **9/2/22 1:28:00 PM**

English (US)

Page 32: [202] Formatted **Yanda Ou** **9/2/22 1:28:00 PM**

English (US)

Page 32: [202] Formatted **Yanda Ou** **9/2/22 1:28:00 PM**

English (US)

Page 32: [203] Formatted **Yanda Ou** **9/2/22 1:28:00 PM**

English (US)

Page 32: [203] Formatted **Yanda Ou** **9/2/22 1:28:00 PM**

English (US)

Page 32: [203] Formatted **Yanda Ou** **9/2/22 1:28:00 PM**

English (US)

Page 32: [203] Formatted **Yanda Ou** **9/2/22 1:28:00 PM**

English (US)

Page 32: [203] Formatted **Yanda Ou** **9/2/22 1:28:00 PM**

English (US)

Page 32: [203] Formatted **Yanda Ou** **9/2/22 1:28:00 PM**

English (US)

Page 32: [203] Formatted **Yanda Ou** **9/2/22 1:28:00 PM**

English (US)

Page 32: [203] Formatted **Yanda Ou** **9/2/22 1:28:00 PM**

English (US)

Page 32: [203] Formatted **Yanda Ou** **9/2/22 1:28:00 PM**

English (US)

Page 32: [203] Formatted **Yanda Ou** **9/2/22 1:28:00 PM**

English (US)

▲
Page 32: [203] Formatted **Yanda Ou** **9/2/22 1:28:00 PM**

English (US)

▲
Page 32: [203] Formatted **Yanda Ou** **9/2/22 1:28:00 PM**

English (US)

▲
Page 32: [203] Formatted **Yanda Ou** **9/2/22 1:28:00 PM**

English (US)

▲
Page 32: [203] Formatted **Yanda Ou** **9/2/22 1:28:00 PM**

English (US)

▲
Page 32: [203] Formatted **Yanda Ou** **9/2/22 1:28:00 PM**

English (US)

▲
Page 32: [203] Formatted **Yanda Ou** **9/2/22 1:28:00 PM**

English (US)

▲
Page 32: [203] Formatted **Yanda Ou** **9/2/22 1:28:00 PM**

English (US)

▲
Page 32: [203] Formatted **Yanda Ou** **9/2/22 1:28:00 PM**

English (US)

▲
Page 32: [203] Formatted **Yanda Ou** **9/2/22 1:28:00 PM**

English (US)

▲
Page 32: [203] Formatted **Yanda Ou** **9/2/22 1:28:00 PM**

English (US)

▲
Page 32: [203] Formatted **Yanda Ou** **9/2/22 1:28:00 PM**

English (US)

▲
Page 32: [203] Formatted **Yanda Ou** **9/2/22 1:28:00 PM**

English (US)

▲
Page 32: [203] Formatted **Yanda Ou** **9/2/22 1:28:00 PM**

English (US)

▲
Page 32: [203] Formatted **Yanda Ou** **9/2/22 1:28:00 PM**

English (US)

▲
Page 32: [203] Formatted **Yanda Ou** **9/2/22 1:28:00 PM**

English (US)

▲
Page 32: [203] Formatted **Yanda Ou** **9/2/22 1:28:00 PM**

English (US)

English (US)

▲
Page 32: [203] Formatted **Yanda Ou** **9/2/22 1:28:00 PM**

English (US)

▲
Page 32: [203] Formatted **Yanda Ou** **9/2/22 1:28:00 PM**

English (US)

▲
Page 32: [203] Formatted **Yanda Ou** **9/2/22 1:28:00 PM**

English (US)

▲
Page 32: [203] Formatted **Yanda Ou** **9/2/22 1:28:00 PM**

English (US)

▲
Page 32: [203] Formatted **Yanda Ou** **9/2/22 1:28:00 PM**

English (US)

▲
Page 32: [203] Formatted **Yanda Ou** **9/2/22 1:28:00 PM**

English (US)

▲
Page 32: [203] Formatted **Yanda Ou** **9/2/22 1:28:00 PM**

English (US)

▲
Page 32: [203] Formatted **Yanda Ou** **9/2/22 1:28:00 PM**

English (US)

▲
Page 32: [203] Formatted **Yanda Ou** **9/2/22 1:28:00 PM**

English (US)

▲
Page 32: [203] Formatted **Yanda Ou** **9/2/22 1:28:00 PM**

English (US)

▲
Page 32: [204] Formatted **Yanda Ou** **9/2/22 1:28:00 PM**

English (US)

▲
Page 32: [204] Formatted **Yanda Ou** **9/2/22 1:28:00 PM**

English (US)

▲
Page 32: [204] Formatted **Yanda Ou** **9/2/22 1:28:00 PM**

English (US)

▲
Page 32: [204] Formatted **Yanda Ou** **9/2/22 1:28:00 PM**

English (US)

▲
Page 32: [204] Formatted **Yanda Ou** **9/2/22 1:28:00 PM**

English (US)

▲

Page 32: [204] Formatted **Yanda Ou** **9/2/22 1:28:00 PM**

English (US)

Page 32: [204] Formatted **Yanda Ou** **9/2/22 1:28:00 PM**

English (US)

Page 32: [204] Formatted **Yanda Ou** **9/2/22 1:28:00 PM**

English (US)

Page 32: [204] Formatted **Yanda Ou** **9/2/22 1:28:00 PM**

English (US)

Page 32: [204] Formatted **Yanda Ou** **9/2/22 1:28:00 PM**

English (US)

Page 32: [204] Formatted **Yanda Ou** **9/2/22 1:28:00 PM**

English (US)

Page 32: [204] Formatted **Yanda Ou** **9/2/22 1:28:00 PM**

English (US)

Page 32: [204] Formatted **Yanda Ou** **9/2/22 1:28:00 PM**

English (US)

Page 32: [204] Formatted **Yanda Ou** **9/2/22 1:28:00 PM**

English (US)

Page 32: [204] Formatted **Yanda Ou** **9/2/22 1:28:00 PM**

English (US)

Page 32: [204] Formatted **Yanda Ou** **9/2/22 1:28:00 PM**

English (US)

Page 32: [204] Formatted **Yanda Ou** **9/2/22 1:28:00 PM**

English (US)

Page 32: [204] Formatted **Yanda Ou** **9/2/22 1:28:00 PM**

English (US)

Page 32: [204] Formatted **Yanda Ou** **9/2/22 1:28:00 PM**

English (US)

Page 32: [204] Formatted **Yanda Ou** **9/2/22 1:28:00 PM**

English (US)

Page 32: [204] Formatted **Yanda Ou** **9/2/22 1:28:00 PM**

English (US)

▲
Page 32: [204] Formatted **Yanda Ou** **9/2/22 1:28:00 PM**

English (US)

▲
Page 32: [204] Formatted **Yanda Ou** **9/2/22 1:28:00 PM**

English (US)

▲
Page 32: [204] Formatted **Yanda Ou** **9/2/22 1:28:00 PM**

English (US)

▲
Page 32: [204] Formatted **Yanda Ou** **9/2/22 1:28:00 PM**

English (US)

▲
Page 32: [204] Formatted **Yanda Ou** **9/2/22 1:28:00 PM**

English (US)

▲
Page 32: [204] Formatted **Yanda Ou** **9/2/22 1:28:00 PM**

English (US)

▲
Page 32: [204] Formatted **Yanda Ou** **9/2/22 1:28:00 PM**

English (US)

▲
Page 32: [204] Formatted **Yanda Ou** **9/2/22 1:28:00 PM**

English (US)

▲
Page 32: [204] Formatted **Yanda Ou** **9/2/22 1:28:00 PM**

English (US)

▲
Page 32: [204] Formatted **Yanda Ou** **9/2/22 1:28:00 PM**

English (US)

▲
Page 32: [204] Formatted **Yanda Ou** **9/2/22 1:28:00 PM**

English (US)

▲
Page 32: [204] Formatted **Yanda Ou** **9/2/22 1:28:00 PM**

English (US)

▲
Page 32: [204] Formatted **Yanda Ou** **9/2/22 1:28:00 PM**

English (US)

▲
Page 32: [204] Formatted **Yanda Ou** **9/2/22 1:28:00 PM**

English (US)

▲
Page 32: [204] Formatted **Yanda Ou** **9/2/22 1:28:00 PM**

English (US)

▲
Page 32: [204] Formatted **Yanda Ou** **9/2/22 1:28:00 PM**

English (US)

English (US)

▲
Page 32: [204] Formatted **Yanda Ou** **9/2/22 1:28:00 PM**

English (US)

▲
Page 32: [204] Formatted **Yanda Ou** **9/2/22 1:28:00 PM**

English (US)

▲
Page 32: [204] Formatted **Yanda Ou** **9/2/22 1:28:00 PM**

English (US)

▲
Page 32: [204] Formatted **Yanda Ou** **9/2/22 1:28:00 PM**

English (US)

▲
Page 32: [204] Formatted **Yanda Ou** **9/2/22 1:28:00 PM**

English (US)

▲
Page 32: [204] Formatted **Yanda Ou** **9/2/22 1:28:00 PM**

English (US)

▲
Page 32: [204] Formatted **Yanda Ou** **9/2/22 1:28:00 PM**

English (US)

▲
Page 32: [204] Formatted **Yanda Ou** **9/2/22 1:28:00 PM**

English (US)

▲
Page 32: [205] Formatted **Yanda Ou** **9/2/22 1:28:00 PM**

English (US)

▲
Page 32: [205] Formatted **Yanda Ou** **9/2/22 1:28:00 PM**

English (US)

▲
Page 32: [205] Formatted **Yanda Ou** **9/2/22 1:28:00 PM**

English (US)

▲
Page 32: [205] Formatted **Yanda Ou** **9/2/22 1:28:00 PM**

English (US)

▲
Page 32: [205] Formatted **Yanda Ou** **9/2/22 1:28:00 PM**

English (US)

▲
Page 32: [205] Formatted **Yanda Ou** **9/2/22 1:28:00 PM**

English (US)

▲
Page 32: [205] Formatted **Yanda Ou** **9/2/22 1:28:00 PM**

English (US)

▲

Page 32: [205] Formatted **Yanda Ou** **9/2/22 1:28:00 PM**

English (US)

Page 32: [205] Formatted **Yanda Ou** **9/2/22 1:28:00 PM**

English (US)

Page 32: [205] Formatted **Yanda Ou** **9/2/22 1:28:00 PM**

English (US)

Page 32: [205] Formatted **Yanda Ou** **9/2/22 1:28:00 PM**

English (US)

Page 32: [206] Formatted **Yanda Ou** **9/2/22 1:28:00 PM**

English (US)

Page 32: [206] Formatted **Yanda Ou** **9/2/22 1:28:00 PM**

English (US)

Page 32: [206] Formatted **Yanda Ou** **9/2/22 1:28:00 PM**

English (US)

Page 32: [206] Formatted **Yanda Ou** **9/2/22 1:28:00 PM**

English (US)

Page 32: [206] Formatted **Yanda Ou** **9/2/22 1:28:00 PM**

English (US)

Page 32: [206] Formatted **Yanda Ou** **9/2/22 1:28:00 PM**

English (US)

Page 32: [206] Formatted **Yanda Ou** **9/2/22 1:28:00 PM**

English (US)

Page 32: [206] Formatted **Yanda Ou** **9/2/22 1:28:00 PM**

English (US)

Page 32: [206] Formatted **Yanda Ou** **9/2/22 1:28:00 PM**

English (US)

Page 32: [206] Formatted **Yanda Ou** **9/2/22 1:28:00 PM**

English (US)

Page 32: [206] Formatted **Yanda Ou** **9/2/22 1:28:00 PM**

English (US)

Page 32: [206] Formatted **Yanda Ou** **9/2/22 1:28:00 PM**

English (US)

▲
Page 32: [207] Formatted **Yanda Ou** **9/2/22 1:28:00 PM**

English (US)

▲
Page 32: [207] Formatted **Yanda Ou** **9/2/22 1:28:00 PM**

English (US)

▲
Page 32: [207] Formatted **Yanda Ou** **9/2/22 1:28:00 PM**

English (US)

▲
Page 32: [207] Formatted **Yanda Ou** **9/2/22 1:28:00 PM**

English (US)

▲
Page 32: [207] Formatted **Yanda Ou** **9/2/22 1:28:00 PM**

English (US)

▲
Page 32: [207] Formatted **Yanda Ou** **9/2/22 1:28:00 PM**

English (US)

▲
Page 32: [207] Formatted **Yanda Ou** **9/2/22 1:28:00 PM**

English (US)

▲
Page 32: [207] Formatted **Yanda Ou** **9/2/22 1:28:00 PM**

English (US)

▲
Page 32: [208] Formatted **Yanda Ou** **9/2/22 1:28:00 PM**

English (US)

▲
Page 32: [208] Formatted **Yanda Ou** **9/2/22 1:28:00 PM**

English (US)

▲
Page 32: [208] Formatted **Yanda Ou** **9/2/22 1:28:00 PM**

English (US)

▲
Page 32: [208] Formatted **Yanda Ou** **9/2/22 1:28:00 PM**

English (US)

▲
Page 32: [208] Formatted **Yanda Ou** **9/2/22 1:28:00 PM**

English (US)

▲
Page 32: [208] Formatted **Yanda Ou** **9/2/22 1:28:00 PM**

English (US)

▲
Page 32: [208] Formatted **Yanda Ou** **9/2/22 1:28:00 PM**

English (US)

▲
Page 32: [208] Formatted **Yanda Ou** **9/2/22 1:28:00 PM**

English (US)

English (US)

▲
Page 32: [209] Formatted **Yanda Ou** **9/2/22 1:28:00 PM**

English (US)

▲
Page 32: [209] Formatted **Yanda Ou** **9/2/22 1:28:00 PM**

English (US)

▲
Page 32: [209] Formatted **Yanda Ou** **9/2/22 1:28:00 PM**

English (US)

▲
Page 32: [209] Formatted **Yanda Ou** **9/2/22 1:28:00 PM**

English (US)

▲
Page 32: [209] Formatted **Yanda Ou** **9/2/22 1:28:00 PM**

English (US)

▲
Page 32: [209] Formatted **Yanda Ou** **9/2/22 1:28:00 PM**

English (US)

▲
Page 32: [209] Formatted **Yanda Ou** **9/2/22 1:28:00 PM**

English (US)

▲
Page 32: [209] Formatted **Yanda Ou** **9/2/22 1:28:00 PM**

English (US)

▲
Page 32: [209] Formatted **Yanda Ou** **9/2/22 1:28:00 PM**

English (US)

▲
Page 32: [209] Formatted **Yanda Ou** **9/2/22 1:28:00 PM**

English (US)

▲
Page 32: [209] Formatted **Yanda Ou** **9/2/22 1:28:00 PM**

English (US)

▲
Page 32: [209] Formatted **Yanda Ou** **9/2/22 1:28:00 PM**

English (US)

▲
Page 32: [209] Formatted **Yanda Ou** **9/2/22 1:28:00 PM**

English (US)

▲
Page 32: [209] Formatted **Yanda Ou** **9/2/22 1:28:00 PM**

English (US)

▲
Page 33: [210] Formatted **Yanda Ou** **9/2/22 1:28:00 PM**

English (US)

▲

Page 33: [210] Formatted **Yanda Ou** **9/2/22 1:28:00 PM**

English (US)

Page 33: [210] Formatted **Yanda Ou** **9/2/22 1:28:00 PM**

English (US)

Page 33: [210] Formatted **Yanda Ou** **9/2/22 1:28:00 PM**

English (US)

Page 33: [210] Formatted **Yanda Ou** **9/2/22 1:28:00 PM**

English (US)

Page 33: [210] Formatted **Yanda Ou** **9/2/22 1:28:00 PM**

English (US)

Page 33: [210] Formatted **Yanda Ou** **9/2/22 1:28:00 PM**

English (US)

Page 33: [210] Formatted **Yanda Ou** **9/2/22 1:28:00 PM**

English (US)

Page 33: [211] Formatted **Yanda Ou** **9/2/22 1:28:00 PM**

English (US)

Page 33: [211] Formatted **Yanda Ou** **9/2/22 1:28:00 PM**

English (US)

Page 33: [211] Formatted **Yanda Ou** **9/2/22 1:28:00 PM**

English (US)

Page 33: [211] Formatted **Yanda Ou** **9/2/22 1:28:00 PM**

English (US)

Page 33: [211] Formatted **Yanda Ou** **9/2/22 1:28:00 PM**

English (US)

Page 33: [211] Formatted **Yanda Ou** **9/2/22 1:28:00 PM**

English (US)

Page 33: [211] Formatted **Yanda Ou** **9/2/22 1:28:00 PM**

English (US)

Page 33: [211] Formatted **Yanda Ou** **9/2/22 1:28:00 PM**

English (US)

Page 33: [211] Formatted **Yanda Ou** **9/2/22 1:28:00 PM**

English (US)

▲
Page 33: [211] Formatted **Yanda Ou** **9/2/22 1:28:00 PM**

English (US)

▲
Page 33: [211] Formatted **Yanda Ou** **9/2/22 1:28:00 PM**

English (US)

▲
Page 33: [211] Formatted **Yanda Ou** **9/2/22 1:28:00 PM**

English (US)

▲
Page 33: [211] Formatted **Yanda Ou** **9/2/22 1:28:00 PM**

English (US)

▲
Page 33: [211] Formatted **Yanda Ou** **9/2/22 1:28:00 PM**

English (US)

▲
Page 33: [212] Formatted **Yanda Ou** **9/2/22 1:28:00 PM**

English (US)

▲
Page 33: [212] Formatted **Yanda Ou** **9/2/22 1:28:00 PM**

English (US)

▲
Page 33: [212] Formatted **Yanda Ou** **9/2/22 1:28:00 PM**

English (US)

▲
Page 33: [212] Formatted **Yanda Ou** **9/2/22 1:28:00 PM**

English (US)

▲
Page 33: [212] Formatted **Yanda Ou** **9/2/22 1:28:00 PM**

English (US)

▲
Page 33: [212] Formatted **Yanda Ou** **9/2/22 1:28:00 PM**

English (US)

▲
Page 33: [212] Formatted **Yanda Ou** **9/2/22 1:28:00 PM**

English (US)

▲
Page 33: [212] Formatted **Yanda Ou** **9/2/22 1:28:00 PM**

English (US)

▲
Page 33: [212] Formatted **Yanda Ou** **9/2/22 1:28:00 PM**

English (US)

▲
Page 33: [212] Formatted **Yanda Ou** **9/2/22 1:28:00 PM**

English (US)

▲
Page 33: [212] Formatted **Yanda Ou** **9/2/22 1:28:00 PM**

English (US)

English (US)

▲
Page 33: [212] Formatted **Yanda Ou** **9/2/22 1:28:00 PM**

English (US)

▲
Page 33: [213] Formatted **Yanda Ou** **9/2/22 1:28:00 PM**

English (US)

▲
Page 33: [213] Formatted **Yanda Ou** **9/2/22 1:28:00 PM**

English (US)

▲
Page 33: [213] Formatted **Yanda Ou** **9/2/22 1:28:00 PM**

English (US)

▲
Page 33: [213] Formatted **Yanda Ou** **9/2/22 1:28:00 PM**

English (US)

▲
Page 33: [213] Formatted **Yanda Ou** **9/2/22 1:28:00 PM**

English (US)

▲
Page 33: [213] Formatted **Yanda Ou** **9/2/22 1:28:00 PM**

English (US)

▲
Page 33: [213] Formatted **Yanda Ou** **9/2/22 1:28:00 PM**

English (US)

▲
Page 33: [213] Formatted **Yanda Ou** **9/2/22 1:28:00 PM**

English (US)

▲
Page 33: [213] Formatted **Yanda Ou** **9/2/22 1:28:00 PM**

English (US)

▲
Page 33: [213] Formatted **Yanda Ou** **9/2/22 1:28:00 PM**

English (US)

▲
Page 33: [213] Formatted **Yanda Ou** **9/2/22 1:28:00 PM**

English (US)

▲
Page 33: [214] Formatted **Yanda Ou** **9/2/22 1:28:00 PM**

English (US)

▲
Page 33: [214] Formatted **Yanda Ou** **9/2/22 1:28:00 PM**

English (US)

▲
Page 33: [214] Formatted **Yanda Ou** **9/2/22 1:28:00 PM**

English (US)

▲

English (US)

